REFERENCE ONLY

UNIVERSITY OF LONDON THESIS

Degree PhD Year 2006 Name of Author HANUOT, S.A

The role of *Sall4* in vertebrate limb development

Steven Andrew Harvey

The Division of Developmental Biology,

MRC National Institute for Medical Research (NIMR),

UCL.

Submitted in 2006 for the degree of doctor of philosophy

ProQuest LLC
789 East Eisenhower Parkway
P.O. Box 1346
Ann Arbor, MI 48106-1346

Acknowledgements

I have thoroughly enjoyed my time at NIMR and this has been made possible by several people. Firstly, I would like to thank Malcolm for his support, encouragement and patience throughout my project. I am also grateful for the help, critical input and stimulating conversations provided by past and present lab members, including Anna, April, Babis, Carolina, Jeff, Jo, Jutta and Peleg. I am forever in debt to the work of the aquatics unit, laidlaw green and NIMR procedural services. Finally, I would like to thank my family, friends and, most importantly, Lindsay for her continual support.

Abstract

Genes required for limb development have, in several instances, first been identified by studies of human diseases in which the limbs are affected. In humans, mutations in the transcription factor *SALL4* results in Okihiro syndrome (OS), which is characterised by forelimb defects and the eye disorder, Duane anomaly. OS patients forelimb defects range from subtle thumb abnormalities to truncated limbs. Mutations in another gene, *TBX5*, cause Holt-Oram syndrome (HOS), which is defined by heart and forelimb defects. OS and HOS patients limb defects are very similar, in fact, patients that have mutations in *SALL4*, and thus OS, have in some cases been misdiagnosed with HOS. Studies have shown that *Tbx5* performs an evolutionary conserved role in forelimb development. The similar limb phenotypes of OS and HOS patients may suggest that *Tbx5* and *Sall4* act in a common pathway and that *Sall4* is also required for forelimb development.

During my thesis work, I have investigated the function of *Sall4* and I have explored the hypothetical relationship between *Sall4* and *Tbx5* during limb development. To perform this analysis I have used zebrafish, chick and mouse model systems. I demonstrate that in the developing zebrafish pectoral fins *sall4* acts downstream of *tbx5*, and that *sall4* is essential for pectoral fin (forelimb) development. I show that *tbx5* initiates a feedforward transcriptional motif that is required to establish FGF signalling in the pectoral fin bud. My studies of sall gene family redundancy and *tbx5* offer explanations for the similarity of OS and HOS patients limb defects.

Declaration

I Steven Andrew Harvey declare that the work presented in this thesis was performed in the laboratory of Dr. Malcolm Logan in the Division of Developmental Biology at the MRC National Institute for Medical Research (NIMR). This work has been submitted for the degree of the degree of doctor of philosophy. I confirm that the work included in this thesis is my own. Where reagents have been obtained from other sources this has been stated within the thesis.

Contents

List of figures

List of abbreviations

AER	apical ectodermal ridge
dpf	days post fertilisation
DRRS	Duane radial ray syndrome
ES cells	embryonic stem cells
FGF	fibroblast growth factor
FGFR	fibroblast growth factor receptor
HOS	Holt-Oram syndrome
hpf	hours post fertilisation
HSPGs	heparin sulphate proteoglycans
Ig	immunoglobulin
MO	antisense morpholino oligonucleotide
OS	Okihiro syndrome
RA	retinoic acid
TBS	Townes-Brocks syndrome
ZPA	zone of polarising activity

1. INTRODUCTION

Limb development

During vertebrate embryonic development cells from discrete zones within the lateral plate mesoderm produce two pairs of limb buds at specific locations along the rostrocaudal axis of the embryo (Fig. 1). Signalling centres drive the growth and patterning of these limb buds to eventually form the mature limb, which consists of many tissues (e.g, bone, muscles, tendons) in a specific arrangement (Fig. 1). The developing limbs can be used as a model to understand how, during embryonic development, tissues grow in a controlled manner and how an apparently morphologically uniform population of cells can be patterned to form distinctive structures. As the developing limbs are easily accessible, it has been possible to carry out classical grafting experiments in the developing chick embryo that have identified the signalling centres required for limb outgrowth and patterning. In conjunction with these chick experiments, mouse and zebrafish genetics have also contributed to our understanding of the genes required for the function of these signalling centres.

Initiation of limb development

Before limb bud outgrowth occurs, the domain that will form the forelimbs and hindlimbs must first be specified. One of the first steps in this process is thought to be the expression of a diffusible factor from the intermediate mesoderm (IM), which lies adjacent to the lateral plate mesoderm (LPM). Evidence for this came from chick experiments in which placement of a foil barrier between the LPM and IM, adjacent to the limb-forming region and prior to the initiation of limb

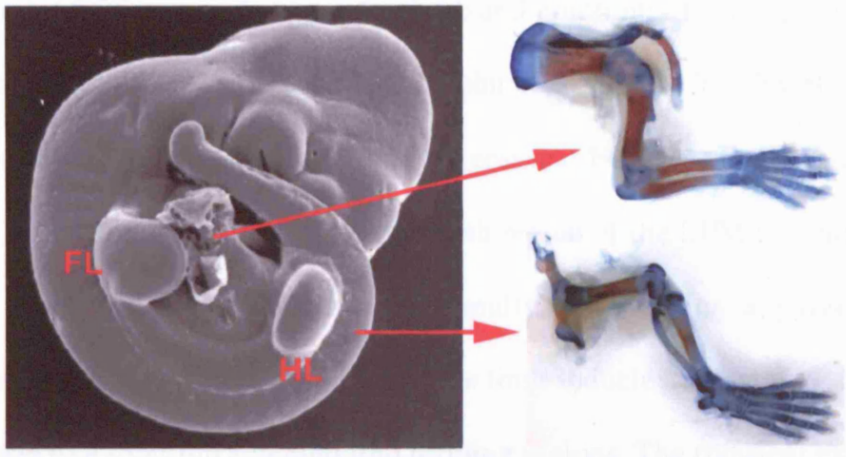

Figure 1. Mouse limb development. A scanning electron micrograph of an E10.5 mouse embryo. The forelimb (FL) and hindlimb (HL) buds form at specific locations along the rostrocaudal axis of the embryo. Alcian blue and alizarin red staining of the limb skeletal elements from an E17.5 embryo. SEM adapted from http://www.med.unc.edu/embryo_images/ and E17.5 limbs from Minguillon et al., 2005.

bud outgrowth, inhibits limb development (Stephens and McNulty, 1981). Similar experiments in which the mesonephros (an IM derivative) is ablated, resulted in an inhibition of limb development (Geduspan and Solursh, 1992).

Fibroblast growth factors (FGFs) are a family of secreted signalling molecules that have a potent effect on limb development. Placing a bead soaked in recombinant FGF protein between forelimb and hindlimb - forming regions, can induce the formation of an ectopic limb (Cohn et al., 1995; Crossley et al., 1996; Vogel et al., 1996). These experiments suggest that FGFs are the limb-inducing factor(s) and demonstrates that the inter-limb region of the LPM is competent to form a limb, although it does not normally do so. This apparent broad competence to form a limb suggests that the limb-inducing signal is restricted to the prospective forelimb and hindlimb forming regions. The transient expression of *Fgf8* in the IM prior to limb bud outgrowth has previously lead to the suggestion that *Fgf8* is the IM limb-inducing signal (Crossley et al., 1996; Vogel et al., 1996).

During embryonic development the Wolffian duct, a region of pronephros initially positioned anterior to the forelimb-forming region, elongates in a caudal direction adjacent to the IM, and in doing so progressively induces the differentiation of the IM to form mesonephros (Fernandez-Teran et al., 1997). Implantation of a foil barrier can inhibit the descent of the Wolffian duct and subsequently mesonephros does not form and *Fgf8* expression is not observed in the IM (Fernandez-Teran et al., 1997). When mesonephros development is inhibited in this way, limb development is unaffected, suggesting the

mesonephros and *Fgf8* expression in the IM is not required for limb development (Fernandez-Teran et al., 1997). In support of these results, conditional inactivation of *Fgf8* in the mouse IM does not affect limb development (Boulet et al., 2004). These experiments may suggest that another FGF that is expressed in the IM can compensate for the loss of *Fgf8*. The role played by the derivatives of the IM during the initiation of limb development therefore remains controversial.

Other studies have suggested that Wnt signalling molecules are the limb-inducing factor. In the developing chick embryo *Wnt2b* is expressed in the IM and the LPM of the prospective forelimb-forming region. Implanting cells that express *Wnt2b* into the inter limb region results in the formation of an ectopic limb, demonstrating that *Wnt2b* can induce limb development (Kawakami et al., 2001). Wnt signalling molecules act by binding to Frizzled transmembrane receptors. *Wnt2b* is thought to activate the so-called canonical Wnt signalling pathway, which results in an accumulation of β-catenin protein levels and the movement of β-catenin from the cytoplasm to the nucleus where, in conjunction with the transcription factors Tcf and Lef1 it can affect the transcription of target genes (Bejsovec, 2005). Consistent with the notion that canonical Wnt signalling can induce limb development, placement of cells expressing an active form of β-catenin can also induce the formation of an ectopic limb (Kawakami et al., 2001). Although *Wnt2b* is not expressed in the developing hindlimbs a related Wnt gene, *Wnt8c,* is and it appears that during hindlimb development *Wnt8c* performs an equivalent role to *Wnt2b* in the developing forelimbs (Kawakami et al., 2001).

During zebrafish embryonic development, *wnt2b* is expressed in mesoderm adjacent to the LPM and is required for the initiation of pectoral fin outgrowth (Ng et al., 2002). *wnt2b* is thought to induce the expression of the T-box transcription factor *tbx5,* which is essential for pectoral fin development (see below), within the LPM (Ng et al., 2002). This suggests that *wnt2b* activates a cascade of events that is required for the initiation of pectoral fin development. However, the expression of *tbx5* commences in the pectoral fin primordia at 17hpf, but *wnt2b* was reported to first be expressed at 22hpf (Ng et al., 2002). Despite the evidence for Wnt signalling in the initiation of zebrafish and chick limb development, to date no Wnt genes have been reported in the mouse to be expressed in a similar pattern to chick *Wnt2b* and *Wnt8c*. Similarly loss of both *Lef1* and *Tcf1* transcription factors does not affect the initiation of limb bud outgrowth (Galceran et al., 1999). These observations may reflect differences in the process of initiating limb development between these species.

Retinoic acid (RA) signalling is also required for the specification of the cells that will form the limb. During embryonic development retinaldehyde dehydrogenases synthesise RA from retinol (vitamin A) (Ang et al., 1996). Limb development is severely disrupted in Vitamin A deficient mouse embryos (Morriss-Kay and Sokolova, 1996). Loss-of-function studies have demonstrated that during zebrafish embryonic development the retinaldehyde dehydrogenase *raldh2* (recently renamed *aldh1a2*) is required for the initiation of *tbx5* expression in the LPM and subsequently the initiation of pectoral fin development (Begemann et al., 2001; Grandel et al., 2002). Supplying *raldh2* mutant embryos with exogenous RA can completely rescue pectoral fin

development. Interestingly, pectoral fin development is completely rescued when RA is supplied only transiently prior to pectoral fin outgrowth (Grandel et al., 2002). In these rescued embryos the expression of the mesodermal and ectodermal fin bud markers *tbx5* and *dlx2* is restored (Begemann et al., 2001; Grandel et al., 2002). Homozygous *raldh2* mutant zebrafish embryos die prior to the initiation of pelvic fin development and therefore the role of RA signalling in zebrafish hindlimb development is unknown.

A role for RA in limb formation appears to be conserved across species, as *Raldh2* null mice also fail to form a forelimb bud and the expression of mesodermal and ectodermal limb bud markers *Fgf10* and *Fgf8,* is undetectable in the forelimb-forming region of these embryos (Niederreither et al., 1999). Similar to the situation in zebrafish, supplying *Raldh2*$^{-/-}$ mouse embryos with RA can rescue the initiation of forelimb development, although at later time points the rescued forelimbs appear reduced in size (Niederreither et al., 2002). Interestingly, in these rescued embryos the left forelimb is more truncated than the right forelimb and the hindlimbs appear to be normal (Niederreither et al., 2002). The truncated forelimbs of these embryos may represent a partial rescue of RA signalling during the initiation of forelimb development, or it could suggest that RA is required at later time points for the maintenance of forelimb bud outgrowth. In addition, the apparently normal hindlimbs in rescued embryos could also imply that RA performs different roles in forelimb and hindlimb development.

The T-box transcription factor *Tbx5* is expressed in the developing forelimbs of all vertebrates analysed to date, including zebrafish, chick, mouse, *Xenopus* and newt embryos (Begemann and Ingham, 2000; Chapman et al., 1996; Gibson-Brown et al., 1998; Khan et al., 2002; Takabatake et al., 2000; Tamura et al., 1999). Loss of function experiments have demonstrated that *Tbx5* is essential for mouse forelimb development (Agarwal et al., 2003; Rallis et al., 2003). In embryos in which *Tbx5* has been conditionally inactivated in the developing forelimbs, no forelimb skeletal elements form, including the scapula and clavicle (Rallis et al., 2003). Similarly, loss of zebrafish *tbx5* function produces embryos that lack all pectoral fin (forelimb) skeletal elements, demonstrating that the role of *Tbx5* in forelimb development is evolutionarily conserved (Ahn et al., 2002; Garrity et al., 2002; Ng et al., 2002). *Fgf10,* which is expressed in both the developing mouse forelimbs and hindlimbs, fails to be expressed in the LPM of the forelimb-forming region in *Tbx5* knockout mice (Agarwal et al., 2003; Rallis et al., 2003). Studies have suggested that this relationship is direct and that *Tbx5* binds to the *Fgf10* promoter and activates its expression (Agarwal et al., 2003). *Fgf10* is also essential for limb development as the forelimbs and hindlimbs fail to form in *Fgf10* null mice (Min et al., 1998; Sekine et al., 1999). Despite largely the absence of the limbs, some remnants of the proximal skeletal elements, such as the scapula, do form in *Fgf10* null mice (Min et al., 1998; Sekine et al., 1999). These observations suggest that in the LPM a cascade of events occurs in which *Tbx5* activates the expression of *Fgf10* and this activation is essential for the initiation of forelimb development (Fig. 2A). However, differences in the formation of proximal forelimb skeletal elements in

Tbx5 and *Fgf10* loss of function mice, suggests that *Tbx5* performs more functions than simply the induction of *Fgf10* expression.

Although *Tbx5* is essential for forelimb development, it is not expressed in the developing hindlimbs. However *Tbx4,* which is the gene most closely related to *Tbx5,* is expressed in the hindlimb buds of zebrafish, chick and mouse embryos (Chapman et al., 1996; Gibson-Brown et al., 1998; Tamura et al., 1999). Mouse loss of function studies have shown that *Tbx4* is required for hindlimb development and normal expression of *Fgf10* in the hindlimb buds (Naiche and Papaioannou, 2003). These results suggest that *Tbx4,* in the hindlimbs, performs a similar function to *Tbx5,* in the forelimbs. Loss of *Tbx5* function results in mice with no forelimbs (Agarwal et al., 2003; Rallis et al., 2003). Ectopically expressing *Tbx4* in the forelimbs of the *Tbx5* conditional knockout genetic background can rescue forelimb development, further supporting the model that *Tbx5* and *Tbx4* perform similar functions during forelimb and hindlimb development (Minguillon et al., 2005).

The zebrafish gene *fgf24,* is essential for the initiation of pectoral fin outgrowth as mutants of *fgf24* (named *ikarus*) lack all pectoral fin skeletal elements but form normal pelvic fins (hindlimbs) (Fischer et al., 2003). However, no *Fgf24* gene has been found in chick, mouse or humans, and it appears *fgf24* was lost in the terrestrial vertebrate lineage (Draper et al., 2003; Fischer et al., 2003). In the LPM of the developing pectoral fins the initiation of *tbx5, fgf24* and *fgf10* expression occurs at 17 hours post fertilisation (hpf), 18hpf and 24hpf,

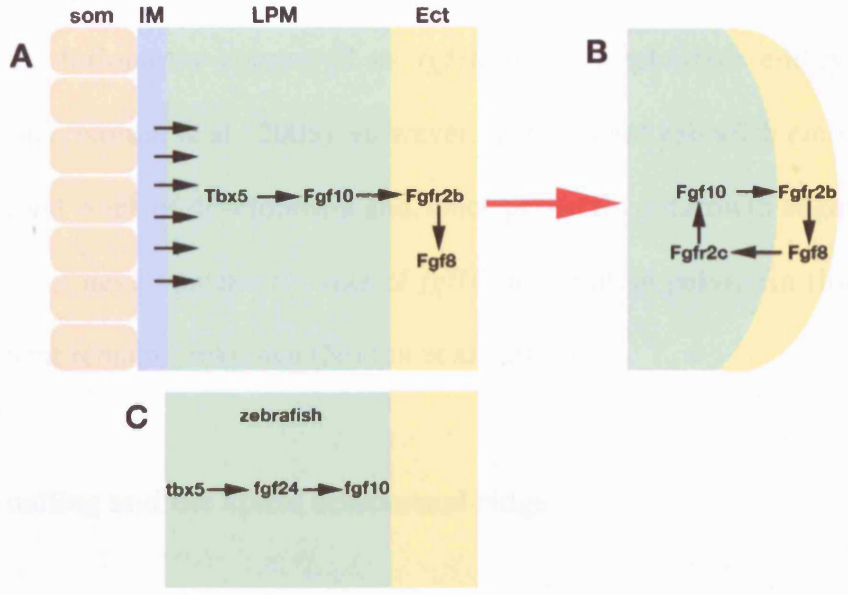

Figure 2. FGF signalling during forelimb development. (A) Chick experiments suggest that the intermediate mesoderm signals to the adjacent lateral plate mesoderm to initiate limb development. In the lateral plate mesoderm of the developing chick and mouse forelimbs *Tbx5* directly activates the expression of *Fgf10*. From the LPM, Fgf10 signals to the overlying ectoderm via Fgfr2b and subsequently induces *Fgf8* expression. (B) Fgf8 then signals back to the mesenchyme via Fgfr2c to maintain *Fgf10* expression. This establishes the *Fgf10/Fgf8* positive feedback loop. (C) In the lateral plate mesoderm of the developing zebrafish pectoral fins *tbx5* activates the expression of *fgf24*, and *fgf24* is required for *fgf10* expression. Ectodermal FGFs fail to be expressed in *fgf24* mutant zebrafish demonstrating mesenchymal FGFs induce the expression of FGFs in the fin bud ectoderm. som=somties, IM=intermediate mesoderm, LPM=lateral plate mesoderm, Ect=ectoderm

respectively (Begemann and Ingham, 2000; Fischer et al., 2003; Ng et al., 2002). Loss of *tbx5* function results in the absence of *fgf24* expression, and *fgf10* fails to be expressed in *fgf24* mutant embryos (Fischer et al., 2003). These results establish an epistatic genetic pathway in which *tbx5* activates *fgf24*, and *fgf24* is required for *fgf10* expression (Fig. 2C). The role of *fgf10* in limb development appears evolutionarily conserved as *fgf10* mutant zebrafish embryos lack pectoral fins (Norton et al., 2005). However, *fgf10* mutant zebrafish embryos die in the second week of development and, since pelvic fin outgrowth begins in the third week of development, the role of *fgf10* in zebrafish pelvic fin (hindlimb) development remains unknown (Norton et al., 2005).

FGF signalling and the apical ectodermal ridge

At the tip of the developing limb bud is a thickening of the ectoderm known as the apical ectodermal ridge (AER). The AER runs along the anterior to posterior axis of the limb bud and divides the dorsal and ventral limb bud ectoderm (Fig. 3A-B). Surgical removal of the AER at early time points in chick limb development, results in limbs that posses only proximal skeletal elements. Removing the AER at later time points produces limbs that lack only the most distal skeletal elements demonstrating that the AER is required to maintain outgrowth of the developing limb and that the skeletal elements of the limb are laid down progressively in a proximal to distal manner (Summerbell, 1974).

The FGF genes, *Fgf4, Fgf8, Fgf9* and *Fgf17* are all expressed in the AER (Martin, 1998; Sun et al., 2000). Removing the AER and replacing it with a

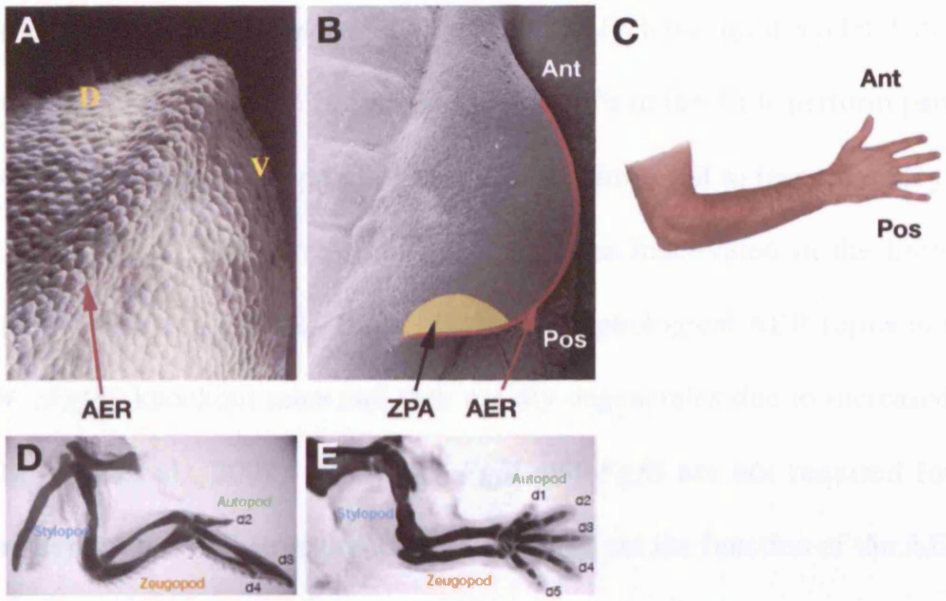

Figure 3. Key signalling centres during limb development. (A) A scanning electron micrograph of a mouse limb bud. The apical ectodermal ridge (AER) is a thickening of the limb bud ectoderm that separates the dorsal (D) and ventral (V) halves of the limb bud. The AER (red) stretches around the distal limb bud from anterior (Ant.) to posterior (Pos.), as shown by a lateral view of a mouse limb bud (B). The zone of polarising activity (ZPA, yellow) is located at the posterior limb bud (B). A picture of a human forelimb. The thumb is the most anterior digit and the little finger the most posterior (C). Skeletal preparations of chick (D) and mouse (E) forelimbs. The stylopod comprises proximal limb skeletal elements such as the humerus, the zeugopod corresponds to the ulna and radius, and the autopod relates to the wrist and hands. Pictures adapted from Logan, 2003 and Niswander, 2003.

bead soaked in recombinant FGF protein can substitute for the loss of the AER and maintain limb outgrowth (Fallon et al., 1994; Niswander et al., 1993). This suggests that FGFs are the signals emanating from the AER that are required for maintenance of limb outgrowth (Fallon et al., 1994; Niswander et al., 1993). Individual genetic loss of mouse *Fgf4* (Sun et al., 2000), *Fgf9* (Colvin et al., 2001), or *Fgf17* function (Xu et al., 2000) does not affect limb development and loss of *Fgf8* function results in limbs that only have mild skeletal defects (Lewandoski et al., 2000). This suggests that FGFs in the AER perform partially redundant functions. In support of this idea, the limbs fail to form in embryos in which *Fgf4* and *Fgf8* have simultaneously been inactivated in the limb bud ectoderm (Sun et al., 2002). Interestingly, a morphological AER forms in these $Fgf4^{-/-};Fgf8^{-/-}$ knockout mice and then rapidly degenerates due to increased cell death (Sun et al., 2002). Therefore *Fgf4* and *Fgf8* are not required for the formation of the AER structure, but instead carry out the function of the AER by signalling to the cells of the underlying mesenchyme.

In *Fgf10* null mice a small limb bud initially develops, however, the AER does not form and subsequently limb bud outgrowth fails (Sekine et al., 1999). Similarly, a pectoral fin bud initially forms in *fgf10* mutant zebrafish but the AER does not develop (Norton et al., 2005). *Fgf10* is required for the induction of *Fgf8* expression in the nascent AER (Min et al., 1998; Sekine et al., 1999). As *Fgf10* is only expressed in the limb bud mesenchyme these results suggest Fgf10 signals to the overlying ectoderm to induce AER formation and *Fgf8* expression. Removing the AER from a chick limb bud results in the downregulation of *Fgf10* expression, suggesting that maintenance of *Fgf10*

expression in the limb bud mesenchyme is AER-dependant (Ohuchi et al., 1997). Furthermore, replacing the AER with *Fgf8* expressing cells, maintains *Fgf10* expression in the limb bud mesenchyme (Ohuchi et al., 1997). Collectively these results show that *Fgf10* and *Fgf8* form a positive feedback loop in which they maintain one another's expression during limb bud outgrowth (Ohuchi et al., 1997).

FGF receptors and limb development

Vertebrates possess four FGF-receptors (*FgfR1-4,* also referred to as high-affinity FGF receptors), which are transmembrane tyrosine kinases with three extracellular immunoglobulin (Ig) domains. FGFs bind to the extracellular Ig domain of the receptors resulting in receptor hetero- and homo-dimerisation, and transphosphorylation of the intracellular domain of the receptor. This phosphorylation results in the activation of a cytoplasmic signal transduction pathway that affects the transcription of target genes. *Fgfr1* and *Fgfr2* are expressed in the developing limb buds of chick (Noji et al., 1993), mouse (Orr-Urtreger et al., 1991; Peters et al., 1992) and zebrafish embryos (Scholpp et al., 2004; Tonou-Fujimori et al., 2002). Alternative splicing of *Fgfr1-3* produces so-called IIIb and IIIc isoforms, in which the third Ig domain differs and results in distinctive FGF binding affinities (De Moerlooze and Dickson, 1997; Ornitz et al., 1996).

The IIIb and IIIc isoforms of *Fgfr2* are differentially expressed in the developing mouse limbs such that the IIIc isoform is expressed in the limb bud

mesenchyme while IIIb is expressed in the ectoderm (Orr-Urtreger et al., 1993; Orr-Urtreger et al., 1991; Revest et al., 2001; Xu et al., 1998). Fgf10 binds with greater affinity to the ectodermally expressed Fgfr2-IIIb isoform, and Fgf4 and Fgf8, which are expressed in the limb bud ectoderm, bind with a higher affinity to mesenchymally expressed Fgfr2-IIIc isoform (Igarashi et al., 1998; Ornitz et al., 1996; Orr-Urtreger et al., 1993). The forelimbs and hindlimbs fail to form in *Fgfr2* loss-of-function mice (De Moerlooze et al., 2000; Revest et al., 2001; Xu et al., 1998). In mice lacking the third Ig domain of *Fgfr2,* the limb buds initially form, however, the AER does not develop and *Fgf8* expression does not initiate (De Moerlooze et al., 2000; Xu et al., 1998). More specifically it has been shown that the ectodermally expressed *Fgfr2-IIIb* isoform is essential for AER formation and limb bud outgrowth (De Moerlooze et al., 2000; Revest et al., 2001). These experiments suggest that isoforms of *Fgfr2* mediate the *Fgf10/Fgf8* positive feedback loop, which is required for limb bud outgrowth (Fig. 2B).

Fgfr1 null mice die prior to limb bud outgrowth due to a gastrulation defect and therefore cannot be used to study the function of *Fgfr1* in limb development (Deng et al., 1994; Yamaguchi et al., 1994). However, recent experiments have conditionally inactivated *Fgfr1* in order to overcome this early lethality (Li et al., 2005; Verheyden et al., 2005). These experiments show that *Fgfr1* is not required for early stages in limb bud outgrowth but is instead required at later time points for autopod development and digit formation (Fig. 3E) (Li et al., 2005; Verheyden et al., 2005).

FGFs can bind to heparin sulphate proteoglycans (HSPGs, sometimes called low affinity FGF receptors) and heparin sulphate (HS) mediates the binding of FGFs to FGF receptors (Schlessinger et al., 2000). UDP-glucose dehydrogenase (Ugdh) is required for the synthesis of glycosaminoglycan side chains of HSPGs, and mutations in the drosophila Ugdh (called *sugarless*), disrupts FGF signalling (Lin et al., 1999). Mutations in the mouse homologue of this gene (called *lazy mesoderm*) disrupts Fgf8 signalling and subsequently results in gastrulation defects (Garcia-Garcia and Anderson, 2003). Exostosin (Ext) and Exostosin-like (Extl) genes are glycosyltransferases that are also required for the formation of HSPG side chains (Zak et al., 2002). Mutations in zebrafish *ext2 (dackel)* and *extl3 (boxer)* were first identified in ENU-induced mutagenesis screens for genes affecting fin development (van Eeden et al., 1996). It has recently been shown *ext2* and *extl3* are required in the pectoral fin bud ectoderm for the reception of *fgf10* signalling (Norton et al., 2005). These experiments provide the first evidence that HSPGs are required for FGF signalling during limb development.

Wnt signalling and the AER

Wnt signalling is also required for the formation and maintenance of the AER. In the developing chick limb buds *Wnt3a* is expressed in the AER and initiation of *Wnt3a* expression precedes that of *Fgf8* (Kengaku et al., 1998). Misexpression of *Wnt3a* in the developing limb bud results in ectopic *Fgf8* expression (Kengaku et al., 1998), and misexpression of *Fgf10* in the inter-limb region induces *Wnt3a* expression in the overlying ectoderm (Kawakami et al.,

2001). This suggests that *Fgf10* induces *Wnt3a* expression, which is required for *Fgf8* expression.

However, *Wnt3a* is not expressed in the mouse AER and loss of *Wnt3a* function does not affect mouse limb development (Roelink and Nusse, 1991; Takada et al., 1994). Instead a related gene, *Wnt3,* is expressed in the mouse limb ectoderm, and appears to play an equivalent role to *Wnt3a* in the developing chick limb. Conditional inactivation of *Wnt3* in the AER and ventral limb bud ectoderm results in an absence of the limbs (Barrow et al., 2003). In the AER of these embryos, *Fgf8* expression is varyingly downregulated. Barrow et al. suggest that *Fgf8* expression is not completely absent as *Wnt3* is not inactivated in the dorsal ectoderm and therefore *Wnt3* emanating from the dorsal ectoderm may partially maintain *Fgf8* expression in the AER. *Wnt3* activates the canonical Wnt signalling pathway and inactivation of β-catenin in the AER also results in an absence of the limbs (Barrow et al., 2003). In these β-catenin conditional knockouts the AER does not form and *Fgf8* is never expressed in the limb bud ectoderm. Later inactivation of β-catenin, after the AER has initially formed, results in a downregulation of *Fgf8* expression (Barrow et al., 2003). These experiments demonstrate that canonical Wnt signalling, activated by *Wnt3,* is initially required for the formation of the AER and the induction, and maintenance, of *Fgf8* expression in the AER.

Signalling between the zone of polarising activity and the AER

Another key signalling centre within the developing limb bud is the zone of

polarising activity (ZPA), which was first identified by classical chick grafting experiments (Fig. 3B, for review see Tickle, 2004). When cells from the posterior limb bud are transplanted into the anterior of a host limb bud it produces a mirror-image duplication of the digits. Subsequent studies have demonstrated that the signalling molecule Shh is the polarising factor expressed within the ZPA and is required for anterior to posterior patterning of the limbs (Riddle et al., 1993). *Shh* is expressed in the ZPA and placement of a bead soaked in Shh, or cells expressing Shh, in the anterior limb bud mimics the grafting of the ZPA and induces the formation of additional digits (Riddle et al., 1993; Yang et al., 1997). The expression of *Shh* in the limb bud mesenchyme is dependant on the AER and therefore *Shh* expression becomes restricted to the distal limb bud (Laufer et al., 1994; Niswander et al., 1994). Shh polarises the AER and restricts the expression of *Fgf4* to the posterior AER (Laufer et al., 1994; Niswander et al., 1994). Implanting a pellet of Shh-expressing cells in the anterior limb bud results in ectopic *Fgf4* expression in the anterior AER, demonstrating that *Shh* can induce *Fgf4* expression in the AER (Niswander et al., 1994). Removing the AER results in a rapid downregulation of *Shh* expression. However, replacing the AER with a bead soaked in recombinant Fgf4 protein maintains *Shh* expression (Laufer et al., 1994). Consistent with this relationship, *Shh* fails to be expressed in *Fgf4;Fgf8* double loss of function mouse limb buds (Sun et al., 2002). Together these results demonstrate that during limb development *Shh* and *Fgf4* form a positive feedback loop in which they maintain each others expression (Laufer et al., 1994; Niswander et al., 1994).

In *Shh*$^{-/-}$ mice the stylopod forms and is apparently normal, however, only one zeugopod element forms and only one digit element of the autopod is present (Fig. 3E) (Chiang et al., 2001; Kraus et al., 2001). The AER forms normally in *Shh*$^{-/-}$ mice and, although initially normal, *Fgf4* expression later becomes downregulated (Zuniga et al., 1999). *shh* is also required for zebrafish pectoral fin development (Neumann et al., 1999; Schauerte et al., 1998; van Eeden et al., 1996). However, the requirement of *shh* during zebrafish pectoral fin development differs from mouse limb development, as *shh* null zebrafish lack all pectoral fin skeletal elements (Neumann et al., 1999).

Sall gene family

The focus of my work has been to understand the function of the gene *Sall4* during vertebrate limb development. *Sall4* belongs to a family of zinc finger transcription factors, which in vertebrates is defined by the presence of an N-terminal Cys2-His-Cys zinc finger. Sall gene family members share characteristic Cys2-His2 type "double" zinc finger domains. *Sall4* has four of these double zinc fingers and in close proximity to the second double zinc finger is an additional zinc finger (Fig. 6B) Sall genes posses a glutamine rich domain which is thought to mediate homo- and heterodimerisation of gene family members (Kiefer et al., 2003; Sweetman et al., 2003). The *Drosophila* gene *spalt (sal)* is the founder member of the Sall gene family (Reuter et al., 1989) and higher vertebrates, such as mice and humans, possess four *Sal-like (Sall)* genes *(Sall1-4)*. Sall genes have also been identified in species such as C.

elegans (Basson and Horvitz, 1996), Medaka (Koster et al., 1997), and zebrafish (Camp et al., 2003).

Sall gene function

Spalt (*sal*), the founder member of the Sall gene family, was first identified as a homeotic gene that is required for specification of the drosophila head and tail. (Kuhnlein et al., 1994). In the *Drosophila* wing imaginal discs, *spalt* acts downstream of the T-box gene *optomotor-blind (omb)* and is required for correct patterning of the wing disc (de Celis et al., 1996; Del Alamo Rodriguez et al., 2004). Subsequent studies have shown that Sall genes are required for a range of developmental functions in several species. Some of these functions include; the correct intercalation of the cells of the developing drosophila trachea system (Ribeiro et al., 2004), the formation of photoreceptor cells in the drosophila eye (Mollereau et al., 2001), the specification of neural cell types in C. elegans (Basson and Horvitz, 1996; Toker et al., 2003) and the determination of the forebrain/midbrain in *Xenopus* (Onai et al., 2004),

Sall1 and *Sall3* are expressed in chick and mouse limb buds, as well as a range of other tissues during embryonic development (Nishinakamura et al., 2001; Ott et al., 2001; Sweetman et al., 2003; Sweetman et al., 2005). *Sall2* is also expressed during mouse embryonic development however the exact temporal and spatial expression pattern has never been reported (Kohlhase et al., 2000). Currently there have been no reports of *Sall2* expression in the developing limbs of chick, mouse or zebrafish embryos. *Sall2* null mice are apparently normal and

have no developmental defects (Sato et al., 2003). *Sall3* null mice have palate and cranial nerve defects and die soon after birth (Parrish et al., 2004). Individual loss of mouse *Sall1, Sall2* or *Sall3* does not affect limb development, despite both *Sall1* and *Sall3* being expressed in the limb buds. This suggests that Sall genes have redundant functions and can compensate for the loss of one another during limb development.

Transcriptional properties of Sall genes

There is currently conflicting data suggesting that Sall genes can act as either transcriptional activators or repressors (Kiefer et al., 2002; Li et al., 2004; Netzer et al., 2001; Onai et al., 2004). Previous studies have shown that *Sall1* can act as a transcriptional repressor, possibly by recruiting a histone deacetylase complex (Kiefer et al., 2002; Netzer et al., 2001; Sweetman et al., 2003). The ability of mouse *Sall1* to act as a transcriptional repressor appears to be mediated by the aminoterminal Cys2-His-Cys zinc finger (Kiefer et al., 2002). Similar to *Sall1,* using GAL4 fusion experiments it has been shown that *Sall3* can act as a transcriptional repressor (Sweetman et al., 2003). Other studies have shown that *Sall2* can bind directly to the promoter of the gene $p21^{WAF1/CIP1}$ and activate its expression (Li et al., 2004). In close proximity to the second double zinc finger domain of *Sall2* is another zinc finger (Fig. 6B). Deletion of these three zinc fingers abolishes the ability of *Sall2* to bind to the $p21^{WAF1/CIP1}$ promoter (Li et al., 2004). Another study has shown that the *Xenopus* Sall gene, *XsalF,* is required for the expression of *Gsk3β* and *Tcf3* during forebrain/hindbrain development, suggesting that this Sall gene can act as a

transcriptional activator (Onai et al., 2004). These observations demonstrate that Sall genes can act as transcriptional activators or repressors and different regions of Sall proteins mediate these effects.

Regulation of Sall gene expression

Sall1 is expressed in the distal mesenchyme and AER of developing chick limb buds (Farrell and Munsterberg, 2000). Implanting a bead soak in Shh in the anterior limb bud results in an expansion in *Sall1* expression. Removing the AER results in a downregulation of *Sall1*, suggesting that maintenance of *Sall1* expression is AER dependant (Farrell and Munsterberg, 2000). Shh cannot upregulate *Sall1* expression in the absence of the AER suggesting that signals from the AER, in conjunction with *Shh,* are required for *Sall1* expression. In the absence of the AER a bead soaked in Fgf4 or cells expressing Wnt3a cannot maintain *Sall1* expression, however, replacing the AER with both a bead soaked in Fgf4 and Wnt3a expressing cells does maintain *Sall1* expression (Farrell and Munsterberg, 2000). This suggests that in the chick limb bud *Wnt3a, Fgf4* and *Shh* all act together to maintain the correct *Sall1* expression pattern.

Further evidence that Shh can upregulate the expression of Sall genes comes from studies of a medaka sall gene homologue that is expressed in the developing eye and midbrain/hindbrain (mhb) boundary, as well as other regions in the developing embryo (Koster et al., 1997). Ectopic expression of *shh* results in an expansion of *sall* gene expression in the mhb boundary and an upregulation of expression in the eye (Koster et al., 1997). Inhibition of hh

signalling by misexpression of a constitutively active form of protein kinase A, results in a downregulation of *sall* expression in the developing eye and mhb boundary (Koster et al., 1997). These results suggest that within these tissues expression of this *sall* gene is positively regulated by *shh*.

SALL4 and Okihiro syndrome

Many human congenital limb abnormalities are caused by the disruption of pathways that are required for embryonic limb development. The human disease Okihiro syndrome, results from mutations in *SALL4* (OS, also called Duane radial ray syndrome (DRRS), OMIM number 607323). OS, which is an autosomal dominant disorder, is characterised by forelimb defects (Fig. 4A) associated with the eye defect, Duane anomaly (Al-Baradie et al., 2002; Kohlhase et al., 2002). The forelimb defects of OS patients range from subtle thumb abnormalities to severely truncated limbs (phocomelia) (Al-Baradie et al., 2002; Kohlhase et al., 2002). The thumb, which is the most anterior digit (Fig. 3C), is most commonly affected in OS (Borozdin et al., 2004). Duane anomaly is an eye movement disorder characterised by limited abduction of the eyes and narrowing of the palpebral fissure (closing of the eye lids) and retraction of the eye globe upon abduction of the eyes. In addition to forelimb defects and Duane anomaly in OS patients, a range of less common abnormalities have been reported in patients with *SALL4* mutations, including ventricular septal defects (hole in the heart), anal stenosis, fused cervical vertebrate, external ear deformities, hearing impairment, kidney agenesis and Hirschsprung's disease (Al-Baradie et al., 2002; Kohlhase et al., 2002). It has

been reported that some OS patients have a widened gap between their first and second toes ("sandal gap") (Kohlhase et al., 2003). Due to the occurrence of these less common features, some OS patients have similar phenotypes to acro-renal-ocular syndrome (AROS), Townes-Brockes syndrome (TBS) and Holt-Oram syndrome (HOS) patients (see below). However the occurrence of kidney agenesis in patients with mutations in *SALL4* has led to the suggestion that AROS and OS are one entity (Kohlhase et al., 2005).

Several different *SALL4* mutations have been identified in OS patients, which all lead to a premature stop codon (Fig. 6C) (Al-Baradie et al., 2002; Borozdin et al., 2004; Brassington et al., 2003; Kohlhase et al., 2005; Kohlhase et al., 2002; Kohlhase et al., 2003). Several larger heterozygous *SALL4* deletions have been described in OS patients (Fig. 6C) (Borozdin et al., 2004). In these pedigrees, two different deletions encompass all four *SALL4* exons, two cover exons 1-3, one covers exon 1 and another exon 4. These larger heterozygous mutations suggest that OS results from *SALL4* haploinsufficiency. A recent study identified a missense mutation that changes amino acid 888 of SALL4 from a Histidine to an Arginine (H888R) (Miertus et al., 2006). The Histidine amino acid that is altered is essential to the aminoterminal zinc finger of the most carboxyterminal double zinc finger domain. Through computational analysis Miertus et al. suggest that this missense mutation results in an increase in SALL4 DNA binding affinity and subsequently affects *SALL4* function. However, only three patients have been described with mutation H888R and these patients have only a mild OS phenotype. All of the three patients described have Duane anomaly, a widened sandal gap and forelimb defects reported

included shortened fingers and thumbs that are positioned slightly more proximal in relation to the fingers. The mild phenotype of these patients suggests that mutation H888R affects the function of *SALL4* but does not completely abolish it. Several other single base pair changes in *SALL4* have been described that do not lead to OS, however due to codon redundancy, only three of these mutations lead to amino acid substitutions (Al-Baradie et al., 2002; Brassington et al., 2003; Kohlhase et al., 2005). As these three amino acid substitutions do not result in OS they most probably do not affect the function of SALL4, or the stability of *SALL4* mRNA.

SALL genes and human disease

Another Sall gene associated with human disease is *SALL1*, which when mutated can lead to Townes-Brocks syndrome (TBS, OMIM number 107480, Kohlhase et al., 1998). TBS is an autosomal dominant disorder, and patients can have a range of abnormalities including limb defects, abnormal ears, imperforate anus and kidney abnormalities (Kohlhase et al., 1998). The limb defects of TBS patients include preaxial polydactyly and triphalangeal thumb in the forelimbs, and syndactyly and club foot in the hindlimbs (Kohlhase et al., 1999). Until recently, all of the *SALL1* mutations described in TBS patients lead to a premature transcription stop codon that is predicted to result in the expression of a truncated SALL1 protein that contains the N-terminal zinc finger, the glutamine rich domain and either one or none of the Cys2-His2 zinc fingers (Botzenhart et al., 2005).

The mouse *Sall1* homologue is expressed in a range of tissues during embryonic development, including the limbs and many other tissues that have defects associated with TBS (Nishinakamura et al., 2001). Loss of function experiments demonstrated that *Sall1* is essential for mouse kidney development but is dispensable in other regions of the embryo. Therefore mice with no functional copies of *Sall1* do not phenocopy TBS defects, despite heterozygous mutations in human *SALL1* being associated with TBS (Nishinakamura et al., 2001). However, mice that express a truncated form of *Sall1,* which is predicted to mimic a TBS-causing mutation, do phenocopy TBS (Kiefer et al., 2003). This truncated form of Sall1 can interact with full length Sall1-4 *in vitro* (Kiefer et al., 2003). Together these results suggest that TBS results from mutations that produce a truncated, dominant-negative form of *SALL1* and is not due to *SALL1* haploinsufficiency.

However, recent work has used quantitative, real-time PCR to identify large heterozygous *SALL1* deletions in patients with mild TBS phenotypes (Borozdin et al., 2006). Using this method Borozdin et al. studied the *SALL1* locus in 240 TBS patients, in which no *SALL1* mutations had previously been identified. Patients in three of the pedigrees studied had large, heterozygous *SALL1* deletions, two of which covered all of the *SALL1* exons. These results show that *SALL1* haploinsufficiency can lead to TBS. However, Borozdin et al. suggest haploinsufficiency of *SALL1* leads to a milder phenotype than that observed in patients with premature stop codon in *SALL1*. These observations also suggest that the function of *Sall1* differs between humans and mice. To date mutations in *SALL2* or *SALL3* have not been directly linked to a human disease.

T-box genes

In the 1920s a mutation within a gene was identified, which resulted in mice with truncated tails. This so-called *T* gene (now more commonly referred to as *Brachyury*) is the founder member of the T-box gene family and members of this family are defined by the presence of a conserved DNA-binding domain, known as the T-domain. T-box genes have been reported in many diverse species and there are 17 known T-box genes in humans (Minguillon and Logan, 2003). T-box genes are required for a range of developmental processes and several have been associated with human disease (for review see Packham and Brook, 2003).

TBX4 and *TBX5* in human disease

As previously mentioned *Tbx4* and *Tbx5* perform essential roles in hindlimb and forelimb development, respectively (See section Initiation of limb outgrowth). Mutations in human *TBX5* results in Holt-Oram syndrome (HOS, OMIM number 142900) (Basson et al., 1997; Li et al., 1997). HOS, which results from *TBX5* haploinsufficiency, is defined by heart and forelimb abnormalities (Packham and Brook, 2003). The limb deformities seen in HOS patients range from thumb defects to phocomelia (Basson et al., 1997; Li et al., 1997). There is an anterior bias to the limb defects of HOS patients such that the thumb and radius bones are predominantly affected (Fig. 4B). Less common defects reported in HOS patients include absent pectoral muscles and eye problems, such as Duane anomaly (Newbury-Ecob et al., 1996). Although *TBX5* mutations

are associated with HOS it has been predicted that these mutations only account for ~30% of HOS patients (Cross et al., 2000).

Mutations in human *TBX4* results in small patella syndrome (SPS, also referred to as Scott-Taor syndrome, OMIM number 147891) (Bongers et al., 2004). *TBX4* mutations have not been described as extensively as mutations in *TBX5*. SPS patients suffer from abnormal pelvic bone structure and recurring dislocation of the patella due to its abnormally decreased size. SPS patients also have an increased gap between their first and second toes ("sandal-gap", Bongers et al., 2004).

The role of *Sall4* during limb development

The forelimb defects in OS (*SALL4* mutations) and HOS (*TBX5* mutations) patients are very similar. In both sets of patients there is an anterior bias to the limb defects and the left limb is more severely affected than the right (Fig. 4). In addition to the phenotypic similarity, several patients previously diagnosed with HOS, but lacking *TBX5* mutations, have been subsequently shown to have mutations in *SALL4* (Brassington et al., 2003). Apart from the association of *SALL4* mutations and OS syndrome, the function of *Sall4* during limb development is unknown. I have investigated the role of *Sall4* in the limb and the relationship between *Sall4* and *Tbx5* during limb development, as the similarities of OS and HOS patients may suggest that *Sall4* and *Tbx5* act in a common signalling pathway that is required for forelimb development. To perform my analysis I have used chick, mice and zebrafish embryos. However,

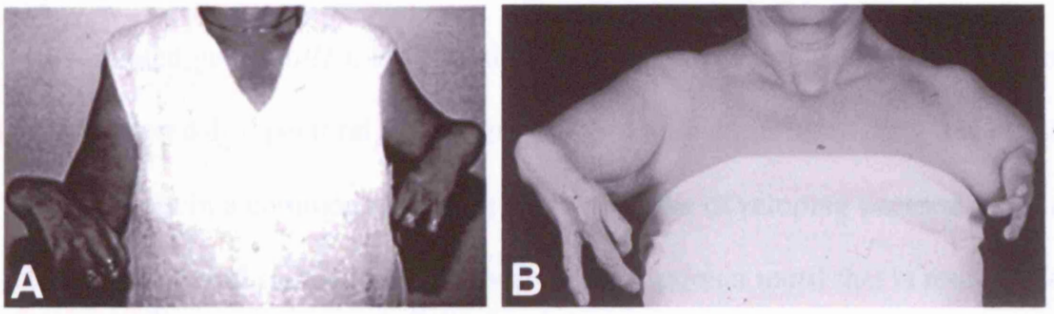

Figure 4. Limb development is disrupted in Okihiro and Holt-Oram syndrome patients. (A) A picture of an Okihiro syndrome patient who has a mutation in the gene *SALL4*. (B) A picture of a Holt-Oram syndrome patient who has a mutation in the gene *TBX5*. In both sets of patients the left limb is more severely affected than the right limb. There is also an anterior bias to their limb defects, such that the most anterior digits (i.e. the thumb and index finger) are most commonly affected. Pictures adapted from Kohlhase et al., 2002 and Basson et al., 1994, respectively.

the majority of my thesis work has focused on using zebrafish embryos. I have used morpholinos to knockdown *sall4* and *tbx5* function during zebrafish embryonic development. Mouse genetics was also used to perform *Sall4* loss of function experiments, and to analyse a fragment of the *Sall4* promoter. I have also carried out misexpression experiments in the developing zebrafish embryo and the forelimbs of chick embryos.

My experiments demonstrate that during zebrafish embryonic development *sall4* and a related gene, *sall1a,* have partially redundant functions, and that they are both required for pectoral fin outgrowth. I demonstrate that *tbx5, sall4* and *sall1a* all act in a common signalling pathway in the developing pectoral fins. In this pathway, *tbx5* initiates a feedforward transcriptional motif that is required to establish FGF signalling in the pectoral fin mesenchyme. This feedforward motif provides insights into the dynamics of FGF signalling during the initiation of forelimb bud outgrowth. These results have clinical significance as they not only offer explanations to the similar limb phenotypes of OS and HOS patients, but could also improve the clinical diagnosis of OS and HOS.

2. MATERIALS AND METHODS

Sall4 cloning

Zebrafish and mouse *Sall4* clones were isolated using RT-PCR. Zebrafish *sall4* was cloned using whole embryo RNA prepared from a sample of 20 embryos at 24hpf. Mouse *Sall4* was cloned using RNA isolated from one whole E10.5 embryo. The RNA for the RT-PCRs was prepared by: (1) The sample(s) were homogenised in 800µl of Trizol reagent (Gibco), and incubated at room temperature for 5mins. (2) The sample was then spun at 14,000 rpm for 10mins at room temperature. (3) The supernatant was removed, and the pellet, which contains high molecular weight DNA, was discarded. (4) 160µl of chloroform was added to the supernatant, vortexed for ~15secs and left at room temperature for 2mins. (5) Then spun at 14,000 rpm for 15mins. (6) The aqueous phase was removed and the RNA was precipitated by adding 400µl of isopropanol and incubating at room temperature for 10mins. (7) The sample was then spun at 14,000 rpm for 10mins. The pellet was washed with 1ml of 75% ethanol, and re-spun for 1min. The ethanol was removed and the pellet was air-dried and re-suspended in RNAse and DNAse free water (Sigma).

Mouse *Sall4* was cloned into the plasmid bluescript pKS (Stratagene) using RT-PCR with E10.5 whole embryo RNA as a template. PCR primers were designed using the cDNA sequence GenBank accession number AK049188. An internal SpeI restriction enzyme site was utilized to clone m*Sall4* in two steps. ClaI and NotI restriction enzyme sites were incorporated into 5' and 3' primers to aid cloning. The 5' fragment of m*Sall4* was first cloned using the primers: (1) 5' – tcaatcgatatgtcgaggcgcaagcaggcg – 3' (ClaI restiction enzyme site) and (2) 5' –

atgttctccactagttgctgc – 3' (SpeI restiction enzyme site). The 3' fragment was cloned using the primers: (3) 5' – ttgcagcaactagtggagaac – 3' (SpeI restiction enzyme site) and (4) 5' – tcagcggccgcttagctgacagcaatcttattttcc – 3' (NotI restiction enzyme site).

Zebrafish *sall4* was cloned into the plasmid Bluescript pKS (Stratagene), in a similar two-step strategy, using RT-PCR with 24hpf whole embryo RNA as a template. Primers were designed using the Ensembl cDNA sequence ENSDART00000007860. An internal ClaI restriction enzyme site was used to clone zf*sall4* in two steps. SpeI and SalI restriction enzyme sites were incorporated into the 5' and 3' primers to aid cloning. I first cloned the 5' fragment with the primers: (1) 5' – ctactagtgtcttactattcgcccctgat – 3' (SpeI restiction enzyme site) and (2) 5' – cagaagaaatcgatgcaccat – 3' (ClaI restiction enzyme site), and then cloned the 3' fragment with the primers: (3) 5' – gatggtgcatcgatttcttct – 3' (ClaI restiction enzyme site) and (4) 5' – atgtcgacgtaagccaatcagcacaac – 3' (SalI restiction enzyme site).

All RT-PCRs were performed using QIAGEN OneStep RT-PCR kit, following the manufacturers protocol. To increase proof-reading fidelity, High Fidelity Taq (BD Biosciences, Advantage HF Taq) was added to the RT-PCR after cDNA synthesis.

C-terminal truncated forms of zebrafish and mouse *Sall4* (*Sall4*Δ) were generated using high fidelity Taq (BD Biosciences, Advantage HF Taq), following the manufacturers protocol, in a PCR using the full - length clones as

templates. Stop codons were incorporated into the 3' primers. The primers used to clone m*Sall4*Δ were (1) 5' – acgggtctcccatgtcgaggcgcaagcaggcg – 3' (BsaI restiction enzyme site) and (2) 5' – acgggatcctgaatcgagcgacagagctgggtt – 3' (BamHI restiction enzyme site, and stop codon). This results in a clone spanning from amino acids 1 to 289 of m*Sall4*. BsaI and BamHI restiction enzyme sites were incorporated into the primers to aid cloning. Digestion of the PCR product with BsaI creates an NcoI-compatible sticky end. This strategy allows cloning of m*Sall4*Δ into the NcoI restriction enzyme site of the shuttle vector pSlax-13 (Logan and Tabin, 1998). m*Sall4*Δ was then removed from the shuttle vector using the restriction enzyme ClaI, and cloned into the retroviral vector RCASBP(A). Orientation was then confirmed by digesting clones with the restriction enzyme NcoI. Using this cloning strategy ensures m*Sall4*Δ is cloned into the correct position of the retrovirus that favours optimal translation and expression of the protein product of the cloned cDNA (Logan and Tabin, 1998).

Zebrafish *sall4*Δ construct was generated by PCR using high fidelity Taq (BD Biosciences, Advantage HF Taq) and the primers: (1) 5' – cgatcgatatgtcgcggcgcaagcagtcc – 3' (ClaI restiction enzyme site) and (2) 5' – cgaattctgatgcttccaaggacaaagactgg – 3' (EcoRI restiction enzyme site). This clone spans from amino acids 1 to 271 of zf*sall4*. ClaI and EcoRI restriction enzyme sites were incorporated into the primers to aid cloning directly into the vector pCS2+. The construct used to create RNA encoding GFP was generated by cloning a fragment of zf*sall4* into a pSlax-13 plasmid, which contained a fusion of bacteriophage λ-hinge and GFP (pSlax13λGFP, provided by J. Francis and M. Logan). This cloning created a fusion of bases –32 to +164 of zf*sall4* to

the λ-hinge GFP. The primers: (1) 5'-agccatggttactattcgcccctgatggt-3' and (2) 5'-agaattccgcaaacccttgtctcctccg3' were used to the PCR amplify, from my full-length clone, the fragment of zf*sall4*. NcoI and EcoRI restriction enzyme sites were incorporated into the primers to aided in-frame cloning into the pSlax λ-hinge GFP plasmid. This GFP construct was then removed from the pSlax plasmid using the restriction enzyme ClaI and cloned into the plasmid pCS2+.

All clones were sequenced at ABC biosciences (Imperial College London). All restriction enzyme digests were performed at 37^0C apart from BsaI, which was performed at 50^0C, and using the manufacturers recommended buffers. Digestion reactions were carried out for 1-2hours.

Ligation reactions were carried using T4 DNA ligase (New England Biolabs) and the manufacturers buffer and performed at room temperature. Sticky end ligations were performed for 1 hour and blunt end ligations for 2 hours. Ligation reactions were performed in a volume of 10μl using 1μl of ligase (4units). Following incubation 5μl of reaction mix was added to 25μl of DH5α competent cells (Invitrogen, thawed on ice) and incubated for 10mins on ice. The cells were then heat shocked by placing in a 42°C water bath for 45 secs. Following heat shock 300μl of 2xTY media (antibiotic free) was added to the cells, which were then placed in a 37°C shaker for ~1hour. Cells were then plated on an agar dish containing antibiotics and incubated at 37°C overnight.

Zebrafish RNA injections

RNA for injections was created by linearsing pCS2+ plasmids with NotI restriction enzyme and using Sp6 mMESSAGE mMACHINE (Ambion), and following the manufacturers protocol, I *in vitro* transcribed 5'capped, sense, RNA that also contained a polyA+ tail. RNA was purified using spin columns (chroma spin-100, BD Bioscience). Transcribed RNA was run on a 1% agarose gel, and quantified using a spectrophotometer.

RNA was injected into the yolk of 1-, 2- or, 4-cell zebrafish embryos. Injections were performed using a pneumatic microinjector (Pneumatic PicoPumP) and compressed air. The needles were held and manipulated using a micromanipulator (Kanetec). The volume to be injected was calibrated using a graticule underneath a petri dish that contained mineral oil. Ten injections into the mineral oil were calibrated to a diameter of 0.3mm. This calibration ensures that one injection corresponds to approximately 1.4nl, based on the volume calculated as $4/3\pi r^3$.

Chick misexpression

m*Sall4*Δ reteroviral supernatant was produced by: (1) DF1 cells (immortalised chick fibroblasts) were grown in 6cm dishes (Nunc) until approximately 50% confluent. DF1 cells were then transfected with the m*Sall4*Δ RCASBP(A) construct using SuperFect transfection reagent with the manufacturers protocol (Qiagen). The cells were incubated with 5μl of m*Sall4*Δ RCAS construct +

Superfect reagent for 3 hours. After this time the media was replaced. (2) Cells were then grown and expanded into 15cm dishes until 100% confluent. Cells were then moved into harvest media, which contains $1/10^{th}$ the concentration of serum. (3) The media (10mls), which contains virus, was then harvested every 24hours for 3 days. Cells were grown in an incubator at 37°C + 5% CO_2. (4) The harvested media was then filtered and ultra-centrifuged (21,000 rpm, 4^0C, for 14hours). Excess media was discarded leaving the pellet and minimal amounts of solution. The pellet was then placed on a shaker, and on ice, and agitated for one hour to re-suspend the pellet. Concentrated virus was stored at -80^0C. m*Sall4*Δ virus was injected into the prospective forelimb-forming region at approximately HH stage 10 as described (Logan and Tabin, 1998).

Embryo staining

Whole – mount RNA *in situ* hybridisation was performed as described for mouse and chick (Riddle et al., 1993). Zebrafish whole-mount RNA *in situ* hybridisations were performed essentially as described (Thisse et al., 1993), but with the following modifications: Embryos greater than ~30hpf were treated with proteinase K (5μg/μl) for 10mins, for mesenchymal fin bud markers, and 5mins for ectodermal fin bud markers. Proteinase K reaction was stopped by washing in 4% PFA for 15mins. Hybridisation was performed overnight in a shaking water bath at 65^0C. To improve the quality of staining, *fgf10* and *fgf24* probes were hybridised over two nights. Hybridisation was performed by adding 1ml of hybridisation buffer and 3μl of re-suspended probe (from 100μl, see below). Following hybridisation embryos were washed in: (1) 50%

hybridisation buffer/50% 2X SSC, for 5mins, 65^{0}C. (2) 2X SSC for 15mins, 65^{0}C. (3) 0.2X SSC, 2 times for 30mins, 65^{0}C. (4) 50% 0.2X SSC/50% PBT, 10mins, at room temperature. (5) PBT, 10mins, at room temperature. (6) PBT/2% sheep serum/2% BSA, for greater than 1 hour, at room temperature. (7) Embryos were then incubated overnight in PBT/2% sheep serum/2% BSA, plus anti-digoxygenin antibody at a dilution of 1 in 5000. (8) Embryos were then washed in PBT at room temperature very briefly. (9) Then 3 times for 5mins. (10) Then 4 times for 15mins. (11) Embryos were then washed in NTMT (100mM NaCl + 100mM tris HCL pH9.5 + 50mM $MgCl_2$) 2 times for 5mins. Embryos were stained in 10mls NTMT + 35µl BCIP (50mg/ml) + 30µl NBT (75mg/ml). Once stained embryos were washed 2 times, 10min in PBT, then fixed in 4% PFA. All *in situ* hybridisations were performed in scintillation vials.

All digoxygenin labelled RNA *in situ* probes were transcribed using the manufacturers protocols (Roche). Transcription reactions were performed at 37^{0}C for 2 hours. Transcription was tested by running 1µl of the transcription reaction on a 1% agarose gel. DNA was digested by adding 1µl of DNAse (RNAse free) and incubating for 15mins at 37^{0}C. RNA was precipitated by adding 100µl TE-8 + 10µl 4M LiCl + 300µl Ethanol, and then incubated overnight at -20^{0}C. RNA was then microcentrifuged 14K, for 10mins. Pellet was washed in 70% ethanol, re-spun at 14K for 1min, and then air-dried. Pellet was re-suspended in 50µl TE-8 + 50µl hybridisation buffer.

The following *in situ* probes have been described previously: zf*dlx2*, zf*fgf8*, zf*fgf10*, zf*fgf24*, zf*erm* (Fischer et al., 2003), zf*sp9* (Norton et al., 2005) m*Fgf8*

(Crossley and Martin, 1995), m*Fgf10* (Bellusci et al., 1997) zf*fgfr2* (Poss et al., 2000), zf*tbx5* (Begemann and Ingham, 2000), m*Tbx5* (Bruneau et al., 1999) and zf*wnt5a* (Kilian et al., 2003). A cDNA clone was used for a zf*sall1a in situ* probe template (IMAGE consortium - accession number BI880033, linearised with EcoRI and RNA transcribed with the polymerase T7) and zf*tcf3b in situ* probe template (IMAGE consortium – accession number AI497195, linearised with SalI and RNA transcribed with the polymerase Sp6). The 5' half of zf*sall4* (1.6kb SpeI-ClaI fragment, see above) was used as an *in situ* probe template. The vector was linearised with SpeI and RNA transcribed using T3 polymerase. My full-length mouse *Sall4* clone was used as *in situ* probe template. The vector was linearised with ClaI and RNA transcribed with the polymerase T7.

Zebrafish section *in situ* analysis was performed by wax imbedding and sectioning whole mount preparations. Embryos were wax imbedded by washing in (1) 70% ethanol 2 times, 30 mins. (2) 85% ethanol, 30mins. (3) 95% ethanol, 30mins. (4) 100% ethanol 2 times, 30mins. (5) histoclear 2 times, 30mins. (6) A 1:1 ration of histoclear/wax for 30mins at 60^{0}C. (7) Wax, at 60^{0}C, 3 times, 30mins. (8) Samples were then embedded in moulds, and embryos were orientated using heated forceps. The moulds were incubated at 4^{0}C overnight. Wax blocks were then removed from moulds and sectioned. Sections were de-waxed by washing in (1) histoclear, 15mins. (2) 100% ethanol 2 times, 2mins. (3) 75% ethanol, 2mins. (4) 50% ethanol, 2mins. (5) 25% ethanol, 2 mins. (6) PBS 2 times, 2mins. Sections were then mounted under cover-slips using Aquamount (BDH chemicals).

Alcian blue staining of zebrafish embryos was performed by: (1) Fix in 4% PFA overnight. (2) Washed in PBT (PBS + 0.1% tween) 2 times, 10 mins. (3) Dehydrated in ascending series of ethanol until 100%, then left overnight. (4) Embryos were stained throughout the day (i.e. 9 hours) at room temperature with alcian blue (1mg alcian blue per 10mls of ethanol:acetic acid 8:2 ratio). (5) Washed 3 times, 20 mins in 95% ethanol, then re-hydrated by washing in an increasing percentage of PBT. (6) Pigment was removed by washing overnight at room temperature with hydrogen peroxide (0.6% H_2O_2) in KOH (1%). (7) Samples were then washed in PBT 3 times, 10 mins. (8) The muscles were rendered transparent by digesting with trypsin (50mg/ml) in 3ml Sodium Borate (from 1% stock) plus 7mls water. The trypsin used, which was obtained from Sigma-Aldrich (T4799), was from a porcine pancreas and in a lyophilised powder. Digestion with trypsin takes approximately 15-30 mins. (9) Samples were then washed in PBT 2 times. (10) Then washed in 30% glycerol, then 60% glycerol in order to photograph. Pictures of alcian blue stained pectoral fins were obtained by removing the pectoral fins and then mounting them on a slide.

Methylene blue staining of cryostat sections was performed by: (1) Sections were stained for 3mins in 20mls sodium borate (1%) plus 15mls ethanol plus 10mls methylene blue (0.13% in water) + 7.5mls water. (2) After stained the sections were washed in H_2O, 4 times, 2mins. (3) Slides were then mounted with Aquamount (BDH chemicals) and photographed immediately.

Zebrafish embryos were prepared for cryostat sectioning by: (1) Embryos were fixed in 4% PFA overnight at 4°C. (2) Embryos were then transferred into a

solution of 30%/PBS, until the embryos sank to the bottom of the solution. (3) Embryos were then transferred into OCT compound (Gurr, BDH) and once orientated were placed on dry ice to freeze. Embedding and cryostat sectioning was performed by Malcolm Logan, The Division of Developmental Biology, NIMR.

Morpholinos

To overcome problems with morpholino (MO) design I cloned a fragment of *sall4* that spans that start codon of *sall4* in the lines I intended to inject. To clone this fragment I used RT-PCR with 40hpf whole embryo RNA with the primers: 5'-ctactagtgtcttactattcgcccctgat–3' and (2) 5'–gctacagctgtttcatctgactctgcaccg–3'. SpeI and SalI restriction enzyme sites were incorporated into the primers to aid cloning into the Bluescript pKS plasmid. I used the sequence of this clone (Fig. 5A) to design *sall4* MO 1 (sequence: 5'-GACATGGTAACCTACAACCATCAGG-3') and *sall4* MO 2 (sequence: 5-GTTTGGACTGCTTGCGCCGCGACAT-3'). To design the *sall4* splice blocking MO I also cloned a fragment of *sall4* pre-mRNA that spans the boundary between exon 1 and intron 1, using RT-PCR with whole embryo 24hpf RNA from zebrafish lines that I intended to inject. The primers used to clone this fragment are: (1) 5'-gacatgcgcatttctactcgag-3' and (2) 5'-tacaaaacttctcgaattcac-3'. XhoI and EcoRI restriction sites were incorporated into the primers to aid cloning into the Bluescript pKS plasmid. Primers were designed upon sequence alignments of my zf*sall4* clone and zebrafish genomic DNA. Using the sequence of this clone (Fig. 5B) I designed a MO that is

antisense to the boundary between exon 1 and intron 1 of *sall4* pre-mRNA: 5'-CGCTCCAAACTCACCATTTTCTGTC-3'. I also obtained a 5bp mismatch control of this MO: 5'-CGgTCgAAACTgACgATTTTCTgTC-3' (lower case letters indicate altered bases).

To test the efficiency of the *sall4* MO and control MO, RT-PCR was performed using whole embryo RNA from 20 embryos at 24hpf, using the primers 5'-tacaaaacttctcgaattcac-3', 5'-gacatgcgcatttctactcgaggg-3' and 5'-agaattccgcaaacccttgtctcctccg-3' to detect spliced and un-spliced *sall4* mRNA transcripts.

A. *sall4* MO 1 and 2 design

5′-GTCTTACTATTCGCCCCTGATGGTTGTAGGTTACC**ATGTC**GCGGCGCAAGCAGTCCAAACCACAGCATATCAATTCG
GACGACCCCGCTTCGACAGAAAATGGGATCTTGCACAATAGTCAAAGTGAAGAGGATGGCAGTGATGCTAAGAGGCGACG
ATCGGAGGAGACAAGGGTTTGCG-3′

B. *sall4* splice MO design

5′-**CGCGGCGCAAGCAGTCCAAACCACAGCATATCAATTCGGACGACCCCGCTTCGACAGAAAATGGT**GAGTTTGGAGCG
ATTAAAACTAATGTAAACTTTGTTTATGTTTCTACCTTGGAGTGATCTAGGAATCTCGCGTGCTCCCTTTTACATCTGAA
TTATGTAATTGGGCATGAATGGGTTCGCGACTCTTAAA-3′

Figure 5. *sall4* morpholino design. Sequence of the clones that were used to design morpholinos targeted against the start codon of *sall4* (A) and the exon1/intron1 boundary of *sall4* (B). (A) Bold font shows the predicted start codon of *sall4*. Underlined font shows the bases that *sall4* MO 1 is antisense to and font highlighted in yellow are the bases that *sall4* MO 2 is antisense to. (B) Bold font represents exon 1 and other font intron sequence. The underlined font highlights the bases that the *sall4* splice blocking MO is antisense to.

The sequence of the *sall1a* MO, which is antisense to the 5'UTR, is 5'-GGCTCACGCATCAGCCACGAAAGAA-3'. The *tbx5* and *fgf24* MOs 5'-GAAAGGTGTCTTCACTGTCCGCCAT-3' and 5'-GACGGCAGAACAGACATCTTGGTCA-3', respectively, have previously been described (*tbx5*: Ahn, et al., 2002 and Garrity, et al., 2002, *fgf24*: Fischer, et al., 2003).

All MOs were obtained from Gene Tools, LLC (http://www.gene-tools.com/). When the MOs were received they were re-suspended in 60µl of water (DNAse and RNAse free water, Sigma). MOs were then purified using microspin G25 columns (Amersham Bioscience) and quantified using a spectrophotometer.

The concentration and volume of morpholino to be injected and the injections procedure were performed as mentioned above (See: Zebrafish RNA injection).

Embryo staging

Zebrafish embryos were laid at 10am and this time was taken as 0hpf. Embryos were incubated at 28°C and were further staged using criteria previously established (Grandel and Schulte-Merker, 1998, and Kimmel, et al., 1995). Mouse embryos were staged according to Kaufmann, 1992, and noon on the day of vaginal plug was taken to be E0.5 days of development. Chick eggs were obtained from Winter's farm were incubated at 37°C and staged according to Hamburger and Hamilton (1951).

Mouse *Sall4* promoter cloning

I used an approximately 900bp antisense probe corresponding to a fragment of m*Sall4* exon 2 to screen high density filters, provided by MRC geneservice, that contained clones for the mouse genomic PAC library RPCI21 (Osoegawa et al., 2000). Positive clones were then obtained from MRC geneservice. I used PCR to screen these clones for a fragment that spanned from the m*Sall4* start codon to 2kb upstream. Using PCR with high fidelity Taq (BD biosciences) and primers (1) 5'–cgactagtcgtggccgcagccgcactcac-3' and (2) 5'–ctatcctgactgacgtggccg–3' I cloned this 2kb fragment into the vector bluescript pKS (Stratagene). This fragment was cloned into two vectors (pLena and pBGZA) upstream of LacZ and with or without a minimal promoter. Two transgenic embryos were created using the vector without the minimal promoter and 16 were created using the vector with the minimal promoter. The vectors were linearised and pronuclear injection was used to create transgenic mice. DNA was prepared for microinjection by (1) The plasmid was linearised (~5μg of DNA), run on a 0.8% agarose gel and then gel isolated using QIAquick gel isolation kit (Qiagen). (2) Isolated DNA (50μl) was then phenol extracted by adding 150μl H_2O and 200μl of phenol, vortexing for ~15secs and microcentrifuging for 10mins at 14,000rpm. The aqueous layer was removed (~200μl) and ethanol precipitated by adding 500μl of ethanol + 10μl 3M sodium acetate + 1μl of glycogen and storing at -20°C for 1hour to overnight. The sample was then spun at 14,000rpm for 10mins. The ethanol was removed and the pellet washed in 500μl of 70% ethanol and then re-spun at 14,000rpm for 1min. The 70% ethanol was removed and the pellet was air-dried at room

temperature. The pellet was re-suspended in 30μl of 10mM tris pH7.4 + 0.1mM EDTA. (3) The concentration of the linearised DNA was then determined using a spectrophotometer, and then diluted to a concentration of 5ng/μl. The pronuclear injection procedure was performed by Sophie Wood, Procedural Services Section, NIMR.

Sall4 gene trap mice

Mouse *Sall4* gene trap ES cell lines (RRK077 and RRP015) were identified by BLAST searches of the BayGenomics website (http://baygenomics.ucsf.edu/). *Sall4* gene trap lines were obtained from BayGenomics and these ES cells were injected into c57bl6 blastocysts. The ES cells are derived from a male mouse and carry the *agouti* coat colour gene, which is dominant over black. Chimeric mice are therefore identifiable by the presence of *agouti* coat colour. If the ES cells have contributed to the germ line (and will pass the transgene) the chimera will be male. Male chimeras were crossed with female c57bl6 females to generate heterozygous gene trap F1's, which will be *agouti*. Preparation of the ES cells for blastocyst injection was performed as described by http://baygenomics.ucsf.edu/. ES cell preparation was performed by Jo Del Buono and Malcolm Logan, The Division of Developmental Biology, NIMR. Blastocyst injection of ES cells was performed by Cynthia Akufo-Addo, The Division of Molecular Neurobiology, NIMR.

Gene trap mice were genotyped using primers targeted against LacZ, which is contained within the trap. The sequence of the primers used is: (1) 5'-

agcggcgtcagcagttgttttt-3' and (2) 5'-ggtcggcttacggcggtgattt-3'. The PCR reaction mix was: 1μl DNA + 1μl primer 1 (10pmol) + 1μl primer 2 (10pmol) + 0.5μl Taq + 10μl 5X PCR buffer + 36.5μl of water. The 5X PCR buffer is: 250μl 1M KCL + 50μl 1M tris (pH8.4)-HCL + 12.5μl 1M $MgCL_2$ + 10μl 100mM dATP +10μl 100mM dTTP + 10μl 100mM dGTP + 10μl 100mM dCTP + 85μl BSA (10mg/ml) + 562.5μl. The PCR programme was: (1) 95°C for 5mins. (2) 95°C for 30secs. (3) 61°C for 30secs. (4) 72°C for 45secs. (5) Go to 2, for 25 cycles. (5) 72°C for 5mins.

X-Gal staining of transgenic mouse embryos was performed by fixing embryos for 15mins (fixative=1% formaldehyde + 0.2% gluteraldehyde + 2mM $MgCl_2$ + 5mM EGTA + 0.02% NP-40), washing three times for 5mins in PBS/0.0.2% NP-40 and then staining for 30mins to overnight at 37°C. Embryos were then washed three times in PBS and post-fixed in 4% paraformaldehyde.

3. RESULTS

Zebrafish *sall4* cloning

To begin to understand the limb defects of OS patients I sought to identify and then clone the zebrafish homologue of *sall4*. I chose to begin my analysis of *Sall4* using zebrafish as antisense morpholino oligonucleotide (MO) can be used to easily and efficiently knockdown the translation of specific mRNAs during zebrafish development (Nasevicius and Ekker, 2000). Therefore MOs are commonly used to investigate the requirement of a given gene during embryonic development. Using the ensembl zebrafish database (www.ensembl.org/Danio_rerio/) I identified a gene predicted from ESTs that shared a high degree of similarity to human *SALL4*. I used this sequence to design PCR primers and used RT-PCR to clone the full-length cDNA of this gene. Phylogenetic comparison of the predicted amino acid sequence of this clone and other Sall genes reveals that this clone is most closely related to human and mouse *Sall4* (Fig. 6A). As with human and mouse *Sall4* the predicted amino acid sequence of this clone contains an N-terminal Cys2-His-Cys zinc finger followed by a glutamine rich domain and then a further seven Cys2-His2 zinc fingers which are arranged in a similar fashion to human *SALL4* (Fig. 6B and D). Alignments of this cDNA clone and zebrafish genomic sequence shows that, similar to human *SALL4,* zebrafish *sall4* consists of four exons. It has been suggested that during evolution a round of whole genome duplication took place in the teleost lineage, followed by the loss of some of the duplicated genes (Amores et al., 1998). Searches of ensembl and NCBI cDNA databases (http://www.ensembl.org/index.html,

http://www.ncbi.nlm.nih.gov/BLAST/), suggests that another functional copy of *sall4* does not exist. I have therefore assigned this clone as zebrafish *sall4*.

sall4 expression during zebrafish embryonic development

To begin to understand the role of *sall4* during zebrafish embryonic development, I studied the expression pattern of *sall4* using *in situ* hybridisation. *sall4* mRNA transcripts are first detectable in the mesenchyme and not the overlying ectoderm of the pectoral fin primordia at 22 hours post fertilisation (hpf) (Fig. 7A). During early pectoral fin bud stages (32hpf), *sall4* is expressed throughout the fin bud mesenchyme (Fig. 7B). As the pectoral fins mature, transcripts remain detectable throughout the mesenchyme, with highest levels at the distal tip of the fin (Fig. 7C). *sall4* is also expressed in other tissues during embryonic development. At 24hpf, transcripts are detectable in the eye, the midbrain/hindbrain junction, the pharyngeal arches, the presomitic mesoderm and posterior neural tube (Fig. 7D). This analysis shows that during zebrafish embryonic development *sall4* is expressed in the two main tissues affected in OS, namely the eye and forelimbs (pectoral fins).

sall4 is required for pectoral fin development

To investigate the function of *sall4* during pectoral fin development, I designed two different MOs that are antisense to the start codon of zebrafish *sall4* (called *sall4* MO 1 and 2). Embryos injected with these MOs were allowed to develop until 3dpf and their pectoral fins were compared with those of wild type

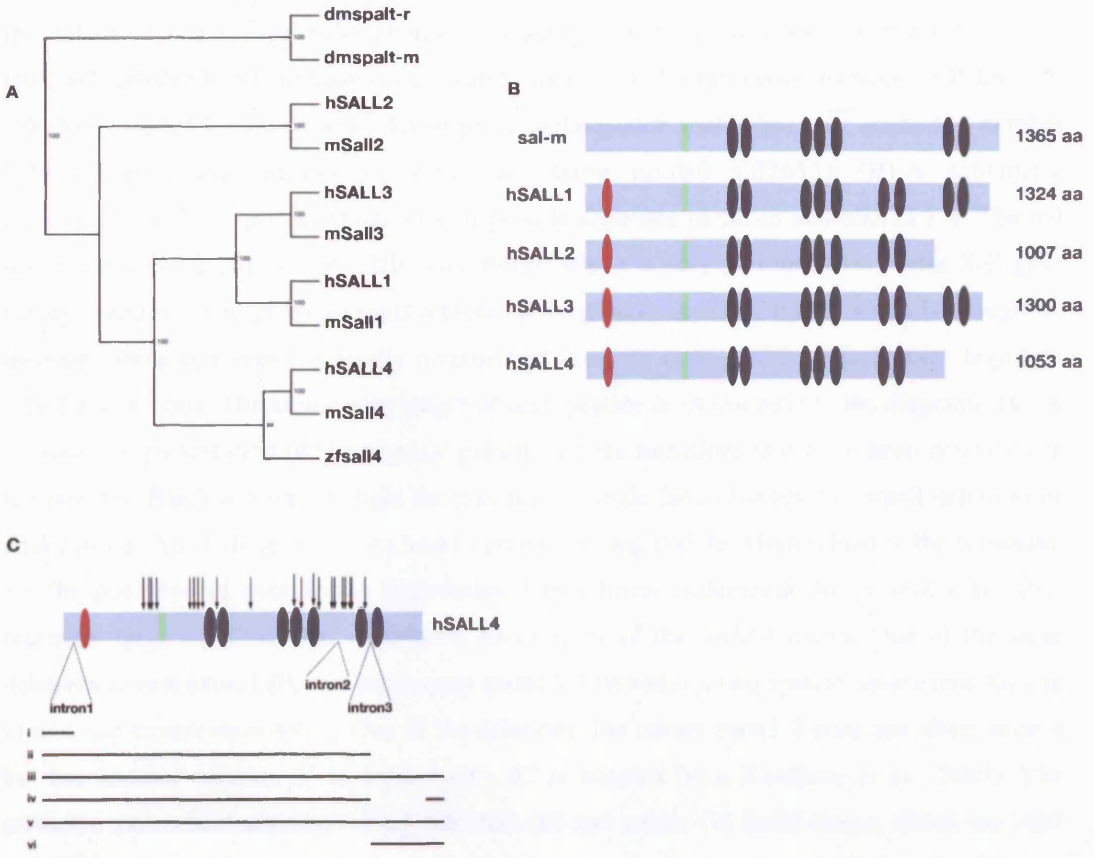

D zfsall4

MSRRKQSKPQHINSDDPASTENGILHNSQSEEEGSDAKRRRSEETRVCEKCCAEFFDEAEFLEHERNCTKSQQVVIMKDG
DGSEVPPEFSQRSPGDVLSDPCDQSTNSYSKHGAESDEMMEGEFMLNQDNPSNHDQEVSGSPGYVASSKLQDSNVTLESM
AATKVAVTQHSSNSSSQKSPPPQPHQDTLLAIPMILEQLVSLQQQQLQQIQLTEQIRIQVAMVAPPSLHAAVGAVMDPLK
ALGAHLSQQLSAAAALIGKRTGSQSLSLEALKQAKLPQSATIPTSLPGGLGSIPLKPDLKGLPDLASRLPALLPQSPGVI
GLQSPFNNLATSMDPSKKAKTKGPVVSEPPKNVSVEHSFKHKCKFCGKTFGNDSALQIHLRSHTGERPFKCNICGNRFTT
KGNLKVHFQRHKEKYPHIKMNPHPVPEHLDNMPSNNGIPYGMSVPMEENGFSETKPVLGVPTTGPPAGPHPPVLQAFKPS
FDIPAAGDPYSQRPSSSGSDGASISSGMFGQDIAGSDQSKDSPDAMVGLHHINGNSLTGENGSGTAKLQQMVDCLEKRTN
DPNECVICHRVLSCQSSLKMHYRTHTGERPYKCKICGRAFSTKGNLKAHYGVHRANTPLKMQHSCPICHKKFTNAVVLQQ
HIRMHMGGQIPNTPLPENQFESPEALDSSMTEDKTIDSNGHEESMEEQDFELDNQEKLNYSTGPQPVTKDDQTFPGQPSM
FTGITALENHMKNLTSALNLQRQSSTASESDSGLKDSPLGSGEVDYKNDRSPVVSDSVSFHSLSPIDGPPSNGPSKSPES
TNLDDSVKSRPDTDAPQDFSENNGALDLTSSFTSKPIKEEPGLSFASGEYGSSQLPFMRVPPSLVKLEMQIPPETPMGAH
GLYSSQLPQGAATPPASSSAPRRSTKQHLCNMCGKNFSSASALQIHERTHTGEKPFACSICGRAFTTKGNLKVHVGTHMW
NNTARRGQRLSLDNPMALMAMGNEPKMMPDMLPPPKDLIPPPINFDPSMWNQYAAAFTNGLTMKTNEISVIQNGGIPLPG
SLGGPLVGSTGGITKMESSQMGIPGTVAEMEKNGSESIAKFPHFMEEGKVN.

E mSall4

MSRRKQAKPQHINWEEGQGEQPQQLPSPDLAEALAAEEPGAPVNSPGNCDEASEDSIPVKRPRREDTHICNKCCAEFFSL
SEFMEHKKSCTKTPPVLIMNDSEGPVPSEDFSRAALSHQLGSPSNKDSLQENGSSSGDLKKLGTDSILYLKTEATQPSTP
QDISYLPKGKVANTNVTLQALRGTKVAVNQRGAEAPMAPMPAAQGIPWVLEQILCLQQQQLQQIQLTEQIRVQVNMWAAH
ALHSGVAGADTLKALSSHVSQQVSVSQQVSAAVALLSQKASNPALSLDALKQAKLPHASVPSAASPLSSGLTSFTLKPDG
TRVLPNFVSRLPSALLPQTPGSVLLQSPFSAVTLDQSKKGKGKPQNLSASASVLDVKAKDEVVLGKHKCRYCPKVFGTDS
SLQIHLRSHTGERPYVCPICGHRFTTKGNLKVHLQRHPEVKANPQLLAEFQDKGAVSAASHYALPVPVPADESSLSVDAE
PVPVTGTPSLGLPQKLTSGPNSRDLMGGSLPNDMQPGPSPESEAGLPLLGVGMIHNPPKAGGFQGTGAPESGSETLKLQQ
LVENIDKATTDPNECLICHRVLSCQSSLKMHYRTHTGERPFQCKICGRAFSTKGNLKTHLGVHRTNTTVKTQHSCPICQK
KFTNAVMLQQHIRMHMGGQIPNTPLPESPCDFTAPEPVAVSENGSASGVCQDDAAEGMEAEEVCSQDVPSGPSTVSLPVP
SAHLASPSLGFSVLASLDTQGKGALPALALQRQSSRENSSLEGGDTGPANDSSLLVGDQECQSRSPDATETMCYQAVSPA
NSQAGSVKSRSPEGHKAEGVESCRVDTEGRTSLPPTFIRAQPTFVKVEVPGTFMGPPSMPSGMPPLLASQPQPRRQAKQH
CCTRCGKNFSSASALQIHERTHTGEKPFVCNICGRAFTTKGNLKVHYMTHGANNNSARRGRKLAIENPMVALSAEGKRAP
EVFSKELLSPAVSVDPASWNQYTSVLNGGLAMKTNEISVIQSGGIPTLPVSLGASSVVSNGTISKLDGSQTGVSMPMSGN
GEKLAVPDGMAKHQFPHFLEENKIAVS.

Figure 6. Phylogenetic comparison of the predicted amino acid sequence of Sall gene family members. (A) Neighbour – joining analysis, using ClustalX (Thompson et al., 1994), of my zebrafish and mouse *Sall4* clones with human *SALL1-4* (accession numbers: Q9NSC2, Q9Y467, Q9BXA9, NP_065169 respectively) , mouse *Sall1-3* (accession numbers: NP_067365, Q9QX96, Q62255 respectively), Drosophila melangastor *spalt* (dm*spalt*, accession number X75541) and *spalt-related* (dm*spaltr*, accession number Y07653). (B) A schematic representation of the predicted amino acid peptide sequence of sal-m and hSALL1-4. The red disc represents the N-terminal C2HC zinc finger, which is only present in vertebrate Sall gene family members. The green sections represents the glutamine rich domain which is thought to mediate interaction between family members (Sweetman et al., 2003). Black discs highlight C2H2 zinc fingers. The amino acid length of each peptide is shown next to the diagrams. (C) A schematic representation of the h*SALL4* protein and the mutations that have been described in OS patients. Black arrows highlight the position of single base changes and small deletions or duplications. All of these mutations lead to premature stop codons. Highlighted in the schematic are the positions of exon/intron boundaries. Black lines, underneath the protein schematic, represent large deletions that encompass all or some of the *SALL4* exons. One of the large deletions covers exon 1 (i), two encompass exons 1-3 (ii and iv), two span all four exons (iii and v) and one covers exon 4 (vi). One of the deletions that covers exon1-3 does not affect exon 4 but has another deletion 3' to exon 4 (iv). (C is adapted from Kohlhase et al., 2005). The predicted amino acid sequence of my zebrafish (D) and mouse (E) *Sall4* clones, which are 1067 and 1091 amino acids, respectively. Amino acids in green represent the glutamine rich domain. Other bold font highlights the zinc fingers, with Cys and His amino acids, which are essential to the zinc finger structure, in red.

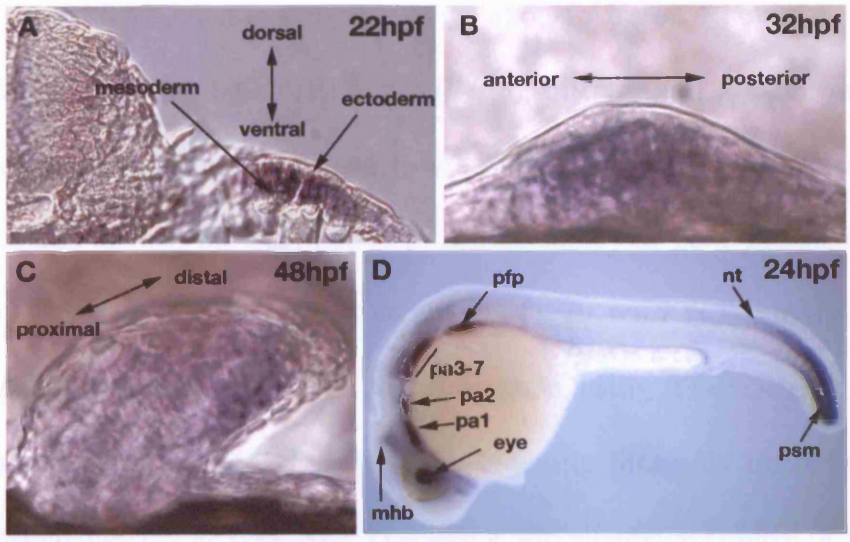

Figure 7. Analysis of zebrafish *sall4* expression. (A) Using whole mount *in situ* hybridisation *sall4* transcripts are first detectable in the mesenchyme of the pectoral fin primordia at 22hpf. (B) At early time points in pectoral fin development (32hpf) *sall4* is expressed throughout the fin bud mesenchyme. (C) Later in development (48hpf) *sall4* continues to be expressed throughout the fin bud mesenchyme but appears greatest levels in the distal fin bud. (D) At 24hpf, as well as being expressed in the pectoral fin primordia (pfp), *sall4* transcripts are detectable in the eye, midbrain hindbrain boundary (mhb), presomitic mesoderm (psm), the posterior neural tube (nt) and pharyngeal arches (pa1-7).

embryos. I observed no differences in the pectoral fins of wild type embryos and those injected with 5ng of either *sall4* MO 1 or 2 (100%, n=136 and 264 respectively). This may suggest that these MOs do not efficiently knockdown *sall4* mRNA translation.

I also obtained a MO that is antisense to the exon 1 / intron 1 boundary of *sall4* and is designed to inhibit splicing of *sall4* pre-mRNA and knockdown *sall4* function (Fig. 8A). Using such a splice-blocking MO is more advantageous than those targeted against the start codon as the efficiency of gene knockdown can be tested using RT-PCR (Draper et al., 2001). In wild type embryos, both spliced and unspliced *sall4* mRNA was detectable, using RT-PCR (Fig. 8B). In embryos injected with 5ng of *sall4* splice blocking MO only unspliced *sall4* transcripts are detectable (Fig. 8B). I created a 5bp mismatch control of the *sall4* MO to test the specificity of splice blocking. I observed no inhibition of *sall4* mRNA transcript splicing in embryos injected with 5ng of the control MO (Fig. 8B). This demonstrates that the *sall4* splice blocking MO can efficiently inhibit splicing of *sall4* pre-mRNA and subsequently knockdown *sall4* function. I therefore continued my analysis of the function of *sall4* during pectoral fin development using only the *sall4* splice blocking MO, which I will now refer to simply as the *sall4* MO.

I allowed embryos injected with the *sall4* MO to develop until 3 days post fertilisation (dpf) and compared their pectoral fins with those of wild type embryos. *sall4* morphants have a range of pectoral fin defects, from a complete absence of both pectoral fins to those that develop to approximately wild-type

size but are positioned perpendicular to the body (Fig. 8D-G). Injection of higher concentrations of *sall4* MO results in an increase in the severity of pectoral fin defects (Fig. 8, table). All embryos injected with 5ng of the mismatch control MO are apparently wild type at 3dpf (100%, n=64). Some *sall4* morphant embryos have pectoral fins that turn rostrally, towards the head of the embryo (Fig. 8F). Significantly I, and others (Garrity et al., 2002), have observed a similar pectoral fin phenotype when embryos are injected with low concentrations of a *tbx5* MO (Fig. 8H).

I stained 5dpf *sall4* morphant embryos with alcian blue to study the individual elements that have been disrupted in the affected pectoral fins. At 5dpf wild-type zebrafish pectoral fins consists of a scapulocoracoid, postcoracoid process, endoskeletal disc and actinotrichs (Fig. 8I, Grandel and Schulte-Merker, 1998). During the third week in development these larval pectoral fins are remodelled to form the adult pectoral fin. The scapulocoracoid and postcoracoid process will form the scapula, while the endoskeletal disc will form the proximal radials which articulate the lepidotrichia (fin rays), which form from the actinotrichs (Grandel and Schulte-Merker, 1998; Sordino et al., 1995). The most severely affected *sall4* morphant pectoral fins possess proximal elements such as the scapulocoracoid, and postcoracoid process (Fig. 8J). Some *sall4* morphant pectoral fins also retain a severely truncated endoskeletal disc (Fig. 8K). I also observe *sall4* morphant pectoral fins that have an endoskeletal disc that is decreased in size and less well developed in distal areas when compared to proximal areas (Fig. 8L). Any actinotrichs that form in *sall4* morphant pectoral fins are truncated and scattered when compared to wild type embryos (Fig. 8L).

These loss of function experiments demonstrate that while *sall4* is not required for the initiation of pectoral fin development, it is essential for outgrowth of the pectoral fins. These results also show that proximal pectoral fin elements such as the scapulocoracoid form independantly of *sall4* function.

Misexpression of a truncated form of *Sall4* disrupts limb development

As previously mentioned, mutations in *SALL1* that lead to a premature stop codon result in Townes-Brocks syndrome (TBS). Previously it has been suggested that these mutations lead to the expression of a truncated dominant-negative form of SALL1, which contains the N-terminal Cys2-His-Cys zinc finger, glutamine rich domain and either one or none of the Cys2-His2 zinc fingers (Botzenhart et al., 2005; Kiefer et al., 2003). Previous studies have shown that limb development is disrupted in mice that expressed a truncated, dominant negative, form of *Sall1* (Kiefer et al., 2003). Based on these observations, and as a complimentary approach to my MO experiments, I sought to misexpress a truncated form of zebrafish *sall4* (*sall4*Δ) to study the effect this has on pectoral fin development. I mapped the h*SALL4* mutation 842delG, which was described in a pedigree of OS patients (Kohlhase et al., 2002), to zebrafish *sall4*. The 842delG mutation leads to a premature stop, 8 codons 3' to the mutation. I introduced a premature stop codon into this position in zf*sall4*, which is predicted to result in the expression of a truncated sall4 protein, sall4Δ, that contains the N-terminal Cys2-His-Cys zinc finger and glutamine rich domain, but none of the seven Cys2-His2 zinc fingers (Fig. 9A). I misexpressed this truncated form of *sall4* by injecting 2-cell stage embryos with sense, *sall4*Δ

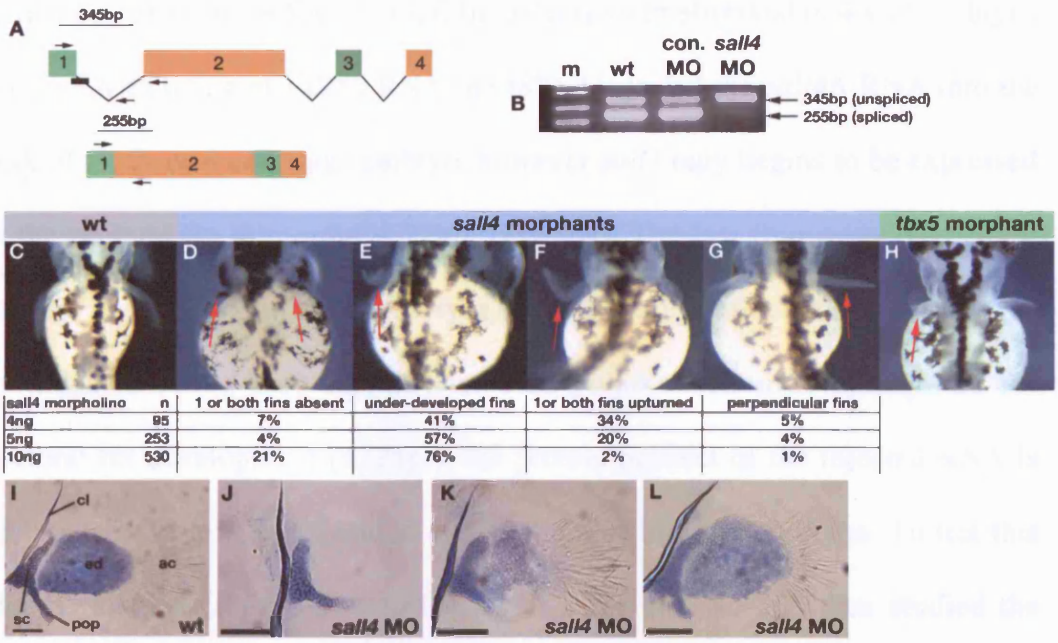

Figure 8. *sall4* is required for pectoral fin outgrowth. (A) Schematic of the RT-PCR used to test the efficiency of a *sall4* splice-blocking MO. Bands of 255bp and 345bp represent spliced and un-spliced *sall4* mRNA, respectively. Arrows represent primers used in the RT-PCR and the black box represents the *sall4* MO. (B) The RT-PCR, schematised in (A), was performed on wild type embryos and embryos injected with either 5ng of the *sall4* MO or 5ng of the mismatch control MO. Splice blocking occurs in embryos injected with the *sall4* MO and not those injected with the control MO (con. MO) (m=molecular marker). (C-H) Dorsal views of the pectoral fins of 3dpf embryos. (C) Wild type embryo. (D-G) Embryos injected with 5ng of *sall4* MO. The percentages of phenotypes observed at 3dpf following injection of different concentrations of *sall4* MO is listed below each picture. (H) The upturned pectoral fin phenotype produced following injection of 1ng of *tbx5* MO. Arrows highlight the pectoral fin defects in D-H. (I-L) 5dpf pectoral fins stained with alcian blue. (I) Wild type. (J-L) Pectoral fins of embryos injected with 4ng of *sall4* MO. cl = cleithrum, sc = scapulocoracoid, pop = postcoracoid process, ed = endoskeletal disc, ac = actinotrichs. Scale bars, which represent 75μm, are shown in the lower right corner of I-L.

RNA. Injected embryos were allowed to develop until 3dpf and their pectoral fins compared to those of wild type embryos. At 3dpf, I observed truncated (Fig.9B) and rostrally turned (Fig. 9C) pectoral fins in those embryos injected with 0.6ng of *sall4*Δ RNA. Pectoral fin defects were observed in 4% of embryos injected with 0.5ng of *sall4*Δ RNA (n=388). I injected the *sall4*Δ RNA into the yolk of 1-, 2- or 4-cell stage embryo, however *sall4* only begins to be expressed in the pectoral fin primordia at 22hpf (Fig. 7A). The low frequency of pectoral fin defects in *sall4*Δ injected embryos most probably reflects the instability of the injected RNA, such that at later time points when *sall4* is required for pectoral fin development (>22hpf), the protein product of the injected RNA is only present at low levels and in a proportion of injected embryos. To test this idea, I injected GFP RNA into the 2-cell stage embryo and then studied the levels of GFP at 24hpf. I observed that, at 24hpf, GFP was undetectable in 58% of embryos injected at the 2-cell stage (n=98) (Fig. 9E-F). In the remaining GFP positive embryos, 18% displayed strong GFP expression (Fig. 9E), whereas the remaining 24% had weaker GFP expression. These observations support the idea that the protein product of RNA injected at the 2-cell stage is only present in a proportion of embryos at times when *sall4* is required for pectoral fin development (>22hpf).

I also used avian retroviruses (based upon the RCASBP(A) construct, which is referred to as RCAS) to misexpress m*Sall4*Δ in the developing chick forelimb. Using a similar approach to that used in zebrafish, I mapped the premature stop codon of the mutation 842delG, which is found in OS patients, to mouse *Sall4* and cloned this into the RCAS backbone (See Materials and Methods). This

Sall4Δ construct was used to produce retroviral supernatants. Injection of these supernatants into the limb-forming region will lead to expression of a truncated Sall4 protein (Logan and Tabin, 1998). Injection of *Sall4Δ* retrovirus results in forelimbs that have decreased proximal distal length (shoulder to digits) and appear to lack anterior limb mesenchyme when compared to contra-lateral control forelimbs (Fig. 9D). This data shows that misexpression of a truncated form of *Sall4* can disrupt forelimb development in chick and zebrafish embryos, and that some of the phenotypes observed in zebrafish following misexpression of *sall4Δ* are similar to those found in *sall4* morphant embryos.

Previous studies have shown that a truncated Sall1 protein can interact with full length Sall1-4 proteins (Kiefer et al., 2003; Sweetman et al., 2003). Therefore in my misexpression experiments Sall4Δ may interfere with multiple Sall proteins, and possibly other, unknown, proteins. Also, I only observe pectoral fin defects in a minority of injected embryos. I therefore chose to continue my analysis of *Sall4* function by studying embryos injected with the *sall4* MO.

sall4 is downstream of _tbx5_, but not _fgf24_, in the pectoral fin primordia

OS and HOS patients have very similar limb phenotypes. My expression analysis of *sall4* shows that *tbx5* expression precedes *sall4* in the pectoral fin primordia (Begemann and Ingham, 2000; Ruvinsky et al., 2000). Therefore I investigated if *tbx5* is required for *sall4* expression during pectoral fin development. I used a *tbx5* MO of identical sequence to one previously demonstrated to phenocopy the ENU-induced *tbx5* mutation *heartstrings*

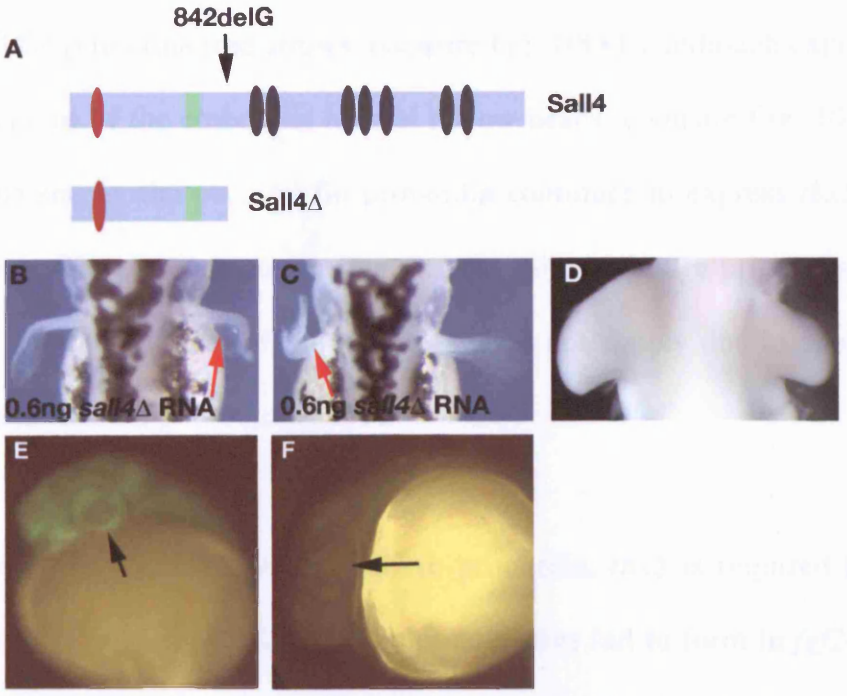

Figure 9. *Sall4*Δ misexpression disrupts forelimb development. (A) A schematic of the structure of hSALL4 protein. The red disc represents the N-terminal C2HC zinc finger and black discs highlight C2H2 zinc fingers. The green section corresponds to a glutamine rich domain that is thought to mediate interactions between Sall gene family members (Sweetman et al., 2003). The black arrow shows the position of a predicted premature stop codon that results from the mutation 842delG (Kohlhase et al., 2002). I cloned a truncated from of my zebrafish and mouse *Sall4* clones (*Sall4*Δ) in order to mimic the mutation 842delG. Red arrows highlight the truncated (B) or upturned (C) pectoral fins that I observed in 3dpf embryos injected with 0.6ng of *sall4*Δ RNA (compare B and C with Fig. 8C). (D) When m*Sall4*Δ was misexpressed in the developing chick forelimb it results in truncated limbs. The limb on the right has been injected with m*Sall4*Δ retroviral supernatants, while the limb on the left is a contra lateral, uninjected, control. (E and F) lateral views of the heads of 24hpf embryos, which were injected at the 2-cell stage with GFP RNA. Arrows highlight the developing eye. At 24hpf GFP is detectable in 42% of embryos (E) (n=98) but not in the remaining embryos (F).

(Ahn et al., 2002; Garrity et al., 2002). As previously described, I also observe that embryos injected with 5ng of *tbx5* MO have no pectoral fins at 3dpf (Fig. 10B). In *tbx5* morphant embryos, *sall4* expression is never detectable in the pectoral fin primordia (red arrows, compare Fig. 10D-E), although expression in other regions of the embryo is normal (arrow heads, compare Fig. 10D-E). At the same stages, the pectoral fin primordia continues to express *tbx5* mRNA transcripts (Fig. 10F) demonstrating that the cells of the fin primordia are still present and that the loss of *sall4* expression is not simply due to apoptosis of these cells following MO knockdown of *tbx5*.

In the mesenchyme of the pectoral fin primordia, *tbx5* is required for *fgf24* expression (Fischer et al., 2003). The pectoral fins fail to form in *fgf24* mutant embryos although the expression of *tbx5* is initiated normally (Fischer et al., 2003). *fgf24* is initially expressed in the fin bud mesenchyme and is required for the induction of *fgf10* expression at 24hpf, also within the mesenchyme (Fischer et al., 2003). As *sall4* expression begins after *fgf24* (Fig. 10A and 7A; Fischer et al., 2003) I tested the possibility that *fgf24* acts downstream of *tbx5* to initiate *sall4* expression in a linear fashion, using an *fgf24* MO demonstrated to phenocopy the *fgf24* mutant, *ikarus* (Fischer et al., 2003). Embryos injected with 6ng of *fgf24* MO have no pectoral fins at 3dpf (Fig. 10C), consistent with previously published results (Fischer et al., 2003). When *fgf24* morphant embryos were analysed at earlier stages (26hpf), *sall4* expression is maintained in the pectoral fin primordia, but in a diffuse pattern, consistent with the reported disruption of cell migration of pectoral fin progenitors following loss of *fgf24* function (Fig. 10G-H) (Fischer et al., 2003). These results demonstrate

that, although induction of *sall4* expression requires *tbx5*, it is independent of *fgf24*.

sall4 is required for FGF signalling during pectoral fin development

Zebrafish with mutations in *fgf10* lack pectoral fins demonstrating *fgf10* is required for pectoral fin development (Norton et al., 2005). As *fgf10* expression begins two hours after *sall4* in the pectoral fin primordia (Ng et al., 2002) I addressed the possibility that *sall4* is required for *fgf10* expression in the developing pectoral fins. I will now refer to embryos injected with 10ng of *sall4* MO as *sall4* morphants. In *sall4* morphant pectoral fins, *fgf10* expression initiates but is reduced when compared with wild type pectoral fins (Fig. 11A-B, reduced in 51% at 30hpf, n=35). At later fin bud stages *fgf10* expression is downregulated in anterior regions of *sall4* morphant pectoral fins (Fig. 11C-D, downregulated in 83%, n=29) demonstrating *sall4* is required for correct *fgf10* expression during pectoral fin development.

During mouse and chick limb development *Fgf10,* which is expressed in the mesenchyme, signals to the overlying ectoderm to activate the expression of *Fgf8* in cells that will form the apical ectodermal ridge (AER). In turn, Fgf8 positively regulates the expression of *Fgf10* in the mesenchyme thereby establishing a positive feedback – loop in which ectodermal and mesenchymal FGFs maintain one another's expression. This loop is essential for limb outgrowth (See Introduction). I therefore predicted that the downregulation of *fgf10* in the mesenchyme of *sall4* morphant pectoral fin buds would lead to the

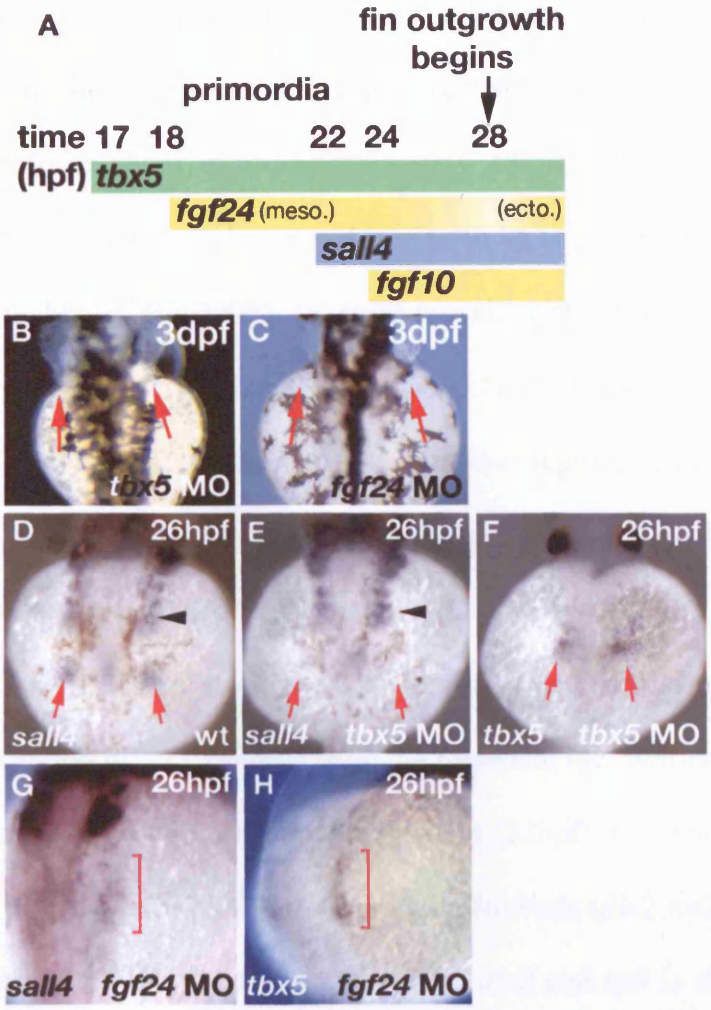

Figure 10. The expression of *sall4* in the pectoral fins is regulated by *tbx5* but not *fgf24*. (A) Schematic representation of *tbx5*, *fgf24*, *sall4* and *fgf10* expression during early stages of pectoral fin development. Expression of *tbx5* initiates at 17hpf, *fgf24* at 18hpf, *sall4* at 22hpf and *fgf10* at 24hpf. The genes are all initially expressed throughout the mesenchyme of the pectoral fin primordia. At the time fin bud outgrowth is initiated, *fgf24* expression becomes downregulated in the mesenchyme and simultaneously upregulated in the overlying ectoderm. Dorsal (B-F) and dorsal lateral (G and H) views of embryos, with red arrows and bars highlighting the pectoral fin primordia. At 3dpf the pectoral fins are absent in embryos injected with 4ng of *tbx5* MO (B) and 6ng of *fgf24* MO (C). *sall4* is expressed in wild type pectoral fin primordia at 26hpf (D), but it is absent in the primordia of embryos injected with 4ng of *tbx5* MO (E). While *sall4* expression is absent in the pectoral fin primordia it continues to be expressed normally in other regions of *tbx5* morphant embryos (arrow heads in D and E). (F) *tbx5* expression in an embryo injected with 4ng of *tbx5* MO at 26hpf. (G) *sall4* is still expressed in the pectoral fin primordia of embryos injected with 9ng of *fgf24* MO although the domain of expression is more dispersed, consistent with a loss of *fgf24* function. This expression pattern is similar to that of *tbx5* in embryos injected with 9ng of *fgf24* MO (H).

downregulation of ectodermal FGFs and a breakdown in FGF signalling in the fin bud. During normal pectoral fin development *fgf24* is expressed in the mesenchyme from 18hpf until approximately 28hpf when it then becomes downregulated in the mesenchyme and begins to be expressed in the overlying ectoderm (Fischer et al., 2003). In *sall4* morphant embryos expression of ectodermal *fgf24* is downregulated (36%, n=28) or often absent (36%) from the fin ectoderm at 40hpf but remains wild type in other regions of the embryo (Fig. 11E-F, and data not shown). I also studied the expression of *dlx2* and *sp9,* two genes that are also expressed in fin bud ectoderm (Fig. 11G and 11I), in *sall4* morphant embryos. In the developing pectoral fins the expression of *dlx2* and *sp9* is dependant on *fgf10* signalling from the mesenchyme (Norton et al., 2005). At early time points in pectoral fin development (32hpf) *dlx2* and *sp9* are both expressed in the ectoderm of all *sall4* morphant fin buds (*dlx2* n=24; *sp9* n=10). At later time points (40hpf) expression of both *dlx2* and *sp9* is downregulated (*dlx2*: 75% n=16; *sp9*: 58% n=12) or absent (*dlx2* 25%; *sp9* 25%) in *sall4* morphant fin buds. In those *sall4* morphant fin buds in which *dlx2* and *sp9* expression is downregulated, I observed that while transcripts remain detectable in the posterior fin bud ectoderm they are absent from the anterior (Fig. 11G-J). The transcription factor *erm* is expressed throughout the fin bud mesenchyme and its expression is positively regulated by FGF signalling (Fischer et al., 2003; Roehl and Nusslein-Volhard, 2001). In *sall4* morphant pectoral fins, *erm* expression is normal initially but is downregulated at more mature fin bud stages (Fig. 11K-L) while remaining normal in other regions of the embryo. These results show that *sall4* is required for *fgf10* expression in the

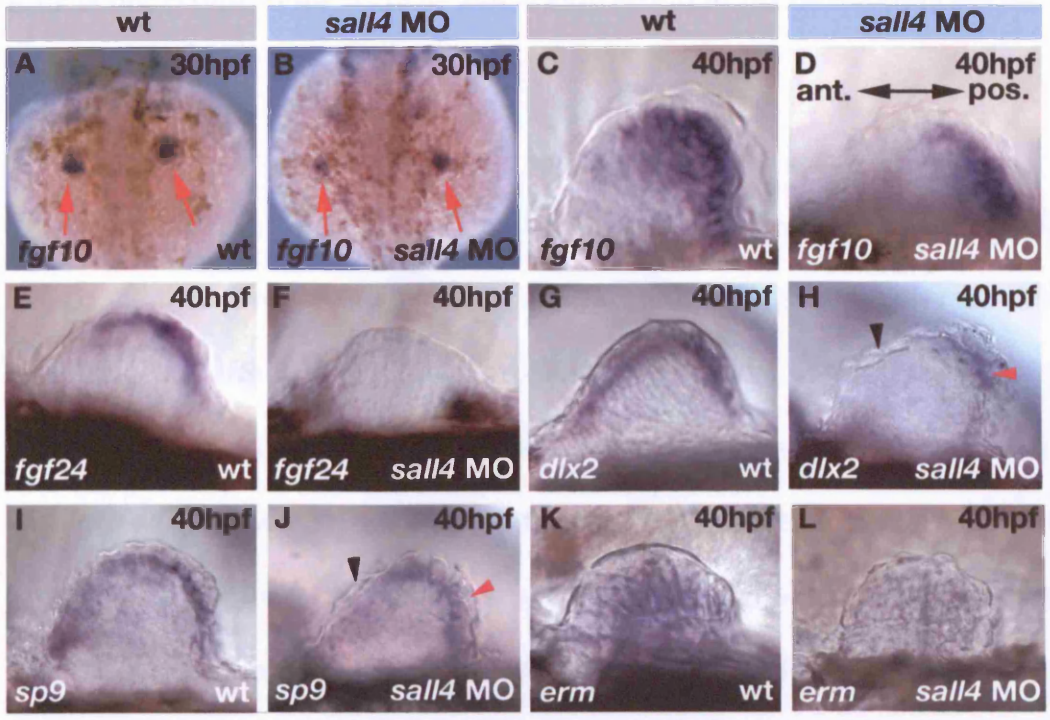

Figure 11. *sall4* is required for FGF signalling in the developing pectoral fins. Comparison of gene expression patterns in wild type (A, C, E, G, I, K) and *sall4* morphant pectoral fins (B, D, F, H, J, L). *fgf10* expression in the pectoral fins at 30hpf (A) is reduced in *sall4* morphant embryos (B), as highlighted by the red arrows. *fgf10* expression at 40hpf (C) is reduced in *sall4* morphant pectoral fins (D). This reduction is most pronounced in the anterior fin bud. At 40hpf *fgf24* is only detected in the ectoderm (E) but is absent in *sall4* morphant fin buds (F). *dlx2* is expressed in the fin bud ectoderm at 40hpf (G). In *sall4* morphant embryos *dlx2* expression is absent in the anterior fin bud ectoderm (black arrow, H) but retained in the posterior (red arrow). *sp9,* which is also expressed in the fin bud ectoderm at 40hpf (I), is downregulated in the anterior ectoderm of *sall4* morphant fin buds (black arrow, J) but retained in the posterior (red arrow). *erm* is expressed in wild type pectoral fins (K) but is reduced in *sall4* morphant pectoral fins (L).

developing pectoral fins and the loss of *fgf10* expression in *sall4* morphant pectoral fins results in a breakdown in FGF signalling in the fin bud.

sall4 is not required for *tcf3b* or *wnt5a* expression in the developing pectoral fins

Previous studies have implicated Sall genes in Wnt signalling (Onai et al., 2004), and therefore I wanted to see if the expression of genes involved in Wnt signalling are affected in *sall4* morphant pectoral fins. The gene *XsalF* is required for the expression of *Tcf3*, which acts to antagonise Wnt signalling during *Xenopus* forebrain/midbrain formation (Onai et al., 2004). *tcf3b* is expressed in the mesenchyme of the developing zebrafish pectoral fins (Fig. 12A). To determine if *sall4* in the zebrafish pectoral fins performs similar functions to *XsalF* in the forebrain/midbrain, I studied the expression of *tcf3b* in *sall4* morphant pectoral fins. No alterations in *tcf3b* expression were seen in the pectoral fin buds of embryos injected with the *sall4* MO (Fig. 12A-B). I also studied the expression of *wnt5a* in *sall4* morphant pectoral fins, as *Wnt5a* is required for forelimb and hindlimb formation during mouse embryonic development (Yamaguchi et al., 1999). I observed no effect on *wnt5a* expression in the pectoral fin buds of *sall4* morphant embryos (Fig. 12C-D). These results demonstrate that during pectoral fin development *sall4* is not required for the expression of *wnt5a* or *tcf3b*.

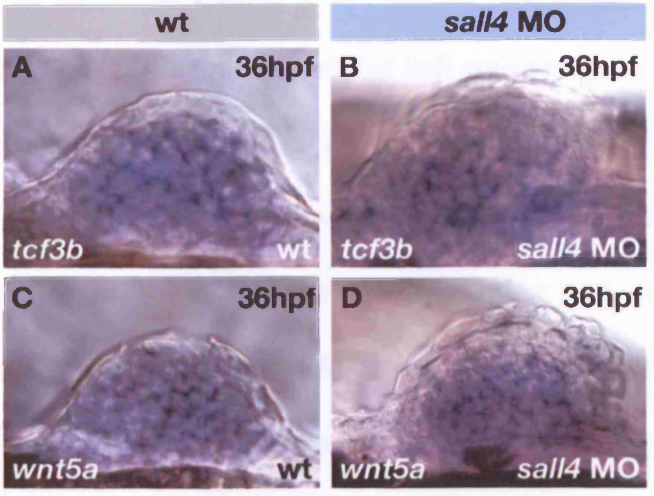

Figure 12. *tcf3b* and *wnt5a* expression is unaffected in *sall4* morphant pectoral fins. Lateral views of the pectoral fins of 36hpf wild type embryos (A and C), and embryos injected with 10ng of *sall4* MO (B and D). The expression of *tcf3b* (B) and *wnt5a* is not affected in *sall4* morphant embryos (D).

sall1a is expressed in the developing pectoral fins

During mouse limb development Sall genes are expressed in overlapping domains and individual loss of *Sall1* or *Sall3* does not affect limb development (See Introduction, section, Sall gene function) (Koshiba-Takeuchi et al., 2005; Nishinakamura et al., 2001; Parrish et al., 2004). This suggests that *Sall1* and *Sall3* may have redundant functions and that Sall genes may compensate for the loss of one another during mouse limb development. In *sall4* morphant embryos, *fgf10* expression is only downregulated in the anterior fin bud (Fig. 11D) suggesting that another sall gene family member may perform a similar function to *sall4* in the posterior fin bud. The expression patterns of *sall1a, sall1b* and *sall3* during zebrafish embryonic development have previously been described (Camp et al., 2003). Of these three genes, only *sall1a* is expressed during pectoral fin development (Camp et al., 2003). I therefore performed a detailed analysis of *sall1a* expression during pectoral fin development. *sall1a* is weakly expressed in the pectoral fin primordia at 24hpf and becomes more visible at 26hpf (Fig. 13A). At later fin bud stages, *sall1a* expression is seen in both the mesenchyme and ectoderm (Fig. 13B). This expression pattern is comparable to that of mouse and chick *Sall1* during limb development (Buck et al., 2001; Farrell and Munsterberg, 2000).

sall1a is required for pectoral fin development

To address whether *sall1a* plays a role in pectoral fin development, I used a MO to knockdown *sall1a* mRNA translation and compared the pectoral fins of 3dpf

sall1a morphants with those of wild type embryos. Embryos injected with the *sall1a* MO have truncated and often absent pectoral fins, demonstrating *sall1a* is required for pectoral fin outgrowth (Fig 13C and table, compare picture with Fig. 8C). *sall1a* morphant pectoral fin defects differ from those of *sall4* morphants, as I never observe upturned pectoral fins in *sall1a* morphants. (table, Fig. 13). I stained 5dpf embryos injected with 2ng of *sall1a* MO to study their pectoral fin defects in greater detail. Proximal skeletal elements such as the postcoracoid process always form in *sall1a* morphant embryos (Fig 13D). I also observed *sall1a* morphant pectoral fins that have small endoskeletal discs and only a few actinotrichs, which also appear scattered (Fig 13E). The *sall1a* morphant pectoral fin defects observed are similar to those seen in embryos injected with the *sall4* MO.

The expression of *sall1a* in the developing pectoral fins is dependant on *tbx5* but not *fgf24*

To understand the regulation of *sall1a* expression during pectoral fin development, and to compare it with that of *sall4,* I studied *sall1a* expression in *tbx5* and *fgf24* morphant embryos. *sall1a* is not expressed in the pectoral fin primordia of *tbx5* morphant embryos (Fig. 13G), but is expressed in a diffuse pattern in the primordia of *fgf24* morphant embryos (Fig. 13H-I). This demonstrates that, similar to *sall4*, the expression of *sall1a* in the pectoral fin primordia is dependant on *tbx5* but not *fgf24*.

sall gene family members have redundant functions during pectoral fin development

Since *sall1a* could be responsible for the maintenance of the posterior domain of *fgf10* expression in the pectoral fin bud of *sall4* morphants, I studied *fgf10* expression in embryos injected with 5ng of the *sall1a* MO. *fgf10* expression initiates in *sall1a* morphant pectoral fin primordia but at reduced levels compared with wild-type embryos (Fig. 13J-K). At later fin bud stages, *fgf10* expression is downregulated but most profoundly in the posterior of *sall1a* morphant fin buds (compare Fig. 13F and 11C). I also studied the expression of the ectodermal fin bud markers *dlx2* and *sp9* in embryos injected with 5ng of *sall1a* MO. *dlx2* and *sp9* expression in the fin bud ectoderm is dependant on *fgf10* signalling from the fin bud mesenchyme (Norton et al., 2005). At 32hpf *sp9* is expressed in all *sall1a* morphant fin buds (n=24) but is downregulated in the posterior ectoderm, while continuing to be expressed in the anterior (compare Fig. 13L and Fig. 14C). *dlx2* is also expressed in all *sall1a* morphant fin buds at 32hpf (n=25), but at 40hpf becomes downregulated (37%) or is absent (63%). In those embryos displaying a downregulation of *dlx2* expression, transcripts are detectable in the anterior fin bud ectoderm but are absent in the posterior (Fig. 13M, compare with Fig. 11G). This expression pattern is complementary to that observed in *sall4* morphant pectoral fins.

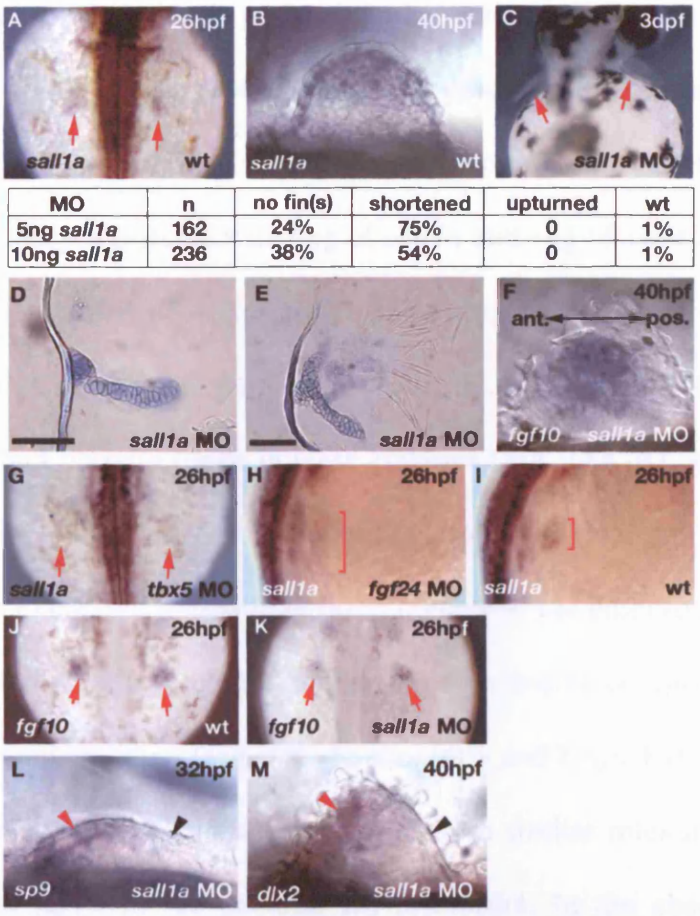

MO	n	no fin(s)	shortened	upturned	wt
5ng *sall1a*	162	24%	75%	0	1%
10ng *sall1a*	236	38%	54%	0	1%

Figure 13. *sall1a* is essential for pectoral fin development. *sall1a* expression during wild type pectoral fin development. (A) Dorsal view of a 26hpf embryo with red arrows pointing to the pectoral fin primordia. (B) Lateral view of a 40hpf pectoral fin showing *sall1a* expression in the fin bud. (C) Dorsal view of a 3dpf embryo injected with 5ng of *sall1a* MO. The pectoral fins are truncated as highlighted by red arrows (compare with wild type in Fig. 8C). The percentages of phenotypes observed at 3dpf following injection of 5ng and 10ng of *sall1a* MO are shown in the table. (D-E) Alcian blue stained pectoral fins of 5dpf embryos injected with 2ng of *sall1a* MO show that pectoral fin development is disrupted in *sall1a* morphant embryos (Compare with wild type pectoral fin in Fig. 8I). (F) A lateral view of *fgf10* expression at 40hpf in an embryo injected with 5ng of *sall1a* MO. The expression of *fgf10* is most profoundly affected in the posterior fin bud (compare with Fig. 11C). *sall1a* is not expressed in the pectoral fin primordia of embryos injected with 4ng of *tbx5* MO (G). Dorsolateral views show that *sall1a* continues to be expressed in the pectoral fin primordia of embryos injected 9ng of *fgf24* MO (H), but in a diffuse pattern when compared with the expression of *sall1a* in wild type primordia (I). Dorsal views of *fgf10* expression at 26hpf in the fin primordia (as indicated with red arrows) of a wild type embryo (J) and an embryo injected with 5ng of *sall1a* MO (K). Expression of the ectodermal fin bud markers *sp9* (L) and *dlx2* (M) are downregulated in the posterior fin bud ectoderm of embryos injected with 5ng of *sall1a* MO (black arrowheads) but continue to be expressed in the anterior fin bud (red arrowheads, compare L with wild type expression in Fig 14C, and M with Fig. 11G).

As *sall1a* and *sall4* appear to perform similar roles in positively regulating the expression of *fgf10* during pectoral fin development, I studied the phenotype of *sall1a/sall4* double morphant embryos. The pectoral fins fail to form in the majority of embryos injected with 4ng of *sall1a* and 4ng of *sall4* MO (table Fig. 14). Staining sections of 48hpf *sall1a/sall4* double morphant embryos with methylene blue shows that, similar to *fgf10* mutant zebrafish (Norton et al., 2005), a fin bud initially forms in these embryos (Fig. 14A-B). At 26hpf, *fgf10* expression is lost in *sall1a/sall4* double morphant pectoral fin primordia although it is expressed normally in other regions of the embryo (Fig. 14G). At 32hpf, *dlx2* and *sp9* expression is absent in the fin bud ectoderm of *sall1a/sall4* double morphant embryos (Fig. 14C-F; *dlx2* 90% n=52; *sp9* 81% n=27). These results demonstrate that *sall1a* and *sall4* perform similar roles in initiating the expression of *fgf10* in the pectoral fin primordia. In the absence of *sall4* function, *sall1a* is able to maintain the posterior domain of *fgf10* expression and similarly, following knockdown of *sall1a* function, *sall4* can maintain the anterior domain of *fgf10* expression.

sall1a and *sall4* are required for the expression of *fgfr2* in the developing pectoral fins

In the developing pectoral fins *fgf10* expression is dependant on *sall1a, sall4* (Fig. 14G) and *fgf24* (Fischer et al., 2003). This raises the question of how both *fgf24* and *sall1a/sall4* regulate *fgf10* expression. For *fgf24* to activate the expression of *fgf10* it must signal via an FGF receptor. I therefore investigated if the expression of an FGF receptor is regulated by *sall1a* and *sall4*. As *fgf10* expression initiates in the pectoral fins of *sall1a* (Fig. 13K) or *sall4* (Fig. 11B)

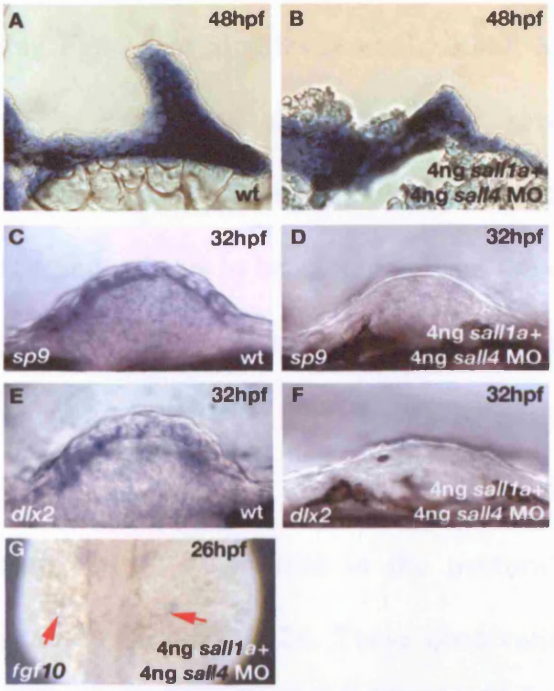

4ng *sall1a*+	n	no fin(s)	shortened	upturned	wt
4ng *sall4* MO	64	77%	23%	0	0

Figure 14. Pectoral fin development is severely disrupted in *sall1a/sall4* double morphant embryos. As shown in the table, co-injection of *sall1a* and *sall4* MOs leads to a significant increase in the most severe phenotype (no fins, compare with tables in Fig. 13 and 8). Methylene blue stained sections of the pectoral fin forming region in a wild type embryo (A) and an embryo injected with 4ng *sall1a* + 4ng *sall4* MO (B) at 48hpf shows that a fin bud initially forms in *sall1a/sall4* double morphant embryos. (C-F) Lateral views of 32hpf pectoral fin buds in wild type embryos (C and E) and embryos injected with 4ng of *sall1a* + 4ng of *sall4* MO (D and F). At this time point *sp9* is expressed in the ectoderm of wild type fin buds (C) but is absent in *sall1a/sall4* double morphant fin buds (D). Likewise, *dlx2* is present in wild type fin bud ectoderm (E) but is absent in *sall1a/sall4* double morphant fins (F). At 26hpf *fgf10* expression fails to initiate in the pectoral fin primordia of *sall1a/sall4* double morphant embryos (compare with wild type in Fig. 13J).

morphant embryos, but does not in those embryos injected with both *sall1a* and *sall4* MO (Fig. 14G), I predicted that expression of this receptor will not initiate in embryos injected with both *sall1a* and *sall4* MO. Limb outgrowth fails to occur in mice lacking *Fgfr2* (De Moerlooze et al., 2000; Xu et al., 1998) and therefore I studied the expression of *fgfr2* during zebrafish embryonic development. *fgfr2* expression is first detectable in the pectoral fin primordia mesenchyme at 23hpf and appears to be excluded from the overlying ectoderm (Fig. 15A). At 24hpf *fgfr2* is expressed in the pectoral fin primordia of wild type (Fig. 15B) and *fgf24* morphant (Fig. 15D) embryos, but is absent from the pectoral fins of embryos injected with both *sall1a* and *sall4* MO (Fig. 15C). This demonstrates that *fgfr2* expression in the pectoral fin primordia is dependant on *sall1a/sall4,* but not *fgf24*. These observations provide a link between *fgf24* and *sall1a/sall4,* and the induction of *fgf10* expression in the pectoral fin primordia.

Collectively my results have enabled me to develop a model of the genetic network that is required to establish FGF signalling in the pectoral fin bud (Fig. 15E). In this model *tbx5* initiates the expression of two sets of target genes – *sall1a/sall4* and *fgf24* – independently. *tbx5, fgf24* and *sall1a/sall4* are required for the expression of *fgf10* in the fin bud mesenchyme. fgf10 then signals to the overlying ectoderm, where it is required for the expression of *dlx2, sp9* and *fgf24*. The function and dynamics of this model will be discussed in depth in the Discussion section.

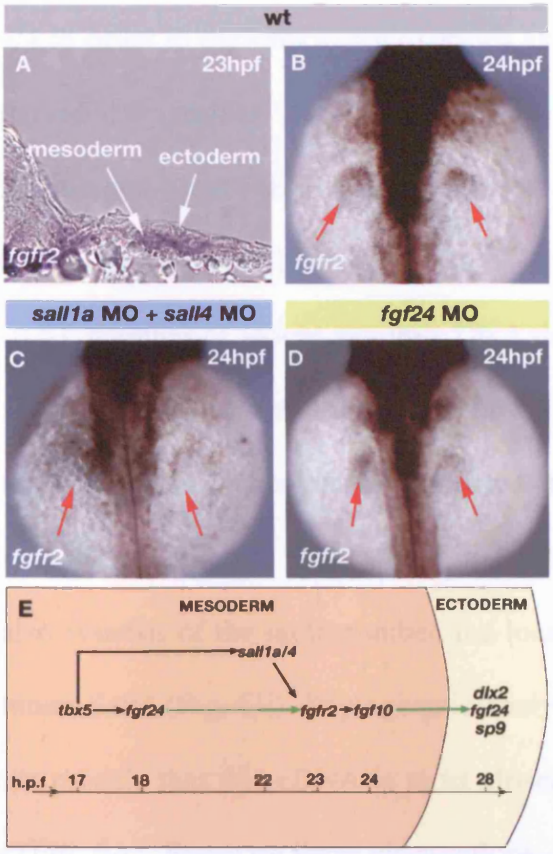

Figure 15. *sall1a* and *sall4* are required for *fgfr2* expression in the pectoral fin primordia. A Section of a 23hpf embryo shows that *fgfr2* is expressed in the pectoral fin primordia mesenchyme but is excluded from the ectoderm (A). Dorsal views highlight *fgfr2* expression in a wild type embryo at 24hpf (B). At the same time point *fgfr2* expression is absent in the pectoral fin primordia of embryos injected with 4ng *sall1a* MO plus 4ng *sall4* MO (C), but continues to be expressed in the primordia of embryos injected with 9ng of *fgf24* MO (D). At this time point *fgfr2* is also downregulated in the trunk of *sall1a/sall4* double morphant embryos (C and data not shown). The red arrows highlight the pectoral fin primordia in B-D. (E) A schematic representation of the regulatory relationships between genes required for pectoral fin development. Green arrows signify relationships between FGF receptors and ligands while black arrows represent transcriptional regulatory relationships.

Isolation of mouse *Sall4*

I cloned mouse *Sall4* in order to perform a cross-species expression analysis of *Sall4*. I identified a mouse cDNA in the NCBI database (http://www.ncbi.nlm.nih.gov/) that shared a high degree of similarity to human *SALL4*. As this mouse cDNA was not publicly available, I isolated this cDNA using RT-PCR. BLAST searches of mouse genomic DNA demonstrates that the genomic location of this cDNA is chromosome 2, and this region is syntenic to a section of chromosome 20 where human *SALL4* is located. The predicted amino acid sequence of this cDNA clone is comparable in length to zebrafish and human *Sall4*, and also consists of the same number and location of zinc fingers as zebrafish and human *Sall4* (Fig. 6E). Phylogenetic analysis of the predicted amino acid sequence reveals that this cDNA is most closely related to human and zebrafish *Sall4* (Fig. 6A). Based on these observations, I have assigned this clone mouse *Sall4*.

Embryonic expression analysis of mouse *Sall4*

To begin to understand the potential roles of *Sall4* during mouse embryonic development, I studied its mRNA expression pattern using *in situ* hybridisation. As the focus of this study is to understand the role of *Sall4* in limb development, I selected a range of embryonic stages from pre-limb formation to more mature limb bud stages. At E8.5, just prior to beginning of limb development, *Sall4* is expressed in the segmental plate and within the rhombomeres (Fig. 16A). At E9.5, *Sall4* transcripts are detectable throughout the forelimb buds (Fig. 16B),

and at later stages is predominantly expressed in the distal limb bud (Fig. 16D). *Sall4* is expressed in both the forelimb and hindlimb buds and appears to be restricted to the limb bud mesenchyme and is not expressed in the apical ectodermal ridge (AER) (Fig. 16D-E). *Sall4* transcripts are also detectable within the developing eye (Fig. 16C), the somites and the hindgut (Fig. 16D). This demonstrates the spatial expression pattern of *Sall4* in the developing limbs, and other regions of the developing embryo, has been conserved from zebrafish to mouse. It also shows that similar to zebrafish *sall4,* mouse *Sall4* is expressed in the developing eye and forelimbs, which are to two main structures affected in OS.

Gene hierarchies during mouse forelimb development

Investigating how *Sall4* may integrate into the signalling cascade that controls mouse limb development, and comparing this with zebrafish pectoral fin development, will enhance our understanding of *Sall4* function. Therefore, I carried out a detailed comparative expression analysis of *Sall4* and three genes essential to mouse forelimb development. Using somite numbers to precisely age the embryos, I identified the exact time that *Sall4* expression begins in relation to *Tbx5, Fgf10* and *Fgf8*. As previously described (see Introduction), *Tbx5* is thought to directly activate *Fgf10* expression in the LPM (Agarwal et al., 2003). Fgf10 subsequently signals to the overlying ectoderm to activate *Fgf8* expression in the nascent apical ectodermal ridge (AER). Fgf8 then signals back to the LPM to maintain *Fgf10* expression and subsequently form the *Fgf10/Fgf8* positive feedback loop that is essential for limb outgrowth (Fig. 2A-B). As

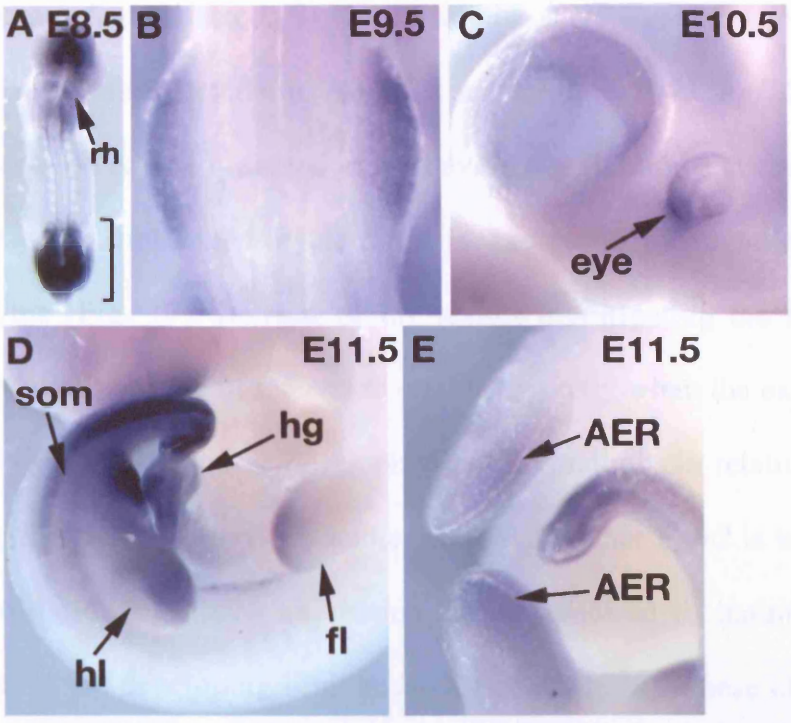

Figure 16. Analysis of *Sall4* expression during mouse embryonic development using whole-mount *in situ* hybridisation. (A) A dorsal view shows that at E8.5 *Sall4* is expressed in the rhombomeres (rh). The black bars highlight *Sall4* expression in the segmental plate and last formed somite (B) A dorsal view of the forelimb region of an E9.5 embryo shows that *Sall4* is initially expressed throughout the forelimb buds. (C) A lateral view of the head of an E10.5 embryo shows that *Sall4* is expressed in the developing eye. (D) A lateral view of an E11.5 embryo shows *Sall4* expression in both the developing forelimbs (fl) and hindlimbs (hl), as well as the hindgut (hg) and somites (som). (E) *Sall4* expression is excluded for the apical ectodermal ridge (AER) of the forelimb and hindlimb buds.

stated earlier no homologue of *fgf24* is thought to exist in amniotes. *Tbx5* is first detected within the developing forelimbs at the 8 somite stage (Fig. 17). Consistent with the model that *Tbx5* acts upstream of *Fgf10,* I first detect *Fgf10* expression at the 12/13 somite stage, which is after the stage that *Tbx5* transcripts are first detected. By the 15 somite stage *Fgf8* is detected in the presumptive forelimb ectoderm. After the induction of *Tbx5, Fgf10* and *Fgf8, Sall4* expression is first observed in the developing forelimbs at the 18 somite stage. At early limb bud stages, *Sall4* is expressed throughout the limb mesenchyme (Fig. 17). In view of my results investigating the function of zebrafish *sall4* it will be of interest to establish exactly when the expression of *Sall1* and *Fgfr2* begins in the developing mouse forelimbs in relation to *Tbx5, Fgf10, Fgf8* and *Sall4*. Previous studies have shown that *Fgfr2* is not required for the initiation of *Fgf10* expression, but is required to maintain *Fgf10* expression in the developing limb buds (Xu et al., 1998). These observations would be consistent with *Sall4* and/or *Sall1* activating the expression of *Fgfr2* in the developing forelimbs, as *Sall4* expression initiates after *Fgf10.*

Mouse *Sall4* gene traps

To investigate the function of mouse *Sall4,* I utilised mouse gene trap lines obtainable from the BayGenomics consortium (http://baygenomics.ucsf.edu/). The vectors used to create these embryonic stem (ES) cell lines contain a cassette of β-geo (β-galactosidase-neomycin resistance fusion) and a stop codon that is flanked by splice acceptor and donor sites (Fig. 18). If the vector incorporates into genomic DNA within an intron, then due to the splice acceptor

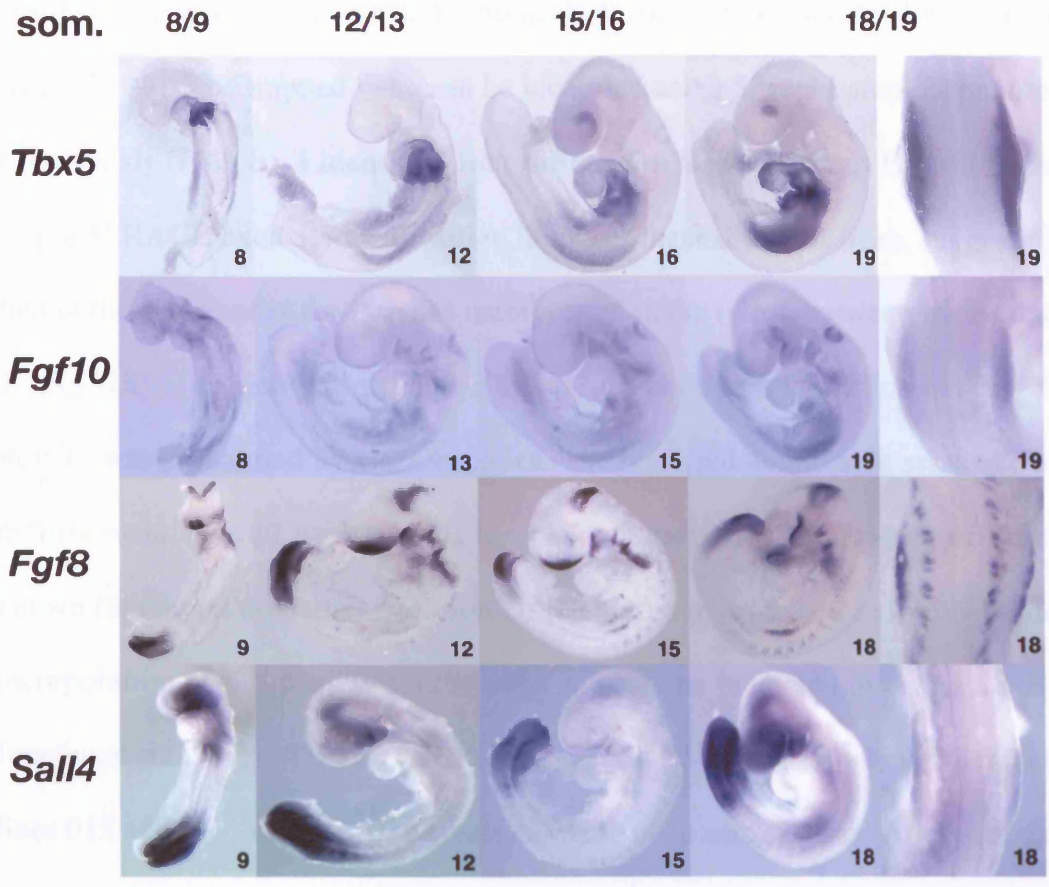

Figure 17. A comparative analysis of the expression patterns of genes essential for early forelimb development. Whole mount *in situ* hybridization for *Tbx5, Fgf10, Fgf8* and *Sall4* in the mouse at early limb bud stages. The numbers in each panel indicate the number of somites the embryo contains. 8 somites = E8.25, 12/13 somites = E8.5, 15/16 somites = E9.0 and 18/19 somites = E9.25. (Kaufmann, 2001). Lateral views of all embryos are shown. Dorsal views of the forelimb region are also shown for embryos with 18/19 somites. som=somites.

and donor sites, the vector will be spliced into the mature mRNA of that gene. Translation of an mRNA that contains such a gene trap results in a protein fusion consisting of β–geo and amino acids encoded by exons that lie 5' to the trap (Fig 18). The trapped gene can be identified using 5' rapid amplification of cDNA ends (RACE). I identified four different m*Sall4* gene trap ES cell lines. Using 5' RACE exon 1 was identified in two of these different lines, suggesting that in these instances the trap has incorporated in the intron between exon1 and 2 (Fig. 18). The generation of the m*Sall4* ES cells and identification, by 5' RACE, was performed by BayGenomics. The predicted amino acid sequence of m*Sall4* exon 1 is 40 amino acids long and contains no zinc fingers or other known functional domains. Therefore, if the gene trap is located in intron 1 then incorporation of this trap into *Sall4* mRNA would be predicted to create a non-functional transcript. These two different m*Sall4* ES cell lines, which I denoted lines 015 and 077, were used to create chimeric mice using blastocyst injections. Male chimeric mice were then crossed with c57bl6 females, to create heterozygous F1 gene traps. ES cells were prepared for injection by M. Logan and J. Del Buono, and injected by C. Akufo-Addo (NIMR). Crosses of heterozygous 077 mice with wild type c57bl6 mice produced 31% heterozygous pups (n=161). Similarly crosses of 015 heterozygous mice with wild type c57bl6 mice produced 41% heterozygous pups (n=32). These observations suggest that heterozygous pups are under-represented at weaning, as Mendelian ratios would predict 50% of the pups should be heterozygous.

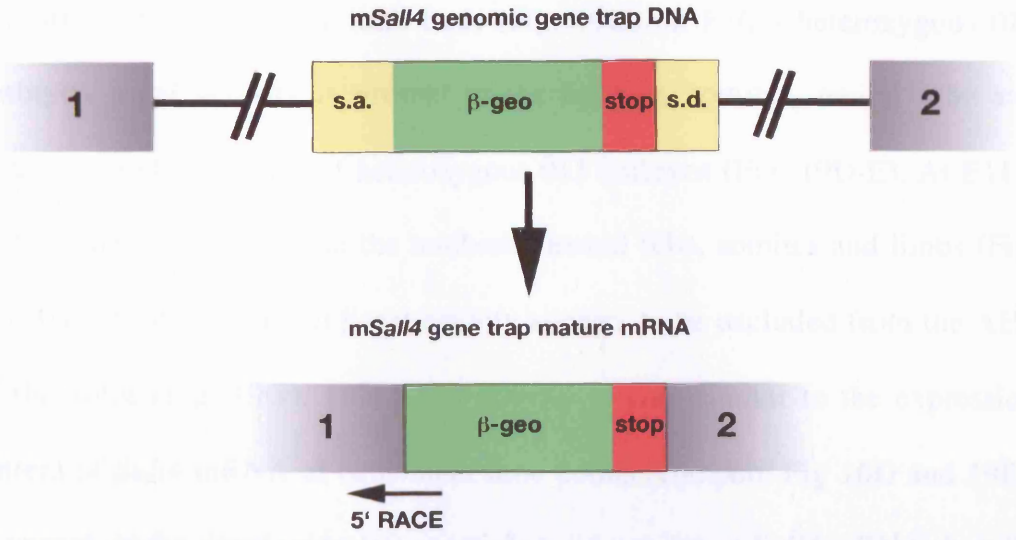

Figure 18. Mouse *Sall4* gene traps. The vectors used to create the gene trap lines contain splice acceptor (s.a.) and splice donor (s.d.) sites that result in the incorporation of the vector into mRNA made from the trapped gene. The trapped gene can then be identified using 5' rapid amplification of cDNA ends (RACE). Using this method, exon1 of *Sall4* was amplified in two different gene trap lines suggesting the vector has incorporated into the intron between exon1 and 2 of *Sall4*. Incorporation of the vector into *Sall4* mRNA results in a protein fusion of β-geo (LacZ geomycin resistance fusion) and amino acids encoded by exon 1. Therefore, β-gal activity can be used to analyse *Sall4* expression.

Sall4 gene trap expression analysis

As the vectors used to create the gene trap lines contain β-geo, *Sall4* expression can be studied by staining transgenic embryos with X-gal. In E10.5 heterozygous 077 embryos β-gal activity is detectable in the midbrain, hindbrain, gut and left ventricle (Fig. 19A-B). I also observed weak β-gal activity in the developing limb buds (Fig. 19C). In E10.5 heterozygous 015 embryos β-gal activity is present in the hindgut, somites, neural tube and forelimbs and hindlimbs of heterozygous 015 embryos (Fig. 19D-E). At E11.5 β-gal remains detectable in the midbrain, neural tube, somites and limbs (Fig. 19F-G). At this time point β-gal activity appears to be excluded from the AER of the limbs (Fig. 19G). This β-gal activity is very similar to the expression pattern of *Sall4* mRNA at equivalent time points (compare Fig 16D and 19E). However, in the developing left ventricle I did not detect *Sall4* mRNA, but did observe β-gal activity in 077 heterozygous embryos (Fig. 19B), suggesting that *Sall4* is expressed at low levels in the developing heart. The level of β-gal activity is greater in heterozygous 015 embryos compared to 077 embryos (compare activity in tail and hindlimbs of Fig. 19C and E). This variation of β-gal activity suggests that the trap is incorporated into *Sall4* mRNA less efficiently in the 077 transgenic line. It also suggests the 077 line is a weaker, hypomorphic, allele than the 015 line, and is likely to not represent a *Sall4* null allele.

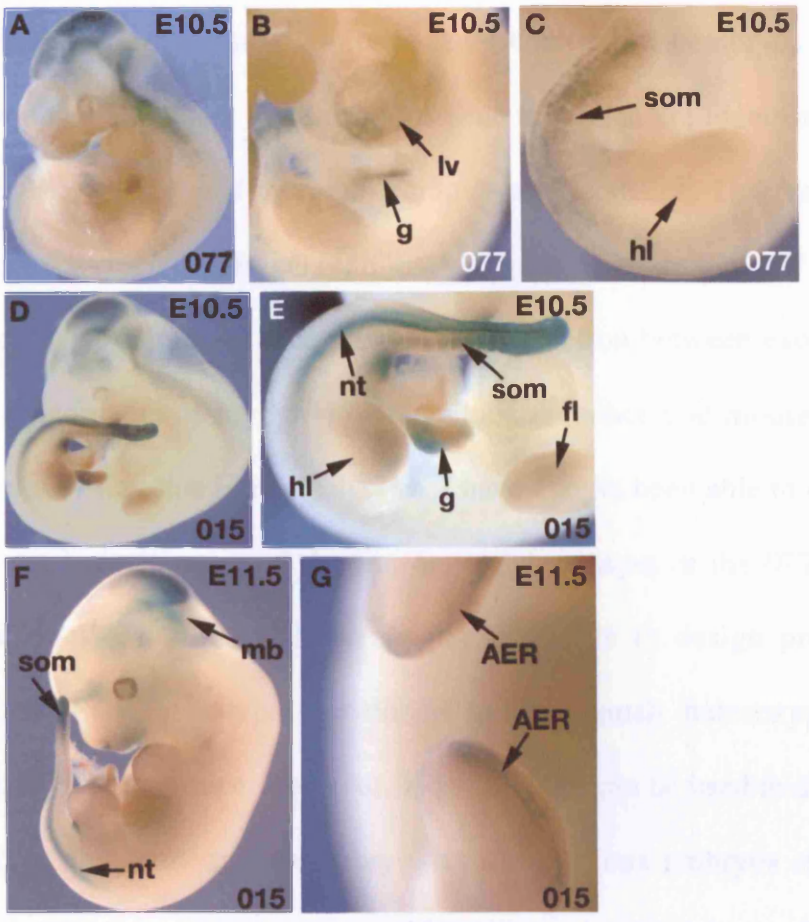

Figure 19. Analysis of β-gal activity in heterozygous 077 and 015 *Sall4* gene trap embryos. X-gal staining of heterozygous 077 (A-C) and 015 (D-G) gene trap embryos. (A) Lateral view of an E10.5 077 embryo stained with X-gal. Magnified views of an 077 E10.5 embryo shows β-gal activity in the gut and the left ventricle (B), and also in the somites (C). Lateral view showing β-gal activity in an 015 heterozygous embryo (D). A magnified view shows β-gal activity in the somites, neural tube, gut, and the forelimb and hindlimbs buds (E) At E11.5 β-gal activity continues to be detectable in the somites, neural tube and midbrain. (D) At E11.5 β-gal activity appears to be excluded from the apical ectodermal ridge of the forelimbs and hindlimbs. Lv=left ventricle, g=gut, som=somites, hl=hindlimb bud, fl=forelimb bud, nt=neural tube, mb=midbrain, AER=apical ectodermal ridge.

Gene trap mice reveal essential functions for *Sall4* during embryonic development

I inter-crossed heterozygous 077 mice to see if homozygous embryos displayed any developmental defects. Heterozygous gene trap mice are identifiable using PCR with primers targeted to amplify trap vector sequence. The results from 5'RACE (performed by BayGenomics) suggests that in the 077 and 015 transgenic lines the trap has incorporated into the intron between exon 1 and 2 of *Sall4*. Alignments of my *Sall4* cDNA clone sequence and mouse genomic sequence shows that this intron is 10.1kb. I have not yet been able to determine the exact genomic location of the trap within this intron in the 077 and 015 transgenic lines. Therefore I have not yet been able to design primers for conventional PCR genotyping methods to distinguish heterozygous and homozygous gene trap mice. However, X-gal staining can be used to distinguish heterozygous and homozygous embryos as homozygous embryos stain more intensely. Intercrosses of heterozygous 077 mice produced embryos that have a midbrain defect where the neural tube has not closed (Fig 20A-D). I observed this midbrain phenotype in 21% of litters harvested from E10.5-15.5 (n= 48), suggesting that this phenotype is seen only in homozygous embryos. In the few litters harvested at E17.5, I did not observe this phenotype (0 out of 13) possibly because these embryos die before E17.5. Those embryos with the midbrain defect display greater β-gal activity than littermates that do not have the phenotype (compare β-gal activity in brain of Fig. 19A and 20A), further supporting the midbrain defect is seen only in homozygous embryos. At later stages in development, embryos that display the midbrain defect have

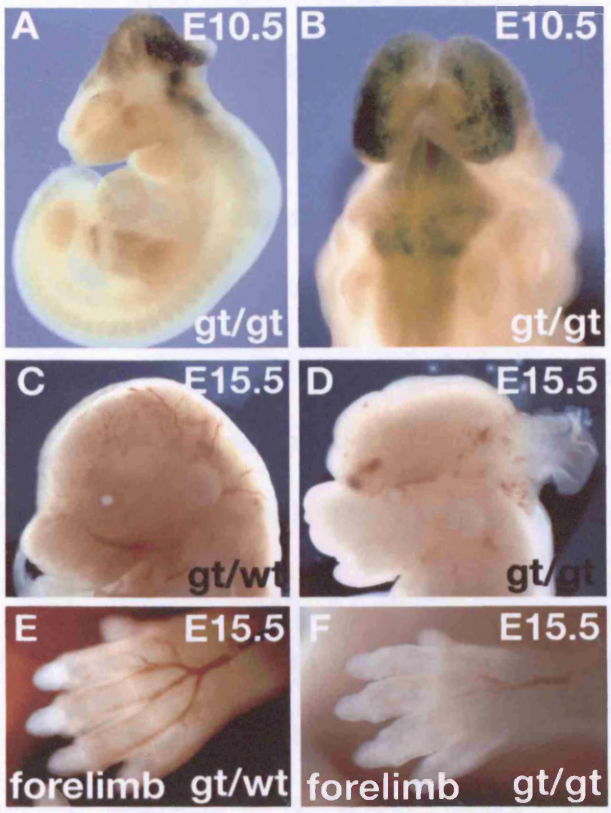

Figure 20. Intercrosses of heterozygous 077 mice results in embryos with a midbrain defect. Lateral (A) and dorsal (B) views of an E10.5 embryo displaying the midbrain defect observed in nearly 25% of litters harvested from intercrosses of heterozygous 077 gene trap mice. X-gal staining of these embryos shows that β-gal activity is greater in embryos displaying the midbrain defect compared to transgenic littermates that are apparently normal (compare with Fig. 19A). At E15.5 the forelimbs of embryos displaying the midbrain defect are apparently normal when compared with littermates not displaying the brain defect (C-F).

apparently normal limbs when compared to wild type littermates (Fig. 20E-F).

Mouse *Sall4* promoter analysis

I have demonstrated that *sall4* expression in the developing zebrafish pectoral fins is dependant on *tbx5* (Fig. 10D-E). In the mouse genome, at 1640bp and 1680bp 5' to the m*Sall4* start codon, are two sequences that match the *Tbx5* binding site consensus and these sequences are also present 5' to human *SALL4* (Fig. 21A) (Ghosh et al., 2001). I isolated mouse *Sall4* genomic BAC clones which span this region in order to test if these *Tbx5* binding sites are required for embryonic m*Sall4* expression. I sub-cloned a fragment that stretches from the m*Sall4* start codon to 2kb upstream, and therefore includes the *Tbx5* binding sites, into a vector upstream of LacZ. Transgenic embryos were then created with these plasmids and X-gal staining was used to test if this 2kb promoter fragment can copy endogenous *Sall4* expression. Transgenic embryos were created by pronuclear injection by S. Wood (NIMR). Eighteen transgenic embryos were created and I detected β-gal activity in only two of these embryos at E10.5. The expression of β-gal was different in these two embryos and did not recapitulate endogenous *Sall4* expression (Fig. 21B-C). β-gal activity was observed in forelimb and hindlimb buds of one of these transgenic embryos (Fig. 21C). This activity was seen in the posterior limb buds but not in most distal regions and therefore differs from endogenous *sall4* expression (compare with Fig. 16 and 19). Also within this embryo β-gal activity was observed in the viscera dorsal to the heart and some anterior somites. I did not detect

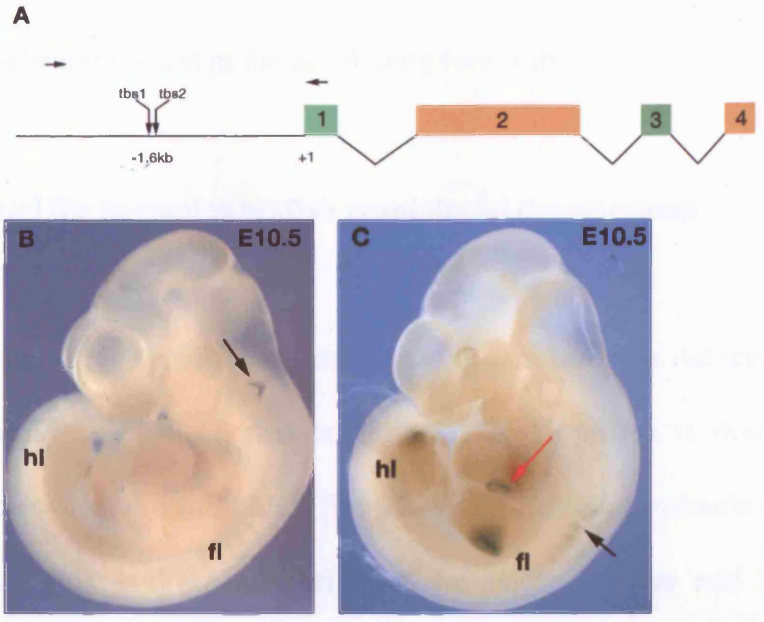

Figure 21. *Sall4* promoter analysis. (A) A schematic of the *Sall4* locus highlights the position of the two potential *Tbx5* binding sites (tbs1 and tbs2). The arrows highlight the position of the primers used to clone the 2kb *Sall4* promoter fragment. (B and C) Lateral views showing the two different E10.5 *Sall4* promoter transgenic embryos, which displayed β-gal activity. In one embryo (B) β-gal was only seen in the otic vesicle, as highlighted by the arrow. In the other embryo (C) β-gal was observed in the posterior forelimb and hindlimb buds, the viscera dorsal to the heart (red arrow) and some anterior somites (black arrow) (fl=forelimb and hl=hindlimb buds).

endogenous *Sall4* expression in these regions of the developing embryo. In summary, these results suggest that elements outside of this 2kb fragment are essential for endogenous m*Sall4* expression and the two transgenic embryos that express LacZ, do so due to random integration events. However, these experiments do not demonstrate whether the *Tbx5* binding sites are, or are not, required for *Sall4* expression in the developing forelimbs.

sall4 is essential for normal zebrafish craniofacial development

While using alcian blue staining to understand the pectoral fin defects of *sall4* morphant embryos, I noticed that craniofacial development is disrupted in embryos injected with the *sall4* MO (Fig. 22A-B). In *sall4* morphants not all of the ceratobranchials (gill arches) form and the palatoquadrate and Meckel's cartilage (upper and lower jaw, respectively), are absent. In order to understand these craniofacial defects I studied the expression of *dlx2,* which is expressed in the neural crest cells that populate the pharyngeal arches (pa) (Piotrowski and Nusslein-Volhard, 2000), in *sall4* morphant embryos. At 18hpf *dlx2* is expressed in three streams, which are then separated by endodermal pouches to give rise to the mandibular arch (pa1), the hyoid arch (pa2) and three remaining domains that form pa3-7 (Fig. 22C) (Piotrowski and Nusslein-Volhard, 2000). The mandibular arch gives rise to the upper and lower jaw, the hyoid arch forms the ceratohyal and pa3-7 form the gill arches. In *sall4* morphant embryos *dlx2* expression is downregulated in the mandibular arch and pa3-7 (Fig. 22D). This downregulation is consistent with the loss of the some gill arches and the jaw in *sall4* morphant embryos (Fig. 22B).

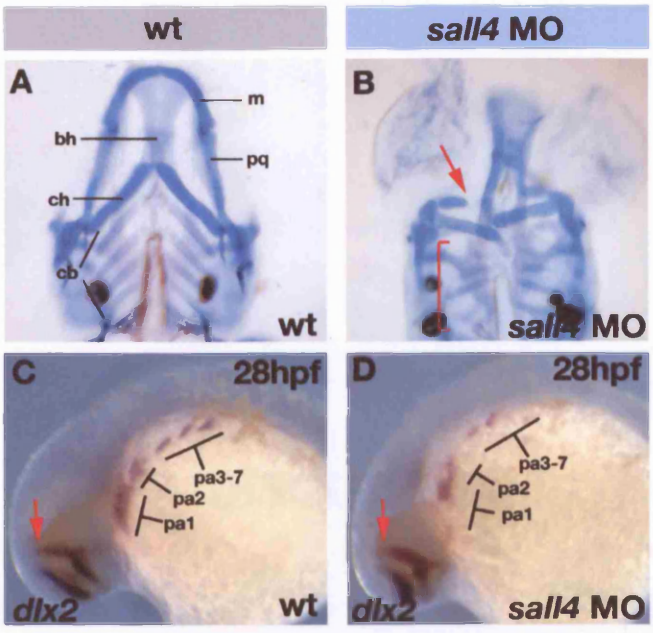

Figure 22. craniofacial development is disrupted in *sall4* morphant embryos. A ventral view of a 5dpf wt embryo stained with alcian blue shows the individual skeletal elements of the head. (B) A ventral view of an embryo injected with 4ng of *sall4* MO shows that craniofacial development is severely disrupted following loss of *sall4* function. The red arrow highlights the absence of the palatoquadrate, and the red bar shows that some ceratobranchials are absent. (C) A lateral view of a 28hpf wild type embryo shows that *dlx2* is expressed in pharyngeal arch (pa) 1 (also called mandibular arch), pa2 (also called hyoid arch) and pa3-7. (D) In an embryo injected with 10ng of *sall4* MO *dlx2* is downregulated in the pa's, but is expressed normally in the brain (red arrow). bh=basihyal, cb=ceratobranchial, ch=ceratohyal, m=Meckel's cartilage and pq=palatoquadrate.

4. DISCUSSION

Zebrafish pectoral fin development is disrupted in *sall4* morphant embryos

During vertebrate limb development a cascade of signals are required to initiate and maintain limb outgrowth (see Introduction). Using zebrafish as a model organism, I have placed *sall4* within the genetic hierarchy that controls limb outgrowth. I have shown that *sall4* is required for outgrowth of the pectoral fins, but not the initiation of pectoral fin development, since *tbx5* and *fgf24* are induced normally and proximal skeletal elements form in *sall4* morphants. The upturned fin phenotype found in some *sall4* morphant embryos (Fig. 8F) and those injected with low concentrations of *tbx5* MO (Fig. 8H, Garrity et al., 2002) demonstrate that reduction of *sall4* and *tbx5* function produces similar pectoral fin defects in zebrafish. This is consistent with the similarity of limb phenotypes seen in OS and HOS patients, which are caused by haploinsufficiency of *SALL4* and *TBX5*, respectively. From fish to mammals, *Fgf10* has an evolutionary conserved function that is essential for limb outgrowth (Min et al., 1998; Sekine et al., 1999; Norton et al., 2005). Using morpholinos, I have demonstrated that *sall4* and *tbx5* are required for the initiation of *fgf10* expression. Therefore, disruption of *Fgf10* signalling is the common cause of the similar abnormalities that arise from fish to humans, following perturbation of either *Tbx5* or *Sall4* function.

sall1a and *sall4* perform similar roles during pectoral fin development

The preferential downregulation of *fgf10* in the anterior of *sall4* morphant fin buds (Fig. 11D) led us to investigate if a *sall4*-related gene is required to

maintain the posterior domain of *fgf10* expression. Although the expression of a *sall2* homologue is yet to be described during zebrafish development, it appears that the only other sall gene expressed in the developing pectoral fins is *sall1a* (Fig. 13A-B). Interestingly, while *sall4* is required for the anterior domain of *fgf10* expression in the fin bud, *sall1a* is required for the posterior domain (Fig. 13F). In *sall1a* (Fig. 13L-M) and *sall4* (Fig. 11G-J) morphant fin buds *dlx2* and *sp9* are preferentially downregulated in the posterior and anterior fin bud ectoderm. These observations are consistent with the downregulation of *fgf10* expression in either the anterior or posterior fin bud and the fact that *dlx2* and *sp9* expression is dependant on *fgf10* (Norton et al., 2005). Although my work demonstrates that *sall1a* and *sall4* are required for posterior and anterior domains of *fgf10* expression in the fin bud (Fig. 11D and 13F), my work does not indicate why *sall1a* and *sall4* are required for these specific domains of *fgf10* expression. One explanation is that, while *sall1a* and *sall4* mRNA is present throughout the fin bud, due to post-transcriptional modifications, sall1a and sall4 proteins are only functional within the posterior and anterior fin buds. Similarly, co-factors within the fin buds may modify the function of sall1a and sall4. In *sall1a* (Fig. 13K) or *sall4* (Fig. 11B) morphant pectoral fin primordia, *fgf10* expression initiates, however it fails to commence in *sall1a/sall4* double morphant embryos (Fig 14G). This suggests that the functions of *sall1a* and *sall4* are partially redundant, such that *fgf10* expression initiates in the primordia in the absence of either gene, but at later stages is absent in either the anterior or posterior fin bud.

The pectoral fin defects observed following loss of *sall1a* function are different from other vertebrates, as *Sall1* null mouse embryos do not have a limb phenotype (Nishinakamura et al., 2001). A possible explanation for this difference in phenotype is the variation in expression of a related gene, *Sall3,* which is expressed in an almost identical pattern to *Sall1* during mouse limb development (Nishinakamura et al., 2001; Ott et al., 2001), but is not expressed in the developing zebrafish pectoral fins (Camp et al., 2003). Based on these observations and because *Sall1* is most closely related to *Sall3*, this suggests that *Sall1* null mice do not have a limb phenotype because *Sall3* can substitute for the loss of *Sall1*. Since *sall3* is not expressed during zebrafish pectoral fin development it cannot compensate for the loss of *sall1a* and therefore *sall1a* morphant embryos have truncated pectoral fins.

Mesenchymal FGFs are required to induce the expression of genes in the pectoral fin ectoderm

Studies in mouse and chick have shown that *Fgf10,* which is expressed in the mesenchyme of the developing limb buds, signals to the overlying ectoderm to induce *Fgf8* expression. These ectodermal and mesenchymal FGFs then form a positive feedback loop that is essential for outgrowth of the developing limbs (See Introduction). Although this positive feedback loop is known to occur in mouse and chick limb buds it has been studied less in zebrafish pectoral fins. The gene *fgf24* is found in zebrafish, but not chicks, mice or humans, and appears to have been lost in the terrestrial vertebrate lineage (Draper et al., 2003). In the zebrafish pectoral fin primordia mesenchyme, *fgf24* is required for

the expression of *fgf10* (Fig. 2C) (Fischer et al., 2003). Ectodermal FGFs fail to be expressed in *fgf24* mutant fin buds (Fischer et al., 2003) demonstrating that, similar to limb development in higher vertebrates, mesenchymal FGFs are required for the induction of ectodermal FGF gene expression. However, previously it has been unclear whether *fgf24,* or its downstream target *fgf10,* were required for induction of ectodermal FGFs. The downregulation of *fgf10* in *sall4* morphant fin buds, and the subsequent loss of ectodermal FGF expression (Fig. 11E-F), suggests that it is *fgf10,* rather than *fgf24,* that is required for the induction of FGF expression in the overlying ectoderm. The induction of ectodermal FGFs only after the time point at which *fgf10* is first expressed, and long after the induction of *fgf24* expression (Fig. 15E), also supports a model in which *fgf10* is the critical mesenchymal signal. As well as being required for the induction of ectodermal FGF gene expression, my studies suggest that *fgf10* is also required for the activation of *dlx2* and *sp9* expression in the fin bud ectoderm (Fig. 11, 13 and 14). These results are also supported by observations of zebrafish *fgf10* mutants (Norton et al., 2005).

tbx5, sall1a and *sall4* are required to establish FGF signalling during the initiation of pectoral fin bud outgrowth

In the pectoral fin primordia *sall1a, sall4* and *fgf24* expression is dependant on *tbx5* (Fig. 10D-E, 13G; Fischer et al., 2003), however expression of either *sall1a/sall4* or *fgf24* can occur independently of one another (Fig. 10G, 13H-I). Therefore, *tbx5* activates the expression of two different target genes, both of which are required for pectoral fin outgrowth (Fig. 15E; Fischer et al., 2003).

sall1a/sall4 and *fgf24* are required for the initiation of *fgf10* expression and I have addressed how this interaction occurs. *fgf24* must signal via a receptor to activate the expression of *fgf10* in the pectoral fin primordia. During zebrafish embryonic development *fgfr2* begins to be expressed in the mesenchyme of the pectoral fin primordia at 23hpf (Fig. 15A), just after *sall1a/sall4* expression is first detected, but just prior to the initiation of *fgf10* expression. *fgfr2* is therefore expressed in the correct spatial and temporal pattern required for the induction of *fgf10* expression. Similarly, as *sall1a* and *sall4* are zinc finger transcription factors they are good candidates to directly regulate the expression of *fgfr2*. My results support a model (Fig. 15E) in which *sall1a/sall4* act as transcriptional activators to positively regulate *fgfr2* transcription, and that fgf24 signals via fgfr2 to initiate *fgf10* expression in the fin bud mesenchyme.

Currently there is conflicting data existing regarding whether Sall genes act as transcriptional activators or repressors (Kiefer et al., 2002; Li et al., 2004; Netzer et al., 2001; Onai et al., 2004; Sweetman et al., 2003). Sall2 can bind directly to the promoter of the gene $p21^{WAF1/CIP1}$ and activate transcription (Li et al., 2004). Other studies have suggested the Sall1 acts as a transcriptional repressor by recruiting a histone deacetylation complex (HDAC) (Kiefer et al., 2002). Sall1 can interact with full length Sall1-4 proteins (Kiefer et al., 2003; Sweetman et al., 2003). The heterodimerisation of Sall1 and other Sall proteins may therefore alter the transcriptional properties of Sall1, such that in different situations Sall1 acts as either a transcriptional activator or repressor. A mechanism for altering the transcription functions of Sall proteins was demonstrated by studies of the cellular localisation of chick Sall1 and Sall3

(Sweetman et al., 2003). Sall1 was shown to mainly localise to the nucleus whereas Sall3 is predominantly cytoplasmic. Co-transfection of *Sall1* and *Sall3* altered the distribution of Sall1 such that it was retained within the cytoplasm. The exclusion of Sall1 from the nucleus, by interactions with Sall3, would therefore alter the transcriptional functions of Sall1.

Studies using yeast-two hybrid screens, have shown that SALL1 interacts with the small ubiquitin-like modifier-1 (SUMO-1), and SUMO-1 becomes conjugated to SALL1 through a process called SUMOylation (Netzer et al., 2002). Post-transcriptional modification of proteins by SUMOylation has been proposed to alter the subcellular localisation and transcriptional properties of transcription factors (Gill, 2004). For example, the transcription factor Sp3 is post-transcriptionally modified by SUMO-1. Inhibition of Sp3 SUMOylation results in an increase in the ability of Sp3 to activate transcription, suggesting that SUMOylation acts to modulate the transcriptional functions of Sp3 (Ross et al., 2002; Sapetschnig et al., 2002). SUMOylation may therefore act as another mechanism of post-transcriptional regulation that affects the function of Sall1. If Sall1 and Sall4 act as a complex to affect the transcription of target genes then SUMOylation of Sall1 may alter the transcriptional function of such a Sall1/Sall4 protein complex. However, my experiments suggest that *sall1a* and *sall4* have partially redundant functions in the developing pectoral fins, such that *fgf10* expression can initiate in the absence of *sall1a* or *sall4,* but does not initiate following loss of both *sall1a* and *sall4*. This suggests that in the developing pectoral fins *sall1a* and *sall4* do not act as a complex.

In view of my findings it will be of interest to perform *fgfr2* loss of function experiments. Based on my model (Fig. 15E), I predict that loss of *fgfr2* function will result in a failure of *fgf10* expression to initiate. Pectoral fin outgrowth will therefore fail to occur in the absence of *fgfr2*. It will also be of interest to analyse the *Fgfr2* promoter. Previous studies have shown that the basic helix-loop-helix transcription factor E2A binds to the *Fgfr2* promoter and is required to repress *Fgfr2* transcription in pre-B cell lymphocytes (Greenbaum et al., 2004). However, nothing is known about the transcription factors that are required for the expression of *Fgfr2* in the developing limbs. The isolation of putative regulatory elements flanking the mouse *Fgfr2* coding sequence could be used to create transient transgenic mouse embryos, and these experiments may lead to the identification of the fragments required for *Fgfr2* expression in the limb buds. These sequences could potentially lie 5' or 3' to the *Fgfr2* locus, or within introns. If such a promoter analysis identifies the fragments required to recapitulate endogenous *Fgfr2* expression in the developing limbs, then luciferase assays could be used to further test if *Sall1* and *Sall4* act as transcriptional activators to initiate *Fgfr2* expression. The specific sequences of DNA that *Sall1* and *Sall4* can recognise and bind to are currently unknown and therefore I have been unable to perform an *in silco* search for *Sall1* and *Sall4* binding sites in close proximity to *Fgfr2* coding sequences. Such DNA binding sites could be identified by performing chromatin immuno-precipitation (ChIP), and/or by *in vitro* binding site selection assays. However, these experiments will require antibodies that recognise *Sall1* and *Sall4,* or the generation of tagged *Sall1* and *Sall4* proteins (i.e Flu or Flag tagged).

tbx5 regulates the expression of *fgf10* in the pectoral fin primordia using a feedforward transcriptional motif

Large scale studies of transcription factors and their downstream target genes in *E. coli* (Shen-Orr et al., 2002), *S. cerevisiae* (Lee et al., 2002) and human ES cells (Boyer et al., 2005) have identified several conserved transcriptional motifs, one of which is called the feedforward transcriptional motif. Collectively my results show that *tbx5* regulates the expression of *fgf10* in the zebrafish pectoral fin primordia using a feedforward motif (Fig. 15E).

In a feedforward transcriptional motif, transcription factor X regulates the expression of transcription factor Y, and then X and Y either act together, or individually, to regulate the expression of gene Z (Fig. 23A). The relationship between X and Y, Y and Z and X and Z can be either to repress or activate transcription. In the most common feedforward transcriptional motif found in *E. coli* and *S. cerevisiae,* X activates the transcription of Y and then X and Y activate the transcription of gene Z (Fig. 23A) (Mangan and Alon, 2003). The function of a feedforward motif, and the transcription of Z, can be affected by the function of X and Y, which can be activated or inhibited by post-transcriptional modification or interactions with other proteins (Mangan and Alon, 2003).

Using mathematical modelling the dynamics of feedforward transcriptional motifs have been proposed to have different functions (Mangan and Alon, 2003; Shen-Orr et al., 2002). It has been suggested that

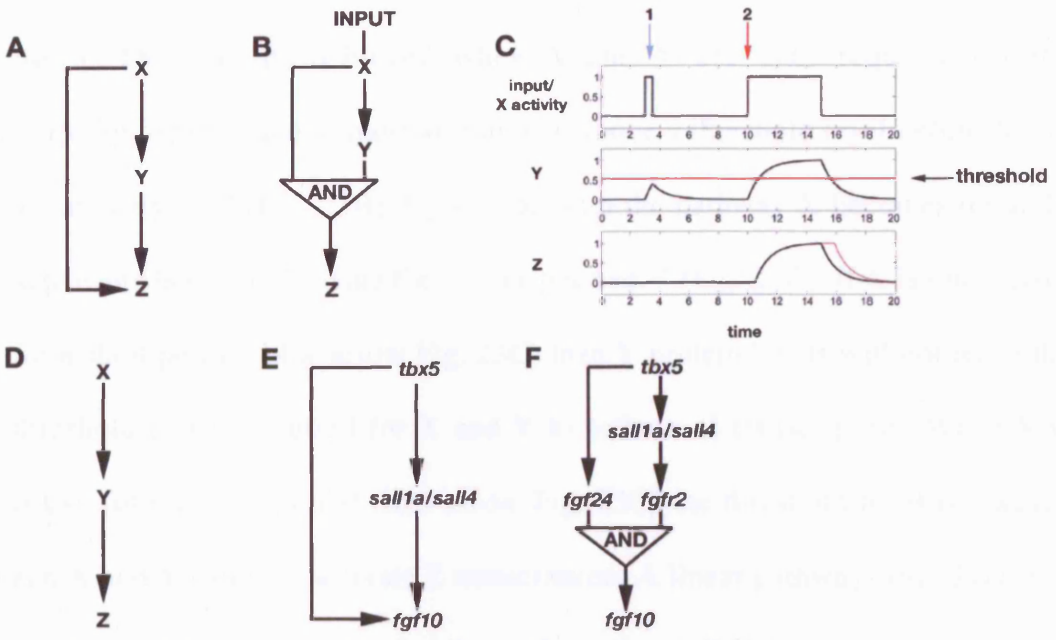

Figure 23. Feedforward transcriptional motifs. (A) An example of a feedforward transcriptional motif in which transcription factor X activates the expression of another transcription factor, Y, and X and Y act either together or individually to activate the expression of gene Z. (B) A feedforward transcriptional motif in which X activates the expression of Y and X AND Y are required for to initiate the transcription of Z. (C) A graphical representation of the feedforward transcriptional motif shown in B. Shown in the boxes is the activity of X and the protein levels of Y and Z. When X becomes active the protein levels of Y accumulate. However, when X is active only transiently (Blue arrow, number 1) the levels of Y do not reach the threshold level (Red line, middle box) that is required for X and Y to activate the transcription of Z. When X is active for a longer period of time (Red arrow, number 2) Y protein levels reach the threshold level and X and Y activate the expression of Z. When X becomes inactive the transcription of Z ceases immediately as X and Y are both required for the transcription of Z. In a linear pathway, as shown in (D), when X becomes inactive the transcription of Z does not immediately cease due to the presence of remaining Y protein. This delay is shown as a red line in the lower box of C. (E) A representation of the feedforward transcriptional motif that my work has uncovered. Transcription factor X is *tbx5*, Y is *sall1a/sall4* and *fgf10* is Z. My work has shown that *tbx5* activates the expression of *sall1a/sall4* and *tbx5* and *sall1a/sall4* then activate the expression of *fgf10*. (F) The feedforward transcriptional motif initiated by *tbx5* also includes *fgf24* and *fgfr2*, which act to initiate the expression of *fgf10*. The temporal events involved in the feedforward motif of F are shown in Fig. 15E. C is adapted from Shen-Orr et al., 2002.

feedforward motifs ensure the transcription of Z is unaffected by transient inputs on the motif and at the same time the transcription of Z can rapidly be shut down. This can be achieved when X and Y are both required for the transcription of Z and Y must accumulate above a threshold level before X and Y can activate Z (Fig. 23B). Upon input into the pathway X becomes instantly active and begins to activate the transcription of Y (Fig. 23C). If X is only active for a short period (blue arrow Fig. 23C) then Y protein levels will not reach the threshold that is required for X and Y to activate Z transcription. When X is active for a longer period (Red arrow Fig. 23C) the threshold level is reached and X and Y can then activate Z transcription. A linear pathway (Fig. 23D) can also be resistant to transient inputs on the pathway if Y must reach a threshold before it can affect the transcription of Z. However, when X becomes inactive the transcription of Z ceases more rapidly in the feedforward motif compared to a linear pathway. In the feedforward motif when X becomes inactive, Y protein levels instantly begin to decline (Fig. 23C). As X and Y are both required for the expression of Z when X becomes inactivated Z transcription will cease immediately and this will occur irrespective of Y protein levels (Fig. 23C). Similarly, in a linear pathway when X becomes inactive the transcription of Y will cease. However, due to the presence of Y protein the transcription of Z will not immediately cease (Fig. 23C).

In the feedfoward transcriptional motif that I have uncovered *tbx5* acts as transcription factor X (Fig. 23E). *tbx5* (X) activates the expression of *sall1a/sall4* (Y) and then *tbx5* and *sall1a/sall4* are required for the expression of *fgf10* (Z). Within this feedforward transcriptional motif *tbx5* activates the

expression of *fgf24* and *sall1a/sall4* activates *fgfr2* expression (Fig. 23F). Therefore *tbx5* activates the expression of different genes, independently, that act in a common pathway to initiate the expression of *fgf10*. The temporal delay between the initiation of *tbx5* and *sall1a/sall4* expression (Fig. 15E) suggests that this regulation may be indirect or that *tbx5* requires a co-factor to activate *sall1a/sall4* expression. A third possibility is that higher threshold levels of tbx5 protein are required to activate different target genes. In the pectoral fin primordia *tbx5* is likely to directly activate the expression of *fgf24* since the expression of each gene initiates only one hour apart (Begemann and Ingham, 2000; Fischer et al., 2003).

The expression of *fgf24* in the pectoral fin primordia begins at 18hpf, approximately six hours before *fgf10* expression commences at 24hpf. *fgfr2* expression is detected at 23hpf (Fig. 15E). During the interval between the initiation of *fgf24* and *fgfr2* expression, it would be predicted that fgf24 protein levels accumulate in the extracellular milieu in the absence of receptor. Presumably when *fgfr2* expression initiates, fgfr2 proteins are rapidly occupied by ligand due to the presence of a reservoir of fgf24. Although, my results do not provide an explanation for the apparent 'priming' of FGF signalling it is possible that in the pectoral fin mesenchyme the dynamics of this regulation would favour a paracrine rather than autocrine mode of signalling and would produce rapid, robust and uniform signalling via the FGF receptor.

Analysing FGF signalling during zebrafish pectoral fin development

In order to test the dynamics of the transcriptional motif that I have identified (Fig. 15E) it would be of interest to misexpress *fgfr2* at an early time point to analyse what effect this has on the initiation of *fgf10* expression and the initiation of fin bud outgrowth. Similarly, *fgfr2* misexpression experiments could be used to try and rescue pectoral fin development in *sall1a/sall4* double morphant embryos. Such experiments can be achieved by injecting full length RNA into the yolk of a 1-, 2- or 4- cell stage zebrafish embryo. However, this technique relies on the RNA and the protein product of that RNA being stable until pectoral fin bud stages. This method has proved successful when trying to rescue the loss of *raldh2* function, which is required at early pectoral fin bud stages to initiate *tbx5* expression (i.e. before 17hpf) (Begemann et al., 2001; Grandel et al., 2002). Other attempts have been less successful when trying to rescue pectoral fin development following loss of *wnt2b* function. Pectoral fin development was only rescued in 43% of embryos co-injected with *wnt2b* MO and *tbx5* mRNA (Ng et al., 2002). When I misexpressed *sall4*Δ RNA by injecting 1-, 2- or 4-cell stage embryos I achieved pectoral fin defects in only 4% of those injected embryos (Fig. 9B-C and text). These experiments could mean that at stages when *sall4* is required for pectoral fin development (22hpf and onwards) the *sall4*Δ RNA and subsequently sall4Δ protein is only stable in a proportion of those injected embryos. This idea is entirely consistent with the observation that only a proportion of embryos injected with GFP RNA are GFP positive at 24hpf (Fig. 9E-F). Therefore the protein product of the injected RNA is present in only a fraction of injected embryos at 24hpf. Trying to rescue

pectoral fin development in *sall1a/sall4* double morphant embryos by injection of *fgfr2* mRNA is therefore beyond the limitations of the reagents currently available to me. An alternative approach to overcome this instability could be to injected embryos with a DNA construct containing *fgfr2*. However, injection of DNA into the zebrafish embryo results in a highly mosaic expression pattern.

The vector pCS2+, which I used for my experiments, is commonly used to create *in vitro* transcribed RNA to perform zebrafish misexpression experiments. The pCS2+ vector was initially created for *Xenopus* misexpression experiments and contains the 5' UTR from the *Xenopus β-globin* gene and an SV40 poly(A) tail (Turner and Weintraub, 1994). Recently one group has created a vector specifically designed for zebrafish misexpression experiments (Ro et al., 2004). This vector, called pcGlobin2, contains the 5' and 3' UTRs from the zebrafish *β-globin* gene and a poly(A) tail. Transcripts made using the pcGlobin2 vector are more stable and translated more efficiently than transcripts made using the pCS2+ vector (Ro et al., 2004). Therefore, in future studies the pcGlobin2 vector will be a more useful tool to misexpress genes in the developing pectoral fins. This vector could be used to misexpress *fgfr2* and also *sall1a* and/or *sall4* in the developing pectoral fins to test the dynamics of my model.

fgfr1 is also expressed in the developing pectoral fins (Scholpp et al., 2004). Previous experiments have shown that *Fgfr1* is required for gastrulation during mouse embryonic development (Deng et al., 1994; Yamaguchi et al., 1994). Conditional inactivation of *Fgfr1* in the developing mouse limbs overcame this

early lethality and demonstrated that *Fgfr1* is not required for early stages in limb bud outgrowth, but is instead required for the formation of the autopod (Li et al., 2005; Verheyden et al., 2005). In light of my findings it will be interesting to establish the function of *fgfr1* during pectoral fin development. However, determining this maybe difficult if *fgfr1* is also required for zebrafish gastrulation.

Identifying the regulatory elements required for *Sall4* expression in the developing limbs

To expand my investigation into the regulation of *Sall4* expression in the developing limbs I used a 2kb fragment of the mouse *Sall4* promoter (start codon to 2kb 5') to create transgenic embryos. However, this fragment alone was unable to drive the expression of a reporter gene (LacZ) in the developing limb buds. This suggests that transcription factors required for *Sall4* expression in the developing limbs bind to regulatory sequences outside of this 2kb fragment. By expanding this analysis and using larger fragments of the mouse *Sall4* promoter, which contain sequences 5' and also 3' to the *Sall4* start codon, it maybe possible to identify the regulatory regions that are required for *Sall4* expression in the developing limb buds. Identifying this region will allow us to test if *Tbx5* directly activates the expression of *Sall4* in the developing limbs.

Differences in the process of initiating forelimb outgrowth between zebrafish and higher vertebrates

It appears that during evolution of terrestrial vertebrates *fgf24* was lost and therefore, while sharks and zebrafish possess *fgf24* it is not found in chicks, mice or humans (Draper et al., 2003; Fischer et al., 2003). *fgf24* is essential for zebrafish pectoral fin development (Draper et al., 2003; Fischer et al., 2003). Therefore the function of *fgf24* during forelimb development in terrestrial vertebrates must have been adopted by another FGF gene. In the developing mouse limbs the only FGF gene expressed in the mesenchyme is *Fgf10*. During zebrafish pectoral fin development *fgf24* expression commences before that of *sall4*, while *fgf10* expression initiates after *sall4* is first expressed (Fig. 24). However, during mouse forelimb development *Fgf10* expression begins before *Sall4* (Fig. 24). In the pectoral fin primordia *tbx5* is required for the expression of *fgf24*, which then activates *fgf10* expression (Fig. 2C) (Fischer et al., 2003). It has also been shown that during mouse forelimb development *Tbx5* directly regulates the expression of *Fgf10* (Agarwal et al., 2003). Collectively these observations are consistent with *Fgf10*, during terrestrial vertebrate forelimb development, performing an equivalent function to that of *fgf24* during early stages in the initiation of zebrafish pectoral fin development.

Loss of mouse *Sall4* function disrupts embryonic development

Using my two different *Sall4* loss of function gene trap lines (077 and 015 lines) I have begun to analyse the function of *Sall4* during mouse embryonic

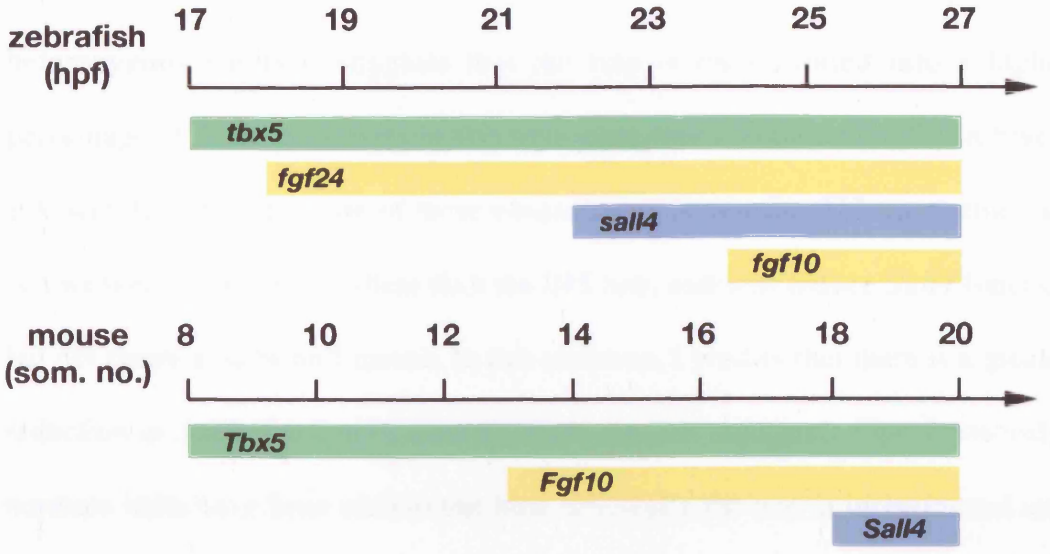

Figure 24. A comparison of gene hierarchies during zebrafish pectoral fin and mouse forelimb development. Schematised is a summary of the time that *Tbx5, Fgf10, Sall4* and *fgf24* begin to be expressed in the zebrafish pectoral fin mesenchyme (top) and the mouse forelimb mesenchyme (bottom). The time is shown as hours post fertilisation for zebrafish embryos and somite numbers for mouse embryos. The data schematised is based on Fig. 6 and 16, and the work of others.

development. When heterozygous 015 and 077 embryos were stained with X-gal I observed greater β-gal activity in 015 embryos (Compare Fig. 19C and E). Currently I have not demonstrated how efficiently the gene trap incorporates into *Sall4* mRNA in the two different transgenic lines. The variation in β-gal activity in the two different lines is likely to reflect differences in the rate the trap is incorporated into *Sall4* mRNA. The greater β-gal activity in 015 heterozygous embryos suggests that the trap is incorporated into a higher percentage of *Sall4* transcripts in this transgenic line compared to 077 embryos. The simplest interpretation of these observations is that the 077 transgenic line is a weaker hypomorphic allele than the 015 line, and will reduce *Sall4* function but not create a *Sall4* null mouse. In this situation, I predict that there is a greater reduction in *Sall4* function in embryos from the 015 transgenic line. Previously, northern blots have been used to test how efficiently the trap is incorporated into a gene trap allele (Pinson et al., 2000). Such experiments could be used to test the efficiency of the 077 and 015 gene trap lines.

Intercrosses of heterozygous 077 mice resulted in homozygous embryos that have an open midbrain, however, as far as could be analysed, limb development appears to be unaffected in these embryos (Fig. 20). I was unable to obtain homozygous 077 embryos that were old enough (E17.5) to perform a detailed analysis of their limb skeletal structure. As I have demonstrated that *sall4* is essential for zebrafish pectoral fin development, the lack of a limb phenotype in homozygous 077 embryos further suggests that the 077 transgenic line is hypomorphic. In this situation the reduction in *Sall4* function in 077 homozygous embryos is not sufficient to disrupt limb development. However,

another possible explanation is that limb development is unaffected in 077 homozygous embryos due to redundancy amongst Sall genes. Individual loss of *Sall1* or *Sall3* function does not affect mouse limb development despite both genes being expressed in the developing limb buds, suggesting Sall genes can substitute for the loss of one another during mouse limb development (Nishinakamura et al., 2001; Parrish et al., 2004). It is therefore not implausible that loss of *Sall4* function in the mouse will not affect limb development as other Sall genes could substitute for the loss of *Sall4* (also see below section: Other investigations using *Sall4* gene trap mice). Further analysis of limb development in homozygous 015 embryos in the future will allow this hypothesis to be tested.

During mouse embryonic development both *Sall1* and *Sall4* are expressed in the developing midbrain (Fig. 16; Buck et al., 2001). *Sall1* null mice do not have a midbrain defect and do not phenocopy Townes-Brocks syndrome (TBS). Instead, mice expressing a truncated form of *Sall1 (Sall1*Δ), which can interact with full-length Sall1-4 proteins, do exhibit TBS-associated phenotypes. These *Sall1*Δ mice have a similar midbrain defect to that seen in homozygous 077 embryos (Kiefer et al., 2003). This midbrain defect has not been reported in *Sall1, Sall2* or *Sall3* null mice (Nishinakamura et al., 2001; Parrish et al., 2004; Sato et al., 2003), suggesting that the midbrain defect of *Sall1*Δ mice arises as Sall1Δ interferes with the function of endogenous Sall4. The co-expression of *Sall1*Δ and *Sall4* in other tissues during embryonic development could result in more similarities between *Sall1*Δ mice and *Sall4* loss of function mice. These observations have implications for the aetiology of TBS and OS. For example,

the absence of thumbs have been reported, with varying penetrance, in OS patients and TBS patients with a premature stop codon in *SALL1* (Kohlhase et al., 2002; Kohlhase et al., 1999). This phenotype has not been described in *Sall1* null mice or *SALL1* haploinsufficient TBS patients, but is present in *Sall1*Δ mice (Borozdin et al., 2006; Kiefer et al., 2003; Nishinakamura et al., 2001). This suggests that during embryonic development *Sall1*Δ interferes with *Sall4* function such that it produces a similar absent thumb phenotype in some OS patients, and TBS patients that have mutations that lead to a premature stop codon in *SALL1*.

Syndactyly is a phenotype that occurs when interdigital programmed cell death (PCD) is disrupted, and results in fused digits. Syndactyly has been reported in the limbs of TBS patients with a premature stop codon in *SALL1* and *Sall1*Δ mice (Kiefer et al., 2003), but not in OS patients, or *Sall1* (Nishinakamura et al., 2001), *Sall2* (Sato et al., 2003) or *Sall3* (Parrish et al., 2004) null mice. The occurrence of syndactylyl only in TBS patients with a premature stop codon in *SALL1* and *Sall1*Δ mice suggests that truncated Sall1 proteins may act dominant negatively to inhibit interdigital PCD. Syndactyly would therefore appear to be specific to TBS patients and not OS patients.

Sall4 function during mouse forelimb development

My analysis has shown that *sall1a* and *sall4* are required for the initiation of *fgfr2* expression in the zebrafish pectoral fin primordia. During mouse limb development *Fgfr2* is thought to mediate the positive feedback loop between

Fgf10 in the limb bud mesenchyme and *Fgf8* in the AER (Xu et al., 1998). The expression of *Fgf10* initiates in the limbs of *Fgfr2* loss of function mice, however, it rapidly becomes downregulated due to a disruption of the *Fgf10/Fgf8* positive feedback loop (Xu et al., 1998). Limb development is severely disrupted in *Fgfr2* knockout mice and the only skeletal elements to form are proximal structures such as the scapula (De Moerlooze et al., 2000; Revest et al., 2001; Xu et al., 1998). Therefore the scapula can form in the absence of *Fgfr2* and this situation is similar to the loss of *Sall4* function in the developing zebrafish pectoral fins (Fig. 8J). Assuming *Sall4* performs an evolutionarily conserved role during zebrafish and mouse forelimb development then *Sall4* will initiate the expression of *Fgfr2* in the limb bud mesenchyme. *Fgfr2* expression will therefore begin after *Sall4* is first detectable, which is after *Fgf10* and *Fgf8* expression has commenced (Fig. 17). In this situation *Fgfr2* will not be required for the initiation of *Fgf10* expression but will mediate the ability of *Fgf8* to maintain *Fgf10* expression. This would be consistent with *Fgfr2* loss of function mice (Xu et al., 1998). In order to test if *Sall4* is required for *Fgfr2* expression, it will be important to establish the exact time point that *Fgfr2* expression commences in the limb mesenchyme, especially in relation to *Sall4*.

Future mouse experiments

As previously mentioned conditional inactivation of *Tbx5* in the developing mouse limbs results in a complete absence of all forelimb skeletal elements (Rallis et al., 2003). *Tbx5* is expressed exclusively in the developing forelimbs

and the closest relative of *Tbx5*, the gene *Tbx4,* is solely expressed in the developing hindlimbs (Chapman et al., 1996). Ectopic expression of *Tbx4* in the developing forelimbs of *Tbx5* conditional knockout mice, using a promoter fragment of the *Prx1* gene, can completely rescue forelimb development (Minguillon et al., 2005). My studies, and others, demonstrate that in the developing mouse and zebrafish forelimbs, prior to forelimb bud formation, *Tbx5* activates the expression of *Fgf10* and *Sall1/Sall4* (Fig. 10E, 13G; Rallis et al., 2003; Agarwal et al., 2003). It will be interesting to see if ectopic expression of these *Tbx5* target genes can also rescue forelimb development in *Tbx5* conditional knockout mice. My studies suggest that ectopic expression of *Fgf10* will not be able to completely rescue forelimb development as, in the absence of *Tbx5,* the expression of *Sall1* and *Sall4* will not initiate. Without *Sall1/Sall4, Fgfr2* will not be expressed in the limb mesenchyme and the *Fgf10/Fgf8* positive feedback loop will not be established. I predict that the feedback loop will only form when both *Fgf10* and *Fgfr2* are expressed in the forelimb-forming region of *Tbx5* conditional knockouts, and in this situation forelimb development will be rescued. The expression of *Fgfr2* in the developing forelimb-forming region maybe achieved by creating transgenic mice that ectopically express *Sall4* and/or *Sall1* using the promoter of the *Prx1* gene. The *Prx1* promoter will drive expression of *Sall4* in the forelimb-forming region prior to the initiation of endogenous *Sall4* expression (P. Hasson and M. Logan, unpublished observation). Therefore, *Prx1-Sall4* transgenic mice could be used to test the transcriptional targets of *Sall4* and the dynamics of FGF signalling in the developing forelimbs.

Other investigations using *Sall4* gene trap mice

Recent work has used a similar approach to my mouse experiments and utilised an available *Sall4* ES cell gene trap line to create heterozygous mice (Koshiba-Takeuchi et al., 2005). Consistent with my studies of the role of *sall4* during zebrafish pectoral fin development, Koshiba-Takeuchi et al suggest that the downregulation of *Sall4* in the forelimbs of heterozygous *Tbx5* null mice indicates that *Sall4* acts downstream of *Tbx5* during forelimb development. Also consistent with my results Koshiba-Takeuchi et al conclude that the downregulation of *Fgf10* in the forelimbs of their heterozygous gene trap mice shows that *Sall4* is required for *Fgf10* expression in the developing forelimbs. Koshiba-Takeuchi et al performed luciferase assays with a fragment of the *Fgf10* promoter and concluded that *Tbx5* and *Sall4* synergistically interact to activate the expression of *Fgf10*. However, my comparative analysis has shown that the expression of *Tbx5, Fgf10, Fgf8* and *Sall4* are initiated sequentially in the developing mouse forelimbs (Fig. 17 and 24). Therefore, as *Fgf10* expression temporally precedes *Sall4* in the forelimb-forming region, the initiation of *Fgf10* expression must be *Sall4*-independent.

The *Sall4* gene trap line used by Koshiba-Takeuchi et al differs from my 015 and 077 gene trap lines, and instead the gene trap has inserted directly into exon 2 of *Sall4*. This results in a predicted fusion of β-geo and the first 383 amino acids of Sall4 (Koshiba-Takeuchi et al., 2005). Functional domains included in these 383 amino acids of *Sall4* are the N-terminal Cys2-His-Cys zinc finger and the glutamine rich domain, but none of the seven Cys2-His2 zinc fingers.

Koshiba-Takeuchi et al show that these heterozygous gene trap mice have a slight elongation of the most anterior digit in the forelimbs, and either a truncation or elongation of the most anterior digit in the hindlimbs. These heterozygous gene trap mice do not have an open midbrain phenotype. The open midbrain phenotype of my homozygous 077 gene trap mice (Fig. 20) suggests that there is a greater disruption of *Sall4* function in these mice compared to the heterozygous gene trap mice described by Koshiba-Takeuchi et al. I did not observe a disruption of limb development in homozygous 077 mice. However, the limb phenotypes described by Koshiba-Takeuchi et al are subtle and only noticeable by analysing the skeletal structure of the limbs. As previously mentioned, I was unable to obtain 077 homozygous embryos old enough (E17.5) to study their skeletal structure.

My experiments have shown that a truncated form of zebrafish and mouse *Sall4* that contains the N-terminal Cys2-His-Cys zinc finger and the glutamine rich domain, can act in a dominant negative fashion and disrupt limb development (Fig. 9). Therefore the *Sall4* gene trap line used by Koshiba-Takeuchi et al may act in a dominant negative fashion. Currently there have been no reports describing an elongation of the most anterior digit of the hindlimbs in OS patients. Therefore the elongation of the anterior digit in the hindlimbs of the gene trap mice described by Koshiba-Takeuchi et al, may result from the truncated *Sall4* protein acting in a dominant negative fashion. Alternatively, such phenotypes may highlight species differences in the role of *Sall4* during hindlimb development.

Holt-Oram and Okihiro syndrome patients have similar limb phenotypes

My studies of *tbx5* and *sall4* function during zebrafish pectoral fin development offer explanations to the similar limb defects seen in HOS and OS patients. I have shown that *tbx5* and *sall4* are required to establish FGF signalling between the mesenchyme and distal ectoderm of the zebrafish pectoral fin bud. The result of disrupting the positive feedback loop between mesenchymal and ectodermal FGFs is demonstrated in classical embryological experiments in the chick in which the AER is surgically removed. When anterior regions of the AER are removed limbs develop that lack anterior skeletal elements (Saunders, 1948). Similarly, alteration of either *Tbx5* or *Sall4* function preferentially leads to a disruption of *Fgf10* in the anterior of the limb bud (Rallis et al., 2003; this study) and it is loss of FGF signalling in this region that ultimately causes the anterior bias of the deletion deformities characteristic of both HOS and OS. My experiments have not resolved the issue of why the anterior fin/limb bud is sensitive to the loss of *Sall4* or *Tbx5* function since both genes are expressed uniformly throughout the early fin bud. A contributing factor could be that partial redundancy amongst Sall–related genes, also present in the limbs, is able to maintain *Fgf10* expression in the posterior of the limb. For example, *Sall3* is expressed in the developing mouse and chick forelimb buds (Ott et al., 2001; Sweetman et al., 2003). If the expression of *Sall3* in the developing limbs is independent of *Tbx5* function then *Sall3* may maintain *Fgf10* expression following a downregulation of *Tbx5*. Such maintenance may occur predominantly in the posterior limb bud. Another, not mutually exclusive, explanation is that *Sall4* is more susceptible to *Tbx5* dosage levels than other

Sall-related genes expressed in the limbs. I have shown that in the developing zebrafish pectoral fin buds *sall1a* is required to maintain *fgf10* expression in the posterior fin bud. I demonstrated that *sall1a* and *sall4* expression is dependant on *tbx5,* however, I could not distinguish if *sall1a* expression is more or less susceptible to tbx5 dosage levels than *sall4*. In humans, if *SALL4* is more susceptible to *TBX5* dosage levels than *SALL1,* then the reduction of *TBX5* function in HOS patients would result in a downregulation of *SALL4* but not *SALL1*. In this situation *FGF10* would become downregulated in the anterior limb bud, but would continue to be expressed in the posterior, subsequently resulting in an anterior bias to HOS and OS patients limb defects.

The specification of proximal limb structures

The scapulocoracoid, a proximal pectoral fin skeletal element that is equivalent to the scapula present in higher vertebrates, is always formed normally in *sall4* morphant embryos (Fig. 8J) and therefore forms independently of *sall4* function. This differs from *tbx5* and *fgf24* mutant embryos which lack all pectoral fin structures, including the scapulocoracoid (Ahn et al., 2002; Garrity et al., 2002). These experiments suggest that specification of proximal pectoral fin structures is dependant on *tbx5* and *fgf24* function and may occur at stages prior to the initiation of *sall4* expression. The formation of these proximal skeletal elements also suggests that *fgf24* performs functions other than just the induction of *fgf10* expression. A parallel situation occurs during mouse limb development as *Tbx5* conditional knockouts lack all forelimb structures including the scapula and clavicle (Rallis et al., 2003) while *Fgf10*-null mice possess a scapula rudiment

(Min et al., 1998; Sekine et al., 1999). This similarly suggests that *Tbx5* not only activates the expression of *Fgf10* in the developing mouse forelimbs but also other target genes. A possible downstream target, or co-factor, of *Tbx5* that is required for scapula formation, is the homeobox gene *Emx2*. Loss of mouse *Emx2* function results in mice that lack a scapula but form more distal limb skeletal elements (Pellegrini et al., 2001).

The differential requirement of *Sall4* and *Tbx5* to form proximal limb skeletal elements is also apparent in humans. Although the limb defects of OS and HOS patients are very similar, there are some important differences. Defects affecting the proximal forelimb, such as hypoplastic clavicles, have been reported in HOS patients and are consistent with *Tbx5* being required for the formation all limb skeletal elements (Newbury-Ecob et al., 1996). However, similar defects in proximal limb skeletal elements have not been reported in OS patients. My data suggests that these proximal forelimb abnormalities are not observed in OS patients as these structures are specified independently of *Sall4* function. These observations are therefore clinically significant as defects affecting proximal limb elements such as the clavicle should be specific to HOS and not OS.

The phenotype of HOS and OS patients can be so similar that previously some patients with mutations in *SALL4* have initially been diagnosed with HOS (Brassington et al., 2003). Also, the absence of detectable *TBX5* mutations in patients diagnosed with HOS has led to the suggestion that HOS is a heterogenous disorder and that *TBX5* mutations only account for approximately 30% of all HOS patients (Cross et al., 2000). The diagnosis of HOS or OS is

complicated by the observations that patients with mutations in *TBX5* and *SALL4* can both have ventricular septal heart defects (Kohlhase et al., 2002; Packham and Brook, 2003). A further problem is that Duane anomaly is thought to be a defining feature of OS, however, it is only present in 70% of patients with mutations in *SALL4* (Kohlhase et al., 2005). Therefore in the absence of Duane anomaly a diagnosis of OS cannot be excluded. My observations should now lead to a better clinical diagnosis of HOS and OS patients. Patients with defects in their clavicle and scapula should be considered as HOS, while patients with a normal scapula and clavicle, and more distal limb defects, should be considered for *SALL4* mutation analysis.

SALL4 mutations and Okihiro syndrome

Previous studies have shown that TBS can result from mutations that lead to a premature transcriptional stop codon, and the expression of a truncated, dominant negative, SALL1 protein (Kiefer et al., 2003; Kohlhase et al., 1999). Several of the mutations in *SALL4* that have been described result in a premature stop codon (Fig. 6C) (Kohlhase et al., 2005). As previously mentioned, misexpression of a truncated form of *Sall4* generated phenotypes that were similar to those obtained from *sall4* knockdown and comparable to the limb phenotypes of OS patients (Fig. 9B-D). This suggests that a truncated Sall4 protein can act in a dominant negative fashion. It is therefore possible that mutations in *SALL4* that lead to a premature stop codon, result in the translation of a truncated, dominant negative, *SALL4* protein. However, there is no evidence from OS patients that these transcripts are translated into dominant

negative proteins. Furthermore, examples have been described in which some OS patients are heterozygous for large deletions which span all, or some, of the four *SALL4* exons (Fig. 6C) (Borozdin et al., 2004). Therefore a truncated *SALL4* protein will not be made in these patients. This observation means that OS can result from *SALL4* haploinsufficiency. Mutations that lead to a premature stop codon in *SALL4* may lead to mRNA degradation, through a process known a nonsense-mediated decay (Frischmeyer and Dietz, 1999), and therefore result in *SALL4* haploinsufficiency. The disruption of limb development through the actions of a dominant-negative Sall4 protein in our animal models may not occur in OS patients. As there are no apparent differences in the phenotypes of OS patients with mutations that lead to a premature stop codon in *SALL4*, or those with large heterozygous deletions in *SALL4*, then it should continue to be assumed that OS results from *SALL4* haploinsufficiency. However, future analysis of the function of *Sall4* should consider that truncated Sall4 proteins can act in a dominant negative fashion.

Asymmetrical limb development

During vertebrate embryonic development the internal organs are subjected to left-right patterning signals that results in their asymmetrical development. However, externally the vertebrate body plan, including the limbs, appears symmetrical. In both OS and HOS patients the left limb is typically more severely affected than the right (Kohlhase et al., 2002; Packham and Brook, 2003) and this is a characteristic of both syndromes. There are very few examples of asymmetrical limb defects. The only other example is that observed

when retinoic acid (RA) is supplied to *Raldh2*$^{-/-}$ mouse embryos (Niederreither et al., 2002). Forelimb development does not initiate in *Raldh2*$^{-/-}$ mouse embryos (Niederreither et al., 1999). When RA is exogenously supplied to *Raldh2*$^{-/-}$ embryos forelimb development is partially rescued, however, the left rescued forelimb is more severely truncated than the right. Three recent studies have shown that RA is required for the symmetrical formation of somites during vertebrate embryonic development (Kawakami et al., 2005; Vermot et al., 2005; Vermot and Pourquie, 2005). Inhibition of RA signalling results in asymmetrical somite formation such that somite development is delayed on the left side.

Previous studies have shown that *raldh2* is required for the expression of *tbx5* in the developing zebrafish pectoral fins (Begemann et al., 2001). I have also demonstrated that *tbx5* is required for the expression of *sall4* in the developing zebrafish pectoral fins (Fig. 10E). These observations suggest a connection between *Tbx5*, *Sall4* and RA signalling during the correct symmetrical development of the forelimbs. Future analysis could use quantitative RT-PCR to test if *Sall4* is asymmetrically expressed in the developing forelimbs. RA synthesis can be blocked by using the chemical inhibitor disulfiram, which inhibits Raldh2 (Vermot and Pourquie, 2005). The relationship between RA, *Tbx5* and *Sall4* could be investigated by blocking RA synthesis and seeing what affect this has on the transcription of *Tbx5* and *Sall4* in the left and right forelimbs.

Interestingly, a recent paper identified some OS patients in which the right limb was more severely affected than the left (Terhal et al., 2006). These OS patients

have in mutation in *SALL4* (c2713C>T) that results in a premature stop codon. The mutation site is 29bp 5' to the splice donor site of the intron between exons 3 and 4 of *SALL4*. Terhal et al. suggest that as this mutation is near to the splice donor site, the mutated *SALL4* mRNA will not undergo nonsense-mediated decay. Such an mRNA would be translated into a truncated SALL4 protein that does not contain the second zinc finger of the most carboxyterminal double zinc finger domain. It is interesting to speculate that the mutation described by Terhal et al. maps a specific domain of *SALL4* that is required for the correct symmetrical development of the limbs. This can be tested using the *Prx1* promoter. I have demonstrated that misexpression of a truncated form *Sall4* (*Sall4*Δ), which was designed to mimic the mutation 842delG, disrupts forelimb development in zebrafish and chick embryos (Fig. 9). Based on these observations, I predict forelimb development will be disrupted when *Sall4*Δ is misexpressed in the mouse limb buds using the *Prx1* promoter. Such experiments may result in a more severely truncated left limb compared to the right, as patients with the mutation 842delG present such asymmetry (Fig. 4A) (Kohlhase et al., 2002). This asymmetry maybe reversed if a truncated form of *Sall4,* which is designed to mimic the mutation c2713C>T, is misexpressed in the developing limbs. If asymmetry is reversed then this will demonstrate the *SALL4* mutation identified by Terhal et al. marks a functional domain of SALL4 that is required for the correct symmetrical development of the limbs.

The role of *Sall4* in hindlimb development

During mouse embryonic development *Sall4* is expressed in the developing

hindlimbs as well as the forelimbs (Fig. 16D). OS is characterised by forelimb defects and the eye disorder Duane anomaly (Al-Baradie et al., 2002; Kohlhase et al., 2002). There have however been reports describing a large gap between the first and second toes of OS patients (Kohlhase et al., 2003). This so-called widened "sandal-gap" phenotype has also been reported in small patella syndrome (SPS) patients, which have mutations in *TBX4* (Bongers et al., 2004). During mouse limb development *Tbx4* and *Tbx5* perform similar roles in hindlimb and forelimb development, respectively (Minguillon et al., 2005). These observations suggest that during hindlimb development *Sall4* and *Tbx4* have a comparable relationship to *Sall4* and *Tbx5* in the developing forelimbs, and subsequently similar sandal gap defects are seen in SPS and some OS patients. Using a MO, I have shown that *sall4* is required for zebrafish pectoral fin development. To investigate the function of genes during pectoral fin development, I injected MOs into the 1-, 2- or 4- cell stage embryo. Pelvic fin development (hindlimb) does not begin until the third week in development. MOs injected into 1-, 2- or 4- cell stage embryos are likely to degrade before hindlimb development commences. Unfortunately, I was therefore unable to investigate the function of *sall4* during pelvic fin development.

The role of *Sall4* in the development of other tissues

My studies have shown that during zebrafish pectoral fin development *sall1a* and *sall4* act downstream of *tbx5,* to initiate FGF signalling (Fig. 15E). My observations have broader implications of the relationship between Sall and T-box genes during FGF signalling in the development of other tissues. In *sall4*

morphant embryos pharyngeal arch development is disrupted, resulting in craniofacial defects (Fig. 22). These observations are consistent with the reported observation that some OS patients have hemifacial microsomia and facial asymmetry (Kohlhase et al., 2002; Terhal et al., 2006). My work, and others (Norton et al., 2005), has shown that during pectoral fin development *dlx2* expression is dependant on FGF signalling, and therefore *dlx2* expression is downregulated in *sall4* morphant pectoral fins (Fig. 11G-H). *dlx2* is also downregulated in the pharyngeal arches of *sall4* morphant embryos (Fig. 22C-D). The development of the pharyngeal arches is also dependent on FGF signalling (*fgf3* and *fgf8*) and the T-box gene *tbx1* (Crump et al., 2004; Piotrowski and Nusslein-Volhard, 2000). Loss of *fgf3, fgf8* or *tbx1* function results in a downregulation of *dlx2* expression in the pharyngeal arches (Crump et al., 2004; Piotrowski and Nusslein-Volhard, 2000). These observations suggest that *sall4* is required for FGF signalling during pharyngeal arch development, as well as pectoral fin development. It is also possible that *tbx1* and *sall4* are required during pharyngeal arch development to establish FGF signalling in an analogous manner to that of *tbx5* and *sall4* during pectoral fin development. Another situation in which a T-box gene is required for the expression of a Sall gene occurs in the drosophila wing imaginal disc. Here the T-box gene *optomotor blind* (*omb)* is required for the expression of *spalt* (*sal*) (Del Alamo Rodriguez et al., 2004). These observations may suggest that Sall and T-box genes form an evolutionarily conserved transcriptional regulatory cassette that is required for the growth of different tissues during embryonic development.

Summary

My investigation into the function of *Sall4* has uncovered a transcriptional motif that is required to establish specific FGF signalling dynamics during early zebrafish pectoral fin development. This establishment is required to initiate the outgrowth of the developing fin bud. It will be interesting to see if future studies uncover similar transcriptional motifs that are required to initiate the development and growth of other tissues during embryonic development. It will now be interesting to firmly establish the function of *Sall4* during limb development in higher vertebrates, especially due to the absence of *fgf24* in terrestrial vertebrates. Such investigations will help to understand species-specific differences during limb development and further understand the growth of tissues during embryonic development. My experiments have highlighted differences between the function of *Tbx5* and *Sall4* during the development of proximal forelimb structures. Hopefully these differences will, in the future, lead to a better diagnosis of HOS and OS.

5. REFERENCES

Agarwal, P., Wylie, J. N., Galceran, J., Arkhitko, O., Li, C., Deng, C., Grosschedl, R. and Bruneau, B. G. (2003). Tbx5 is essential for forelimb bud initiation following patterning of the limb field in the mouse embryo. *Development* **130**, 623-33.

Ahn, D. G., Kourakis, M. J., Rohde, L. A., Silver, L. M. and Ho, R. K. (2002). T-box gene tbx5 is essential for formation of the pectoral limb bud. *Nature* **417**, 754-8.

Al-Baradie, R., Yamada, K., St Hilaire, C., Chan, W. M., Andrews, C., McIntosh, N., Nakano, M., Martonyi, E. J., Raymond, W. R., Okumura, S. et al. (2002). Duane radial ray syndrome (Okihiro syndrome) maps to 20q13 and results from mutations in SALL4, a new member of the SAL family. *Am J Hum Genet* **71**, 1195-9.

Amores, A., Force, A., Yan, Y. L., Joly, L., Amemiya, C., Fritz, A., Ho, R. K., Langeland, J., Prince, V., Wang, Y. L. et al. (1998). Zebrafish hox clusters and vertebrate genome evolution. *Science* **282**, 1711-4.

Ang, H. L., Deltour, L., Hayamizu, T. F., Zgombic-Knight, M. and Duester, G. (1996). Retinoic acid synthesis in mouse embryos during gastrulation and craniofacial development linked to class IV alcohol dehydrogenase gene expression. *J Biol Chem* **271**, 9526-34.

Barrow, J. R., Thomas, K. R., Boussadia-Zahui, O., Moore, R., Kemler, R., Capecchi, M. R. and McMahon, A. P. (2003). Ectodermal Wnt3/beta-catenin signaling is required for the establishment and maintenance of the apical ectodermal ridge. *Genes Dev* **17**, 394-409.

Basson, C. T., Cowley, G. S., Solomon, S. D., Weissman, B., Poznanski, A. K., Traill, T. A., Seidman, J. G. and Seidman, C. E. (1994). The clinical and genetic spectrum of the Holt-Oram syndrome (heart-hand syndrome). *N Engl J Med* **330**, 885-91.

Basson, C. T., Bachinsky, D. R., Lin, R. C., Levi, T., Elkins, J. A., Soults, J., Grayzel, D., Kroumpouzou, E., Traill, T. A., Leblanc-Straceski, J. et al. (1997). Mutations in human TBX5 [corrected] cause limb and cardiac malformation in Holt-Oram syndrome. *Nat Genet* **15**, 30-5.

Basson, M. and Horvitz, H. R. (1996). The Caenorhabditis elegans gene sem-4 controls neuronal and mesodermal cell development and encodes a zinc finger protein. *Genes Dev* **10**, 1953-65.

Begemann, G. and Ingham, P. W. (2000). Developmental regulation of Tbx5 in zebrafish embryogenesis. *Mech Dev* **90**, 299-304.

Begemann, G., Schilling, T. F., Rauch, G. J., Geisler, R. and Ingham, P. W. (2001). The zebrafish neckless mutation reveals a requirement for raldh2 in mesodermal signals that pattern the hindbrain. *Development* **128**, 3081-94.

Bejsovec, A. (2005). Wnt pathway activation: new relations and locations. *Cell* **120**, 11-4.

Bellusci, S., Grindley, J., Emoto, H., Itoh, N. and Hogan, B. L. (1997). Fibroblast growth factor 10 (FGF10) and branching morphogenesis in the embryonic mouse lung. *Development* **124**, 4867-78.

Bongers, E. M., Duijf, P. H., van Beersum, S. E., Schoots, J., Van Kampen, A., Burckhardt, A., Hamel, B. C., Losan, F., Hoefsloot, L. H., Yntema, H. G. et al. (2004). Mutations in the human TBX4 gene cause small patella syndrome. *Am J Hum Genet* **74**, 1239-48.

Borozdin, W., Boehm, D., Leipoldt, M., Wilhelm, C., Reardon, W., Clayton-Smith, J., Becker, K., Muhlendyck, H., Winter, R., Giray, O. et al. (2004).

SALL4 deletions are a common cause of Okihiro and acro-renal-ocular syndromes and confirm haploinsufficiency as the pathogenic mechanism. *J Med Genet* **41**, e113.

Borozdin, W., Steinmann, K., Albrecht, B., Bottani, A., Devriendt, K., Leipoldt, M. and Kohlhase, J. (2006). Detection of heterozygous SALL1 deletions by quantitative real time PCR proves the contribution of a SALL1 dosage effect in the pathogenesis of Townes-Brocks syndrome. *Hum Mutat* **27**, 211-212.

Botzenhart, E. M., Green, A., Ilyina, H., Konig, R., Lowry, R. B., Lo, I. F., Shohat, M., Burke, L., McGaughran, J., Chafai, R. et al. (2005). SALL1 mutation analysis in Townes-Brocks syndrome: twelve novel mutations and expansion of the phenotype. *Hum Mutat* **26**, 282.

Boulet, A. M., Moon, A. M., Arenkiel, B. R. and Capecchi, M. R. (2004). The roles of Fgf4 and Fgf8 in limb bud initiation and outgrowth. *Dev Biol* **273**, 361-72.

Boyer, L. A., Lee, T. I., Cole, M. F., Johnstone, S. E., Levine, S. S., Zucker, J. P., Guenther, M. G., Kumar, R. M., Murray, H. L., Jenner, R. G. et al. (2005). Core transcriptional regulatory circuitry in human embryonic stem cells. *Cell* **122**, 947-56.

Brassington, A. M., Sung, S. S., Toydemir, R. M., Le, T., Roeder, A. D., Rutherford, A. E., Whitby, F. G., Jorde, L. B. and Bamshad, M. J. (2003). Expressivity of Holt-Oram syndrome is not predicted by TBX5 genotype. *Am J Hum Genet* **73**, 74-85.

Bruneau, B. G., Logan, M., Davis, N., Levi, T., Tabin, C. J., Seidman, J. G. and Seidman, C. E. (1999). Chamber-specific cardiac expression of Tbx5 and heart defects in Holt-Oram syndrome. *Dev Biol* **211**, 100-8.

Buck, A., Kispert, A. and Kohlhase, J. (2001). Embryonic expression of the murine homologue of SALL1, the gene mutated in Townes--Brocks syndrome. *Mech Dev* **104**, 143-6.

Camp, E., Hope, R., Kortschak, R. D., Cox, T. C. and Lardelli, M. (2003). Expression of three spalt (sal) gene homologues in zebrafish embryos. *Dev Genes Evol* **213**, 35-43.

Chapman, D. L., Garvey, N., Hancock, S., Alexiou, M., Agulnik, S. I., Gibson-Brown, J. J., Cebra-Thomas, J., Bollag, R. J., Silver, L. M. and Papaioannou, V. E. (1996). Expression of the T-box family genes, Tbx1-Tbx5, during early mouse development. *Dev Dyn* **206**, 379-90.

Chiang, C., Litingtung, Y., Harris, M. P., Simandl, B. K., Li, Y., Beachy, P. A. and Fallon, J. F. (2001). Manifestation of the limb prepattern: limb development in the absence of sonic hedgehog function. *Dev Biol* **236**, 421-35.

Cohn, M. J., Izpisua-Belmonte, J. C., Abud, H., Heath, J. K. and Tickle, C. (1995). Fibroblast growth factors induce additional limb development from the flank of chick embryos. *Cell* **80**, 739-46.

Colvin, J. S., Green, R. P., Schmahl, J., Capel, B. and Ornitz, D. M. (2001). Male-to-female sex reversal in mice lacking fibroblast growth factor 9. *Cell* **104**, 875-89.

Cross, S. J., Ching, Y. H., Li, Q. Y., Armstrong-Buisseret, L., Spranger, S., Lyonnet, S., Bonnet, D., Penttinen, M., Jonveaux, P., Leheup, B. et al. (2000). The mutation spectrum in Holt-Oram syndrome. *J Med Genet* **37**, 785-7.

Crossley, P. H. and Martin, G. R. (1995). The mouse Fgf8 gene encodes a family of polypeptides and is expressed in regions that direct outgrowth and patterning in the developing embryo. *Development* **121**, 439-51.
Crossley, P. H., Minowada, G., MacArthur, C. A. and Martin, G. R. (1996). Roles for FGF8 in the induction, initiation, and maintenance of chick limb development. *Cell* **84**, 127-36.
Crump, J. G., Maves, L., Lawson, N. D., Weinstein, B. M. and Kimmel, C. B. (2004). An essential role for Fgfs in endodermal pouch formation influences later craniofacial skeletal patterning. *Development* **131**, 5703-16.
de Celis, J. F., Barrio, R. and Kafatos, F. C. (1996). A gene complex acting downstream of dpp in Drosophila wing morphogenesis. *Nature* **381**, 421-4.
De Moerlooze, L. and Dickson, C. (1997). Skeletal disorders associated with fibroblast growth factor receptor mutations. *Curr Opin Genet Dev* **7**, 378-85.
De Moerlooze, L., Spencer-Dene, B., Revest, J., Hajihosseini, M., Rosewell, I. and Dickson, C. (2000). An important role for the IIIb isoform of fibroblast growth factor receptor 2 (FGFR2) in mesenchymal-epithelial signalling during mouse organogenesis. *Development* **127**, 483-92.
Del Alamo Rodriguez, D., Terriente Felix, J. and Diaz-Benjumea, F. J. (2004). The role of the T-box gene optomotor-blind in patterning the Drosophila wing. *Dev Biol* **268**, 481-92.
Deng, C. X., Wynshaw-Boris, A., Shen, M. M., Daugherty, C., Ornitz, D. M. and Leder, P. (1994). Murine FGFR-1 is required for early postimplantation growth and axial organization. *Genes Dev* **8**, 3045-57.
Draper, B. W., Morcos, P. A. and Kimmel, C. B. (2001). Inhibition of zebrafish fgf8 pre-mRNA splicing with morpholino oligos: a quantifiable method for gene knockdown. *Genesis* **30**, 154-6.
Draper, B. W., Stock, D. W. and Kimmel, C. B. (2003). Zebrafish fgf24 functions with fgf8 to promote posterior mesodermal development. *Development* **130**, 4639-54.
Fallon, J. F., Lopez, A., Ros, M. A., Savage, M. P., Olwin, B. B. and Simandl, B. K. (1994). FGF-2: apical ectodermal ridge growth signal for chick limb development. *Science* **264**, 104-7.
Farrell, E. R. and Munsterberg, A. E. (2000). csal1 is controlled by a combination of FGF and Wnt signals in developing limb buds. *Dev Biol* **225**, 447-58.
Fernandez-Teran, M., Piedra, M. E., Simandl, B. K., Fallon, J. F. and Ros, M. A. (1997). Limb initiation and development is normal in the absence of the mesonephros. *Dev Biol* **189**, 246-55.
Fischer, S., Draper, B. W. and Neumann, C. J. (2003). The zebrafish fgf24 mutant identifies an additional level of Fgf signaling involved in vertebrate forelimb initiation. *Development* **130**, 3515-24.
Frischmeyer, P. A. and Dietz, H. C. (1999). Nonsense-mediated mRNA decay in health and disease. *Hum Mol Genet* **8**, 1893-900.
Galceran, J., Farinas, I., Depew, M. J., Clevers, H. and Grosschedl, R. (1999). Wnt3a-/--like phenotype and limb deficiency in Lef1(-/-)Tcf1(-/-) mice. *Genes Dev* **13**, 709-17.
Garcia-Garcia, M. J. and Anderson, K. V. (2003). Essential role of glycosaminoglycans in Fgf signaling during mouse gastrulation. *Cell* **114**, 727-37.

Garrity, D. M., Childs, S. and Fishman, M. C. (2002). The heartstrings mutation in zebrafish causes heart/fin Tbx5 deficiency syndrome. *Development* **129**, 4635-45.
Geduspan, J. S. and Solursh, M. (1992). A growth-promoting influence from the mesonephros during limb outgrowth. *Dev Biol* **151**, 242-50.
Ghosh, T. K., Packham, E. A., Bonser, A. J., Robinson, T. E., Cross, S. J. and Brook, J. D. (2001). Characterization of the TBX5 binding site and analysis of mutations that cause Holt-Oram syndrome. *Hum Mol Genet* **10**, 1983-94.
Gibson-Brown, J. J., S, I. A., Silver, L. M. and Papaioannou, V. E. (1998). Expression of T-box genes Tbx2-Tbx5 during chick organogenesis. *Mech Dev* **74**, 165-9.
Gill, G. (2004). SUMO and ubiquitin in the nucleus: different functions, similar mechanisms? *Genes Dev* **18**, 2046-59.
Grandel, H. and Schulte-Merker, S. (1998). The development of the paired fins in the zebrafish (Danio rerio). *Mech Dev* **79**, 99-120.
Grandel, H., Lun, K., Rauch, G. J., Rhinn, M., Piotrowski, T., Houart, C., Sordino, P., Kuchler, A. M., Schulte-Merker, S., Geisler, R. et al. (2002). Retinoic acid signalling in the zebrafish embryo is necessary during pre-segmentation stages to pattern the anterior-posterior axis of the CNS and to induce a pectoral fin bud. *Development* **129**, 2851-65.
Greenbaum, S., Lazorchak, A. S. and Zhuang, Y. (2004). Differential functions for the transcription factor E2A in positive and negative gene regulation in pre-B lymphocytes. *J Biol Chem* **279**, 45028-35.
Hamburger, V. and Hamilton, H. L. (1951). A series of normal stages in the development of the chick embryo. *J. Exp. Morph.* **88**, 49-92.
Igarashi, M., Finch, P. W. and Aaronson, S. A. (1998). Characterization of recombinant human fibroblast growth factor (FGF)-10 reveals functional similarities with keratinocyte growth factor (FGF-7). *J Biol Chem* **273**, 13230-5.
Kaufman, M. H. (1992). The Atlas of Mouse Development. *Academic Press.*
Kawakami, Y., Capdevila, J., Buscher, D., Itoh, T., Rodriguez Esteban, C. and Izpisua Belmonte, J. C. (2001). WNT signals control FGF-dependent limb initiation and AER induction in the chick embryo. *Cell* **104**, 891-900.
Kawakami, Y., Raya, A., Raya, R. M., Rodriguez-Esteban, C. and Belmonte, J. C. (2005). Retinoic acid signalling links left-right asymmetric patterning and bilaterally symmetric somitogenesis in the zebrafish embryo. *Nature* **435**, 165-71.
Kengaku, M., Capdevila, J., Rodriguez-Esteban, C., De La Pena, J., Johnson, R. L., Belmonte, J. C. and Tabin, C. J. (1998). Distinct WNT pathways regulating AER formation and dorsoventral polarity in the chick limb bud. *Science* **280**, 1274-7.
Khan, P., Linkhart, B. and Simon, H. G. (2002). Different regulation of T-box genes Tbx4 and Tbx5 during limb development and limb regeneration. *Dev Biol* **250**, 383-92.
Kiefer, S. M., McDill, B. W., Yang, J. and Rauchman, M. (2002). Murine Sall1 represses transcription by recruiting a histone deacetylase complex. *J Biol Chem* **277**, 14869-76.
Kiefer, S. M., Ohlemiller, K. K., Yang, J., McDill, B. W., Kohlhase, J. and Rauchman, M. (2003). Expression of a truncated Sall1 transcriptional repressor

is responsible for Townes-Brocks syndrome birth defects. *Hum Mol Genet* **12**, 2221-7.

Kilian, B., Mansukoski, H., Barbosa, F. C., Ulrich, F., Tada, M. and Heisenberg, C. P. (2003). The role of Ppt/Wnt5 in regulating cell shape and movement during zebrafish gastrulation. *Mech Dev* **120**, 467-76.

Kimmel, C. B., Ballard, W. W., Kimmel, S. R., Ullmann, B. and Schilling, T. F. (1995) Stages of embryonic development of the zebrafish. *Dev Dyn* **203**, 253-310.

Kohlhase, J., Wischermann, A., Reichenbach, H., Froster, U. and Engel, W. (1998). Mutations in the SALL1 putative transcription factor gene cause Townes-Brocks syndrome. *Nat Genet* **18**, 81-3.

Kohlhase, J., Taschner, P. E., Burfeind, P., Pasche, B., Newman, B., Blanck, C., Breuning, M. H., ten Kate, L. P., Maaswinkel-Mooy, P., Mitulla, B. et al. (1999). Molecular analysis of SALL1 mutations in Townes-Brocks syndrome. *Am J Hum Genet* **64**, 435-45.

Kohlhase, J., Altmann, M., Archangelo, L., Dixkens, C. and Engel, W. (2000). Genomic cloning, chromosomal mapping, and expression analysis of msal-2. *Mamm Genome* **11**, 64-8.

Kohlhase, J., Heinrich, M., Schubert, L., Liebers, M., Kispert, A., Laccone, F., Turnpenny, P., Winter, R. M. and Reardon, W. (2002). Okihiro syndrome is caused by SALL4 mutations. *Hum Mol Genet* **11**, 2979-87.

Kohlhase, J., Schubert, L., Liebers, M., Rauch, A., Becker, K., Mohammed, S. N., Newbury-Ecob, R. and Reardon, W. (2003). Mutations at the SALL4 locus on chromosome 20 result in a range of clinically overlapping phenotypes, including Okihiro syndrome, Holt-Oram syndrome, acro-renal-ocular syndrome, and patients previously reported to represent thalidomide embryopathy. *J Med Genet* **40**, 473-8.

Kohlhase, J., Chitayat, D., Kotzot, D., Ceylaner, S., Froster, U. G., Fuchs, S., Montgomery, T. and Rosler, B. (2005). SALL4 mutations in Okihiro syndrome (Duane-radial ray syndrome), acro-renal-ocular syndrome, and related disorders. *Hum Mutat* **26**, 176-83.

Koshiba-Takeuchi, K., Takeuchi, J. K., Arruda, E. P., Kathiriya, I. S., Mo, R., Hui, C. C., Srivastava, D. and Bruneau, B. G. (2005). Cooperative and antagonistic interactions between Sall4 and Tbx5 pattern the mouse limb and heart. *Nat Genet.* **38**, 175-83.

Koster, R., Stick, R., Loosli, F. and Wittbrodt, J. (1997). Medaka spalt acts as a target gene of hedgehog signaling. *Development* **124**, 3147-56.

Kraus, P., Fraidenraich, D. and Loomis, C. A. (2001). Some distal limb structures develop in mice lacking Sonic hedgehog signaling. *Mech Dev* **100**, 45-58.

Kuhnlein, R. P., Frommer, G., Friedrich, M., Gonzalez-Gaitan, M., Weber, A., Wagner-Bernholz, J. F., Gehring, W. J., Jackle, H. and Schuh, R. (1994). spalt encodes an evolutionarily conserved zinc finger protein of novel structure which provides homeotic gene function in the head and tail region of the Drosophila embryo. *Embo J* **13**, 168-79.

Laufer, E., Nelson, C. E., Johnson, R. L., Morgan, B. A. and Tabin, C. (1994). Sonic hedgehog and Fgf-4 act through a signaling cascade and feedback loop to integrate growth and patterning of the developing limb bud. *Cell* **79**, 993-1003.

Lee, T. I., Rinaldi, N. J., Robert, F., Odom, D. T., Bar-Joseph, Z., Gerber, G. K., Hannett, N. M., Harbison, C. T., Thompson, C. M., Simon, I. et al. (2002). Transcriptional regulatory networks in Saccharomyces cerevisiae. *Science* **298**, 799-804.
Lewandoski, M., Sun, X. and Martin, G. R. (2000). Fgf8 signalling from the AER is essential for normal limb development. *Nat Genet* **26**, 460-3.
Li, C., Xu, X., Nelson, D. K., Williams, T., Kuehn, M. R. and Deng, C. X. (2005). FGFR1 function at the earliest stages of mouse limb development plays an indispensable role in subsequent autopod morphogenesis. *Development* **132**, 4755-64.
Li, D., Tian, Y., Ma, Y. and Benjamin, T. (2004). p150(Sal2) is a p53-independent regulator of p21(WAF1/CIP). *Mol Cell Biol* **24**, 3885-93.
Li, Q. Y., Newbury-Ecob, R. A., Terrett, J. A., Wilson, D. I., Curtis, A. R., Yi, C. H., Gebuhr, T., Bullen, P. J., Robson, S. C., Strachan, T. et al. (1997). Holt-Oram syndrome is caused by mutations in TBX5, a member of the Brachyury (T) gene family. *Nat Genet* **15**, 21-9.
Lin, X., Buff, E. M., Perrimon, N. and Michelson, A. M. (1999). Heparan sulfate proteoglycans are essential for FGF receptor signaling during Drosophila embryonic development. *Development* **126**, 3715-23.
Logan, M. and Tabin, C. (1998). Targeted gene misexpression in chick limb buds using avian replication-competent retroviruses. *Methods* **14**, 407-20.
Logan, M. (2003). Finger to toe: the molecular basis of limb identity. *Development* **130**. 6401-10.
Mangan, S. and Alon, U. (2003). Structure and function of the feed-forward loop network motif. *Proc Natl Acad Sci U S A* **100**, 11980-5.
Martin, G. R. (1998). The roles of FGFs in the early development of vertebrate limbs. *Genes Dev* **12**, 1571-86.
Miertus, J., Borozdin, W., Frecer, V., Tonini, G., Bertok, S., Amoroso, A., Miertus, S. and Kohlhase, J. (2006). A SALL4 zinc finger missense mutation predicted to result in increased DNA binding affinity is associated with cranial midline defects and mild features of Okihiro syndrome. *Hum Genet*, 1-8.
Min, H., Danilenko, D. M., Scully, S. A., Bolon, B., Ring, B. D., Tarpley, J. E., DeRose, M. and Simonet, W. S. (1998). Fgf-10 is required for both limb and lung development and exhibits striking functional similarity to Drosophila branchless. *Genes Dev* **12**, 3156-61.
Minguillon, C. and Logan, M. (2003). The comparative genomics of T-box genes. *Brief Funct Genomic Proteomic* **2**, 224-33.
Minguillon, C., Del Buono, J. and Logan, M. P. (2005). Tbx5 and Tbx4 are not sufficient to determine limb-specific morphologies but have common roles in initiating limb outgrowth. *Dev Cell* **8**, 75-84.
Mollereau, B., Dominguez, M., Webel, R., Colley, N. J., Keung, B., de Celis, J. F. and Desplan, C. (2001). Two-step process for photoreceptor formation in Drosophila. *Nature* **412**, 911-3.
Morriss-Kay, G. M. and Sokolova, N. (1996). Embryonic development and pattern formation. *Faseb J* **10**, 961-8.
Naiche, L. A. and Papaioannou, V. E. (2003). Loss of Tbx4 blocks hindlimb development and affects vascularization and fusion of the allantois. *Development* **130**, 2681-93.
Nasevicius, A. and Ekker, S. C. (2000). Effective targeted gene 'knockdown' in zebrafish. *Nat Genet* **26**, 216-20.

Netzer, C., Rieger, L., Brero, A., Zhang, C. D., Hinzke, M., Kohlhase, J. and Bohlander, S. K. (2001). SALL1, the gene mutated in Townes-Brocks syndrome, encodes a transcriptional repressor which interacts with TRF1/PIN2 and localizes to pericentromeric heterochromatin. *Hum Mol Genet* **10**, 3017-24.
Netzer, C., Bohlander, S. K., Rieger, L., Muller, S. and Kohlhase, J. (2002). Interaction of the developmental regulator SALL1 with UBE2I and SUMO-1. *Biochem Biophys Res Commun* **296**, 870-6.
Neumann, C. J., Grandel, H., Gaffield, W., Schulte-Merker, S. and Nusslein-Volhard, C. (1999). Transient establishment of anteroposterior polarity in the zebrafish pectoral fin bud in the absence of sonic hedgehog activity. *Development* **126**, 4817-26.
Newbury-Ecob, R. A., Leanage, R., Raeburn, J. A. and Young, I. D. (1996). Holt-Oram syndrome: a clinical genetic study. *J Med Genet* **33**, 300-7.
Ng, J. K., Kawakami, Y., Buscher, D., Raya, A., Itoh, T., Koth, C. M., Rodriguez Esteban, C., Rodriguez-Leon, J., Garrity, D. M., Fishman, M. C. et al. (2002). The limb identity gene Tbx5 promotes limb initiation by interacting with Wnt2b and Fgf10. *Development* **129**, 5161-70.
Niederreither, K., Subbarayan, V., Dolle, P. and Chambon, P. (1999). Embryonic retinoic acid synthesis is essential for early mouse post-implantation development. *Nat Genet* **21**, 444-8.
Niederreither, K., Vermot, J., Schuhbaur, B., Chambon, P. and Dolle, P. (2002). Embryonic retinoic acid synthesis is required for forelimb growth and anteroposterior patterning in the mouse. *Development* **129**, 3563-74.
Nishinakamura, R., Matsumoto, Y., Nakao, K., Nakamura, K., Sato, A., Copeland, N. G., Gilbert, D. J., Jenkins, N. A., Scully, S., Lacey, D. L. et al. (2001). Murine homolog of SALL1 is essential for ureteric bud invasion in kidney development. *Development* **128**, 3105-15.
Niswander, L., Tickle, C., Vogel, A., Booth, I. and Martin, G. R. (1993). FGF-4 replaces the apical ectodermal ridge and directs outgrowth and patterning of the limb. *Cell* **75**, 579-87.
Niswander, L., Jeffrey, S., Martin, G. R. and Tickle, C. (1994). A positive feedback loop coordinates growth and patterning in the vertebrate limb. *Nature* **371**, 609-12.
Noji, S., Koyama, E., Myokai, F., Nohno, T., Ohuchi, H., Nishikawa, K. and Taniguchi, S. (1993). Differential expression of three chick FGF receptor genes, FGFR1, FGFR2 and FGFR3, in limb and feather development. *Prog Clin Biol Res* **383B**, 645-54.
Norton, W. H., Ledin, J., Grandel, H. and Neumann, C. J. (2005). HSPG synthesis by zebrafish Ext2 and Extl3 is required for Fgf10 signalling during limb development. *Development* **132**, 4963-73.
Ohuchi, H., Nakagawa, T., Yamamoto, A., Araga, A., Ohata, T., Ishimaru, Y., Yoshioka, H., Kuwana, T., Nohno, T., Yamasaki, M. et al. (1997). The mesenchymal factor, FGF10, initiates and maintains the outgrowth of the chick limb bud through interaction with FGF8, an apical ectodermal factor. *Development* **124**, 2235-44.k
Onai, T., Sasai, N., Matsui, M. and Sasai, Y. (2004). Xenopus XsalF: anterior neuroectodermal specification by attenuating cellular responsiveness to Wnt signaling. *Dev Cell* **7**, 95-106.

Ornitz, D. M., Xu, J., Colvin, J. S., McEwen, D. G., MacArthur, C. A., Coulier, F., Gao, G. and Goldfarb, M. (1996). Receptor specificity of the fibroblast growth factor family. *J Biol Chem* **271**, 15292-7.
Orr-Urtreger, A., Bedford, M. T., Burakova, T., Arman, E., Zimmer, Y., Yayon, A., Givol, D. and Lonai, P. (1993). Developmental localization of the splicing alternatives of fibroblast growth factor receptor-2 (FGFR2). *Dev Biol* **158**, 475-86.
Orr-Urtreger, A., Givol, D., Yayon, A., Yarden, Y. and Lonai, P. (1991). Developmental expression of two murine fibroblast growth factor receptors, flg and bek. *Development* **113**, 1419-34.
Osoegawa, K., Tateno, M., Woon, P. Y., Frengen, E., Mammoser, A. G., Catanese, J. J., Hayashizaki, Y. and de Jong, P. J. (2000). Bacterial artificial chromosome libraries for mouse sequencing and functional analysis. *Genome Res* **10**, 116-28.
Ott, T., Parrish, M., Bond, K., Schwaeger-Nickolenko, A. and Monaghan, A. P. (2001). A new member of the spalt like zinc finger protein family, Msal-3, is expressed in the CNS and sites of epithelial/mesenchymal interaction. *Mech Dev* **101**, 203-7.
Packham, E. A. and Brook, J. D. (2003). T-box genes in human disorders. *Hum Mol Genet* **12 Spec No 1**, R37-44.
Parrish, M., Ott, T., Lance-Jones, C., Schuetz, G., Schwaeger-Nickolenko, A. and Monaghan, A. P. (2004). Loss of the Sall3 gene leads to palate deficiency, abnormalities in cranial nerves, and perinatal lethality. *Mol Cell Biol* **24**, 7102-12.
Pellegrini, M., Pantano, S., Fumi, M. P., Lucchini, F. and Forabosco, A. (2001). Agenesis of the scapula in Emx2 homozygous mutants. *Dev Biol* **232**, 149-56.
Peters, K. G., Werner, S., Chen, G. and Williams, L. T. (1992). Two FGF receptor genes are differentially expressed in epithelial and mesenchymal tissues during limb formation and organogenesis in the mouse. *Development* **114**, 233-43.
Pinson, K. I., Brennan, J., Monkley, S., Avery, B. J. and Skarnes, W. C. (2000). An LDL-receptor-related protein mediates Wnt signalling in mice. *Nature* **407**, 535-8.
Piotrowski, T. and Nusslein-Volhard, C. (2000). The endoderm plays an important role in patterning the segmented pharyngeal region in zebrafish (Danio rerio). *Dev Biol* **225**, 339-56.
Poss, K. D., Shen, J., Nechiporuk, A., McMahon, G., Thisse, B., Thisse, C. and Keating, M. T. (2000). Roles for Fgf signaling during zebrafish fin regeneration. *Dev Biol* **222**, 347-58.
Rallis, C., Bruneau, B. G., Del Buono, J., Seidman, C. E., Seidman, J. G., Nissim, S., Tabin, C. J. and Logan, M. P. (2003). Tbx5 is required for forelimb bud formation and continued outgrowth. *Development* **130**, 2741-51.
Reuter, D., Schuh, R. and Jackle, H. (1989). The homeotic gene spalt (sal) evolved during Drosophila speciation. *Proc Natl Acad Sci U S A* **86**, 5483-6.
Revest, J. M., Spencer-Dene, B., Kerr, K., De Moerlooze, L., Rosewell, I. and Dickson, C. (2001). Fibroblast growth factor receptor 2-IIIb acts upstream of Shh and Fgf4 and is required for limb bud maintenance but not for the induction of Fgf8, Fgf10, Msx1, or Bmp4. *Dev Biol* **231**, 47-62.

Ribeiro, C., Neumann, M. and Affolter, M. (2004). Genetic control of cell intercalation during tracheal morphogenesis in Drosophila. *Curr Biol* **14**, 2197-207.
Riddle, R. D., Johnson, R. L., Laufer, E. and Tabin, C. (1993). Sonic hedgehog mediates the polarizing activity of the ZPA. *Cell* **75**, 1401-16.
Ro, H., Soun, K., Kim, E. J. and Rhee, M. (2004). Novel vector systems optimized for injecting in vitro-synthesized mRNA into zebrafish embryos. *Mol Cells* **17**, 373-6.
Roehl, H. and Nusslein-Volhard, C. (2001). Zebrafish pea3 and erm are general targets of FGF8 signaling. *Curr Biol* **11**, 503-7.
Roelink, H. and Nusse, R. (1991). Expression of two members of the Wnt family during mouse development--restricted temporal and spatial patterns in the developing neural tube. *Genes Dev* **5**, 381-8.
Ross, S., Best, J. L., Zon, L. I. and Gill, G. (2002). SUMO-1 modification represses Sp3 transcriptional activation and modulates its subnuclear localization. *Mol Cell* **10**, 831-42.
Ruvinsky, I., Oates, A. C., Silver, L. M. and Ho, R. K. (2000). The evolution of paired appendages in vertebrates: T-box genes in the zebrafish. *Dev Genes Evol* **210**, 82-91.
Sapetschnig, A., Rischitor, G., Braun, H., Doll, A., Schergaut, M., Melchior, F. and Suske, G. (2002). Transcription factor Sp3 is silenced through SUMO modification by PIAS1. *Embo J* **21**, 5206-15.
Sato, A., Matsumoto, Y., Koide, U., Kataoka, Y., Yoshida, N., Yokota, T., Asashima, M. and Nishinakamura, R. (2003). Zinc finger protein sall2 is not essential for embryonic and kidney development. *Mol Cell Biol* **23**, 62-9.
Saunders, J. W. Jr (1948). The proximo-distal sequence of origin of the parts of the chick wing and the role of the ectoderm. *J. Exp. Zool.* **108**, 363-403.
Schauerte, H. E., van Eeden, F. J., Fricke, C., Odenthal, J., Strahle, U. and Haffter, P. (1998). Sonic hedgehog is not required for the induction of medial floor plate cells in the zebrafish. *Development* **125**, 2983-93.
Schlessinger, J., Plotnikov, A. N., Ibrahimi, O. A., Eliseenkova, A. V., Yeh, B. K., Yayon, A., Linhardt, R. J. and Mohammadi, M. (2000). Crystal structure of a ternary FGF-FGFR-heparin complex reveals a dual role for heparin in FGFR binding and dimerization. *Mol Cell* **6**, 743-50.
Scholpp, S., Groth, C., Lohs, C., Lardelli, M. and Brand, M. (2004). Zebrafish fgfr1 is a member of the fgf8 synexpression group and is required for fgf8 signalling at the midbrain-hindbrain boundary. *Dev Genes Evol* **214**, 285-95.
Sekine, K., Ohuchi, H., Fujiwara, M., Yamasaki, M., Yoshizawa, T., Sato, T., Yagishita, N., Matsui, D., Koga, Y., Itoh, N. et al. (1999). Fgf10 is essential for limb and lung formation. *Nat Genet* **21**, 138-41.
Shen-Orr, S. S., Milo, R., Mangan, S. and Alon, U. (2002). Network motifs in the transcriptional regulation network of Escherichia coli. *Nat Genet* **31**, 64-8.
Sordino, P., van der Hoeven, F. and Duboule, D. (1995). Hox gene expression in teleost fins and the origin of vertebrate digits. *Nature* **375**, 678-81.
Stephens, T. D. and McNulty, T. R. (1981). Evidence for a metameric pattern in the development of the chick humerus. *J Embryol Exp Morphol* **61**, 191-205.
Summerbell, D. (1974). A quantitative analysis of the effect of excision of the AER from the chick limb-bud. *J Embryol Exp Morphol* **32**, 651-60.

Sun, X., Lewandoski, M., Meyers, E. N., Liu, Y. H., Maxson, R. E., Jr. and Martin, G. R. (2000). Conditional inactivation of Fgf4 reveals complexity of signalling during limb bud development. *Nat Genet* **25**, 83-6.
Sun, X., Mariani, F. V. and Martin, G. R. (2002). Functions of FGF signalling from the apical ectodermal ridge in limb development. *Nature* **418**, 501-8.
Sweetman, D., Smith, T., Farrell, E. R., Chantry, A. and Munsterberg, A. (2003). The conserved glutamine-rich region of chick csal1 and csal3 mediates protein interactions with other spalt family members. Implications for Townes-Brocks syndrome. *J Biol Chem* **278**, 6560-6.
Sweetman, D., Smith, T. G., Farrell, E. R. and Munsterberg, A. (2005). Expression of csal1 in pre limb-bud chick embryos. *Int J Dev Biol* **49**, 427-30.
Takabatake, Y., Takabatake, T. and Takeshima, K. (2000). Conserved and divergent expression of T-box genes Tbx2-Tbx5 in Xenopus. *Mech Dev* **91**, 433-7.
Takada, S., Stark, K. L., Shea, M. J., Vassileva, G., McMahon, J. A. and McMahon, A. P. (1994). Wnt-3a regulates somite and tailbud formation in the mouse embryo. *Genes Dev* **8**, 174-89.
Tamura, K., Yonei-Tamura, S. and Belmonte, J. C. (1999). Differential expression of Tbx4 and Tbx5 in Zebrafish fin buds. *Mech Dev* **87**, 181-4.
Terhal, P., Rosler, B. and Kohlhase, J. (2006). A family with features overlapping Okihiro syndrome, hemifacial microsomia and isolated Duane anomaly caused by a novel SALL4 mutation. *Am J Med Genet A* **140**, 222-6.
Thisse, C., Thisse, B., Schilling, T. F. and Postlethwait, J. H. (1993). Structure of the zebrafish snail1 gene and its expression in wild-type, spadetail and no tail mutant embryos. *Development* **119**, 1203-15.
Thompson, J. D., Higgins, D. G. and Gibson, T. J. (1994). CLUSTAL W: improving the sensitivity of progressive multiple sequence alignment through sequence weighting, position-specific gap penalties and weight matrix choice. *Nucleic Acids Res* **22**, 4673-80.
Tickle, C. (2004). The contribution of chicken embryology to the understanding of vertebrate limb development. *Mech Dev* **121**, 1019-29.
Toker, A. S., Teng, Y., Ferreira, H. B., Emmons, S. W. and Chalfie, M. (2003). The Caenorhabditis elegans spalt-like gene sem-4 restricts touch cell fate by repressing the selector Hox gene egl-5 and the effector gene mec-3. *Development* **130**, 3831-40.
Tonou-Fujimori, N., Takahashi, M., Onodera, H., Kikuta, H., Koshida, S., Takeda, H. and Yamasu, K. (2002). Expression of the FGF receptor 2 gene (fgfr2) during embryogenesis in the zebrafish Danio rerio. *Mech Dev* **119 Suppl 1**, S173-8.
Turner, D. L. and Weintraub, H. (1994). Expression of achaete-scute homolog 3 in Xenopus embryos converts ectodermal cells to a neural fate. *Genes Dev* **8**, 1434-47.
van Eeden, F. J., Granato, M., Schach, U., Brand, M., Furutani-Seiki, M., Haffter, P., Hammerschmidt, M., Heisenberg, C. P., Jiang, Y. J., Kane, D. A. et al. (1996). Genetic analysis of fin formation in the zebrafish, Danio rerio. *Development* **123**, 255-62.
Verheyden, J. M., Lewandoski, M., Deng, C., Harfe, B. D. and Sun, X. (2005). Conditional inactivation of Fgfr1 in mouse defines its role in limb bud establishment, outgrowth and digit patterning. *Development* **132**, 4235-45.

Vermot, J., Gallego Llamas, J., Fraulob, V., Niederreither, K., Chambon, P. and Dolle, P. (2005). Retinoic acid controls the bilateral symmetry of somite formation in the mouse embryo. *Science* **308**, 563-6.
Vermot, J. and Pourquie, O. (2005). Retinoic acid coordinates somitogenesis and left-right patterning in vertebrate embryos. *Nature* **435**, 215-20.
Vogel, A., Rodriguez, C. and Izpisua-Belmonte, J. C. (1996). Involvement of FGF-8 in initiation, outgrowth and patterning of the vertebrate limb. *Development* **122**, 1737-50.
Xu, J., Liu, Z. and Ornitz, D. M. (2000). Temporal and spatial gradients of Fgf8 and Fgf17 regulate proliferation and differentiation of midline cerebellar structures. *Development* **127**, 1833-43.
Xu, X., Weinstein, M., Li, C., Naski, M., Cohen, R. I., Ornitz, D. M., Leder, P. and Deng, C. (1998). Fibroblast growth factor receptor 2 (FGFR2)-mediated reciprocal regulation loop between FGF8 and FGF10 is essential for limb induction. *Development* **125**, 753-65.
Yamaguchi, T. P., Harpal, K., Henkemeyer, M. and Rossant, J. (1994). fgfr-1 is required for embryonic growth and mesodermal patterning during mouse gastrulation. *Genes Dev* **8**, 3032-44.
Yamaguchi, T. P., Bradley, A., McMahon, A. P. and Jones, S. (1999). A Wnt5a pathway underlies outgrowth of multiple structures in the vertebrate embryo. *Development* **126**, 1211-23.
Yang, Y., Drossopoulou, G., Chuang, P. T., Duprez, D., Marti, E., Bumcrot, D., Vargesson, N., Clarke, J., Niswander, L., McMahon, A. et al. (1997). Relationship between dose, distance and time in Sonic Hedgehog-mediated regulation of anteroposterior polarity in the chick limb. *Development* **124**, 4393-404.
Zak, B. M., Crawford, B. E. and Esko, J. D. (2002). Hereditary multiple exostoses and heparan sulfate polymerization. *Biochim Biophys Acta* **1573**, 346-55.
Zuniga, A., Haramis, A. P., McMahon, A. P. and Zeller, R. (1999). Signal relay by BMP antagonism controls the SHH/FGF4 feedback loop in vertebrate limb buds. *Nature* **401**, 598-602.